PHYSICAL CHARACTERISATION OF URBAN CYCLISTS FOR ADVANCED BICYCLE TRAVEL MODELS

by

Simone Tengattini

A THESIS SUBMITTED IN PARTIAL FULFILLMENT OF

THE REQUIREMENTS FOR THE DEGREE OF

MASTER OF APPLIED SCIENCE

in

The Faculty of Graduate and Postdoctoral Studies

(Civil Engineering)

THE UNIVERSITY OF BRITISH COLUMBIA

(Vancouver)

April 2017

ABSTRACT

Urban cyclist's physical characteristics are important for advanced modelling of bicycle speed and energy expenditure, with applications including infrastructure design, network analysis, and health and safety assessments. However, representative values for diverse urban travellers have not been established. This study investigates the physical characteristics of real-world urban cyclists, including rolling and drag resistance parameters, and bicycle and cargo masses. Relationships among physical characteristics socio-demographics and travel behaviour are also analysed, and a bicycle cruising speed model is derived to illustrate usefulness of the sought parameters.

Firstly, a 12-sensor, 100-meter coast-down test setup is developed and indoor and outdoor validation tests are performed. Outdoor validation tests generate rolling resistance coefficient estimates of 0.0064 ±0.0013 and effective frontal area estimates of 0.63 ±0.11 m^2.

Secondly, resistance parameters were measured utilizing the novel coast-down test for 557 intercepted cyclists in Vancouver, Canada.. The average (standard deviation) of coefficient of rolling resistance (C_r), effective frontal area ($A_f C_d$), bicycle plus cargo mass, and bicycle-only mass were 0.0077 (0.0036), 0.559 (0.170) m^2, 18.3 (4.1) kg, and 13.7 (3.3) kg, respectively. The range of measured values is wider and higher than suggested in the literature.

Thirdly, the sample of intercepted cyclists is categorised based on observed physical attributes of the bicycle and rider. Three typologies defined through cluster analysis were identified as Road (R), Hybrid (H) and Mountain (M) style urban cyclists. The analysis indicates that cycling efficiency, perceptions, preferences, and habits are related to physical

typology in a complex but consistent manner. M, H, and R cyclists are, in that order, increasingly more efficient, more comfortable in mixed traffic, more consistently year-round cyclists, self-reportedly faster, and engage in more physical activity. Physical typologies might help unveil new motivations in active travel behaviour and encourage urban cycling by a wider range of people.

Finally, a mathematical framework is derived from first principles to determine speed from cyclist characteristics (power output, gearing, resistance parameters) and roadway attributes. Application of the speed estimation framework to the problem of traffic signal clearance interval timing illustrates the utility for probabilistic, context-sensitive roadway design.

PREFACE

This research was conducted with Dr. Alex Bigazzi (Assistant Professor at the University of British Columbia) as thesis supervisor and principal investigator. The author of this thesis, Simone Tengattini, was responsible for the literature review, coast-down test design and instrumentation, planning, managing and administration of the intercept survey, data processing, and analysis. The UBC REACT lab (REsearch on ACtive Transportation) in the persons of Evan Hammer, Andrei Radu and Gurtej Tung collaborated in the data collection. Invaluable continuous feedback and guidance were provided by the principal investigator, who also was the main contributor of chapter 9.4.

Part of Chapter 4 and 5 were used in a peer-reviewed conference paper by Tengattini and Bigazzi (2017).

Intercept survey presented in Chapter 6 was conducted in compliance with the UBC Behavioural Research Ethics Board (BREB) requirements, under the project titled "Incorporating pollution inhalation and energy expenditure into network analysis for active transportation", UBC BREB number H16-00604.

This research was partly funded by Natural Science and Engineering Research Council of Canada (NSERC), grant number RGPIN-2016-04034.

TABLE OF CONTENTS

LIST OF TABLES

LIST OF FIGURES

LIST OF SYMBOLS

Kinematic quantities

t	Time
t_0	Initial time
$t(x)$	Coasting time as a function of distance
$\tau(x)$	Experimentally observed coasting times
$\varepsilon_{i,j}$	Coasting time residual at sensor location i, during test j
x	Coasting distance
x_0	Initial distance
$x(v)$	Coasting distance as a function of speed
Δx_i	Spatial correlation correction factor, at location i
v_{rel}	Bicycle speed, relative to the wind
v	Bicycle speed
v_0	Initial bicycle speed
$\hat{v}_0$	Fitted initial bicycle speed
v_f	Final speed
$v(t)$	Coasting speed as a function of time
$v_{i,j}$	Coasting speed at sensor location i, during test j
$\vec{v}$	Bicycle ground speed vector
w	Wind speed
$\overrightarrow{w_{app}}$	Apparent wind speed vector
$\overrightarrow{w_{abs}}$	Absolute wind speed vector

α	Absolute wind direction
β	Bicycle yaw angle
π	180-degree angle

Dynamic quantities

F_i	Generic force applied on a vehicle
T	Tractive bicycle force
τ_c	Bicycle torque at the crank
c^*	Bicycle cadence for which P_c^* realizes
c	Bicycle Cadence
P	Power output (generic)
P_c	Power output at the bicycle crank
P_c^*	Maximum power in the second-order power-cadence relationship
P_w	Power output at the drive wheel
η	Drivetrain efficiency
γ	Constant term in the torque cadence relationship
δ	Linear term in the torque cadence relationship
g	Gravity acceleration

Resistance-related quantities

c_0	Constant-with-speed term in the generic resistance formulation
c_1	Linear-with-speed term with speed in the generic resistance formulation
c_2	Quadratic-with-speed term in the generic resistance formulation

k_m	Aerodynamic drag per unit mass
C_r	Rolling resistance coefficient
A_f	Frontal area
C_d	Drag Coefficient
$A_f C_d$	Effective frontal area
R	Total resistance
R_r	Rolling resistance
R_d	Aerodynamic resistance
R_g	Grade resistance
ρ	Air density
T_K	Air temperature (absolute)
h	Altitude of test location, above sea level
m	Vehicle mass (usually total mass, bicycle + rider + cargo)
m_μ	Inflated vehicle mass (for rotating parts)
μ	Mass correction factor
G	Road grade
A	Proxy for rolling resistance
$\hat{A}$	Fitted proxy for rolling resistance
B	Proxy for aerodynamic resistance
$\hat{B}$	Fitted proxy for aerodynamic resistance
k_w	Shape parameter Weibull distribution
λ_w	Scale parameter Weibull distribution
α_Γ	Shape parameter Gamma distribution

β_Γ	Rate parameter Gamma distribution

Other quantities

D	Bicycle gear development length
D_{min}	Minimum bicycle gear development length
D_{max}	Maximum bicycle gear development length
r_w	Bicycle drive wheel radius
m_i	Bicycle i^{th} gear conversion ratio
C_i	Clearance interval
w_i	Signalized intersection width in NATCO guideline

LIST OF ABBREVIATIONS

BMI	Body Mass Index
BREB	Behavioural Research Ethics Board
CAD	Canadian Dollar
GNSS	Global Navigation Satellite System
H	"Hybrid" style cyclist (cluster analysis)
IMU	Inertial Measurement Unit
IR	InfraRed light
K-S	Kolmogorov-Smirnov test
LCD	Liquid Crystal Display
M	"Mountain" style cyclist (cluster analysis)
MEMS	Micro Electro-Mechanical Systems
MicroSD	Miniaturized Secure Digital flash memory card
NATCO	National Association of City Transportation Officials
R	"Road" style cyclist (cluster analysis)
WAAS	Wide Area Augmentation System
WGS84	World Geodetic System 1984

ACKNOWLEDGEMENTS

"How could I forget to mention the bicycle is a good invention"
Red Hot Chili Peppers, Bicycle Song (2006)

Having crossed the uncharted waters of a research-based master's program, tastes marvellous like happiness, and *happiness real only when shared*. So, in all fairness, along with bizarre *bench* interludes and *Fringe* marathons filling the sails, I ought to mention many human beings for providing incommensurable energy to this journey.

Of course, Dr. Alex Bigazzi is profoundly thanked for his scientific guidance and support that was indispensable to keep me not only on track, but on the right one. Yacht Rock, music and brews, helped along the way, as well. Clark Lim is also thanked for being so available to students, sharing life advice. Thanks to Prof. Federico Rupi for providing feedback, and passionately teaching my first course in transportation engineering, contributing to my route choice.

Outside faculty, but still in the department, the civil front office and "rusty hut" staff has been fun to hang out with, efficient and greatly useful for all the data collection-related, often last-minute requests. Also, thanks to fellow friends and acquaintances in engineering (or not) who I received any feedback from about my thesis work.

Clearly, life's not circumscribed to uni, so thanks to the *Slackhouse*, my first house, where I had lots of fun and drama too. Also, thanks to *2116* where I was lucky enough to move in with *actual* friends, as opposed to *potential* friends. Luis, Sylvia (member by transitive relation), Alice, Lisa, Moh, and Wes all super chill people, who one can be himself with. Well, how not to mention Ilaria, keeping Italian traditions – especially culinary – alive! Also, a *grazie* to the *Sagra*, a bunch of friends scattered all over the planet and always eager to catch up again. Bologna too, city and people-wise, should be really

thanked, as I still feel belonging there. Loving relatives, in Canada and in Italy, always provided constant affection and support: I’m thankful for all the freedom I could always enjoy in taking life decisions.

1. INTRODUCTION

With the growth in bicycling as an urban transportation mode in cities around the world, there is increasing interest in and need for methods to model bicycle performance and cyclist behaviour in increasing detail. Bicycle performance, for example design speed, is a key input for safe, reliable, and attractive infrastructure design (Navin, 1994; Parkin & Rotheram, 2010). Since the 1970s, there has been growing interest in bicycle infrastructure planning and design techniques, with new guidelines being developed around the world, e.g. (CROW, 2007; National Association of City Transportation Officials, 2014). Also, bicycle speed is a key input for geometric and signal design (Parkin & Rotheram, 2010; Taylor & Mahmassani, 2000), and variability in bicycle speeds is essential for moving toward probabilistic, reliability-based infrastructure designs (Ismail & Sayed, 2009). An appropriate cyclists' physical characterization would refine bicycle performance knowledge fundamental to providing bicycle infrastructure that is both safe and appealing, for example accommodating desired riding speeds, with the additional goal of incentivising bicycle travel. Furthermore, the increase use of microsimulation for operational performance analysis requires more refined ways to model bicycle travel, particularly speed (Twaddle, Schendzielorz, & Fakler, 2014). Better understanding of bicycle performances in terms of energy expenditure, power output and speed could also improve understanding of bicycle route and mode choices (Heinen, van Wee, & Maat, 2010; Iseki & Tingstrom, 2013; Mercat, 1999a). Speed and energy expenditure are also important factors for health effects through air pollution and physical activity, and better cyclists' characterization could improve health assessments for transportation systems and projects (Bigazzi, 2016; Bigazzi & Figliozzi, 2014; Mueller et al., 2015a).

Bicyclist power output and energy expenditure are connected to travel (speed) and roadway (grade and pavement) conditions primarily through three physical parameters describing rolling, aerodynamic resistances and overall cyclist mass (i.e. including machine and cargo, if present) (Bigazzi & Figliozzi, 2015a; Olds, 2001; Wilson & Papadopoulos, 2004). These parameters have been investigated mainly for sport and professional bicycling, while relatively little is known about their values for utilitarian urban bicyclists (Bigazzi & Figliozzi, 2015a; Faria, Parker, & Faria, 2005; Wilson & Papadopoulos, 2004). A better understanding of these physical parameters for real-world urban bicyclists, including their relationship with other non-physical factors, is needed to estimate speed and energy expenditure and to understand how they relate to travel and roadway conditions.

This thesis addresses the lack of real-world urban cyclists' rolling, aerodynamic resistances parameters as well as overall mass (gathered under the term "physical characterization") and uses newly gathered knowledge towards cycling behavioural and speed modelling. To fill the lack, experimental research was carried out, comprising design and validation of an outdoor coast-down test to measure resistances parameters (chapter 4 and 5, respectively), administration of the test in an intercepted survey (chapter 6), and analyses of physical characterization results, exploring how they relate to cyclists' socio-demographics and travel behaviour (chapter 7 and 8, respectively). Finally, a bicycle speed model is derived, using rolling, aerodynamic and mass parameters, to show the importance and usefulness of this research work in one practical example (chapter 9).

This thesis, especially the coast-down test methodology, builds on past work, so a literature review is provided in the following chapter.

2. LITERATURE REVIEW

This literature review is twofold. The first part exposes available body of knowledge regarding land vehicle resistances, with a focus on sport and professional cycling. The second part illustrates available methods to measure bicycle resistances.

2.1. Resistance parameters in land vehicles

Any real-world land vehicle is subject to resistances that must be exceeded to generate motion. Resistance forces are typically subdivided in those that are always present for any vehicle on any route (Rolling and Aerodynamic resistances) and those that might be present depending on route topography (Grade resistance) and vehicle type (Curve resistance in railroad vehicles) (Lupi, 2004).

Rolling resistance

Rolling resistance is mainly due to eccentricity of wheels' pressure distribution along the contact patch (contact area between the wheel and the pavement). When the wheel is not moving, pressure distribution is symmetric so that the resultant perfectly balance out the weight the wheel is supporting. When the wheel is moving, the pressure distribution skews in the direction of travel, resulting in an imbalanced horizontal force (namely, rolling resistance) acting in the opposite direction of motion. Also, because the contact between wheel and pavement is inelastic, energy dissipation occurs when moving.

Generally, rolling resistance depends on contact patch area, which is influenced by tire type, pressure, weight. It also depends on pavement and wheel materials (railroad rolling resistance is much lower than automobiles) and temperature, as well as wheel bearings (in)efficiency. Lastly, it depends on wheel speed, because the eccentricity in contact patch pressure distribution grows with growing speed (Lupi, 2004; Wong, 2008).

Aerodynamic resistance

Aerodynamic (or drag) resistance, is mainly due to air overpressure at the front of the vehicle, depression at the rear of the vehicle, and for long vehicles (e.g. trains or trucks) friction along vehicle's lateral surfaces (bottom included). Hence, drag resistance is proportional to vehicle's external shape and area, as well as travelling speed (wide, non-aerodynamic areas offer more surface, and higher speed generates higher pressure). Also, it is proportional to the medium density (Lupi, 2004; Wong, 2008).

Grade resistance

Grade resistance originates when a vehicle is moving vertically in the gravitational field. It is true that to gain height (i.e. go uphill) a vehicle must exert work so that part of it be transformed in potential energy. Grade resistance depends on the weight of the vehicle and on the road grade itself.

Curve resistance

Curve resistance is usually negligible but for railroad vehicles (Lupi, 2004). The reason lies in the friction generated between wheel flanges and rail heads during a turn. When travelling on a horizontal curve railroad vehicle wheels, being rigidly connected, cannot steer so the flange/head friction is responsible for the turning movement. Also, railroad vehicles are not equipped with differentials (mechanical devices allowing the outer wheels to rotate faster than inner ones when travelling on a curve), generating slippage (Hay, 1982; Lupi, 2004).

2.2. Resistance parameters in bicycles

Major resistance forces for a bicycle can be categorized as the following (Olds et al., 1995; Wilson & Papadopoulos, 2004):

(i) Rolling: due to inelastic deformation of the wheel and friction losses at the bearings;

(ii) Aerodynamic drag: due to the bicycle moving in the medium air;

(iii) Road grade: due to a gain (or loss) of height in the gravitational field.

Other resistances (such as friction losses during turning) can be considered negligible for a bicycle (Wilson & Papadopoulos, 2004). At low speeds, rolling resistance is a main contributor to total resistance force and it can be approximated as independent of speed. Analogously to the Coulombian formulation of friction, the rolling resistance is

$$R_r = mgC_r \quad (1)$$

where C_r is the unit-less rolling resistance coefficient, which depends on parameters such

as tire pressure, tire width, and pavement (roughness and material), and mg is the weight (in N) of the bicycle plus bicyclist. As speed grows, drag can become the main resistance force. The resistance of a body moving in a medium of density ρ (kg/m^3), at speed v_{rel} relative to the wind, having frontal area A_f and drag coefficient C_d, is modelled as (semi-empirical equation, derived from Bernoulli's theorem):

$$R_d = \frac{1}{2}\rho A_f C_d v_{rel}|v_{rel}| \, . \qquad (2)$$

The absolute value in Equation 2 allows for the condition $v_{rel} < 0$ – where the bicyclist has a tailwind that exceeds the travel speed (Knight, 2008). Grade resistance can be modelled as

$$R_g = mg\frac{G}{\sqrt{1+G^2}} \qquad (3)$$

where G is the road grade in direction of travel, expressed as a ratio of vertical to horizontal distance over a fixed length of road (unit-less). For small G Equation 3 approximates

$$R_g = mgG \qquad (4)$$

Total resistance force can then be written as

$$R = mg(C_r + G) + \frac{1}{2}\rho A_f C_d v_{rel}|v_{rel}|. \qquad (5)$$

Mass m can be inflated to m_μ according to the following

$$m_\mu = m(1+\mu) \qquad (6)$$

where μ is a mass correction factor to account for the inertia of rotating parts. It is usually estimated enforcing an energy balance between the bicycle as a rigid body and the actual one (i.e. with rotating parts). Mass inflation in bicycles can be considered negligible for non-professional bicycling purposes (Burke, 2003a), so it was not accounted for in this study. As an example for an average bicycle (80 kg bicycle and cyclists; 0.9 kg per wheel, each having 0.34 and 0.36 m internal and external diameter, respectively) $\mu = 0.02$ is found.

2.3. Resistance parameters methods of assessment

Aerodynamic drag and rolling resistances during bicycling have been investigated using wind tunnels, power meters, the dynamometric method, and the coast-down method, among others. Wind tunnel testing is a common approach, but relatively costly, difficult to apply to a wide range of travellers, and only able to measure drag resistance. Data from bicycles instrumented with power-meters to measure cyclist power output at different speeds can be used to estimate rolling and drag resistance parameters, but again this is difficult to apply to a wide range of travellers, and requires modifying the bicycle for which parameters are sought. Thirdly, the dynamometric method (towing the bicycle on flat ground at constant speeds using a cable paired in series with a dynamometer) can be used to estimate rolling and drag resistance parameters. Finally, coast-down or deceleration methods can be used to measure rolling and drag resistances exploiting Newton's second law (Andersen, Larsen, Fraser, Schmidt, & Dyre, 2014; R. B. Candau et al., 1999; Debraux, Grappe, Manolova, & Bertucci, 2011; Kyle & Burke, 1984).

2.4. Coast-down tests review

Among the methods enumerated previously, coast-down testing, also known as the deceleration method, is appealing for testing of real-world urban bicyclists because it can capture both rolling and drag resistance forces, has been successfully applied to a range of vehicles, and can be implemented *in situ* on bicycle facilities. A coast-down test consists of measuring a vehicle's motion while coasting from a cruising speed to a stop without activating the brakes, and then extracting resistance parameters from the data by fitting a physical equation of motion (R. B. Candau et al., 1999; Debraux et al., 2011; Preda & Ciolan, 2010; White & Korst, 1972). While this method holds promise, most previous bicycle coast-down testing has been conducted indoors, and so the method must be revised for field application by accounting for wind and grade.

In the absence of propulsion or braking forces, vehicle deceleration is primarily determined by rolling and aerodynamic resistance forces. For automobiles, the coast-down test is formalized as a velocity-time curve from the basic equations of motion, and on-board instruments (e.g. accelerometers, tachometers, odometers) can be used to measure instantaneous deceleration, speed, and distance over time (Preda & Ciolan, 2010; White & Korst, 1972). Coast-down deceleration can be represented as the differential equation

$$m \cdot \frac{dv}{dt} = c_0 + c_1 v + c_2 v^2 \qquad (7)$$

where m is the total mass of the vehicle, v is the instantaneous speed over time t, and c_i are resistance parameters. Typically, rolling resistance is considered to be independent of speed (contributing to c_0) and drag proportional to v^2 (contributing to c_2); c_1 is usually low, related to the rotational inertia, and sometimes assumed to be zero (di Prampero, Cortili,

Mognoni, & Saibene, 1979).

On-board measurement is more difficult for bicycles (for example, using power meters or cycle computers) – particularly during a short field test with intercepted travellers. Waltham and Copeland (1999) manually recorded velocity over time with an audio recorder, while de Groot et al. (1995) logged cycle computer data and used Equation 7 with $c_1 = 0$ to develop the fitting equation for $v(t)$:

$$v(t) = \sqrt{\frac{c_0}{k_m}}\, tan\left(atan\left(v_0\sqrt{\frac{k_m}{c_0}}\right) - \sqrt{c_0 k_m}\; t\right) \qquad (8)$$

where v_0 is the initial bicycle speed and k_m is aerodynamic drag per unit mass (c_2/m). Cycle computers to measure speed are problematic for a field survey because each bicycle would have to be instrumented before testing. In addition there are resolution errors at low speeds for most off-the-shelf cycle computers.

As an alternative to direct speed measurements, time measurement at fixed locations has been used for bicycle coast-down test instrumentation. Kyle and Burke (1984) performed coast-down tests with bicyclists coasting down a hill and then slowing to a stop on flat land. Initial coasting speed was measured using time traps (two timing switches a short distance apart) and the total coasted distance was recorded. The equation developed for the test coasting distance was:

$$x = \frac{m}{2c_2} ln\left(\frac{-mgG+c_0+c_2(v_0-w)^2}{-mgG+c_0+c_2 w^2}\right) + \frac{mw}{\sqrt{c_2(-mgG+c_0)}}\left(-atan\left(\frac{-w\sqrt{c_2}}{\sqrt{-mgG+c_0}}\right) + atan\left(\frac{c_0-mgG+c_2 {v_0}^2}{-mgG+c_0}\right)\right) \qquad (9)$$

where m is the mass of rider and bicycle, c_0 and c_2 are rolling and drag resistance parameters, g is gravitational acceleration, G is road grade, and w is wind speed. Results of the on-road testing were inconclusive, possibly due to lack of accounting for varying wind

and grade.

Candau at al. (1999) developed an indoor coast-down test using three timing switches (pneumatic tubes) in a flat hallway, with spacing of 1 m and 20 m. Trigger times were recorded using computer chronometer with resolution of 30 μs. They developed a mathematical framework from Equation 7 with $c_1 = 0$, similar to Equation 9 but without grade and wind effects. A first estimate of v_0 was obtained from the first two timing sensors with spacing of x_0 and initial time t_0, and then the timing for the third switch estimated by

$$x(t) = \frac{m}{2c_2} \ln \left[\frac{1+\tan\left(t\sqrt{c_0 c_2/m^2} - \operatorname{atan}\left(\frac{\cos\left(t_0\sqrt{c_0 c_2/m^2}\right) - e^{\frac{c_2}{m}x_0}}{\sin\left(t_0\sqrt{c_0 c_2/m^2}\right)} \right) \right)^2}{1+\frac{c_2}{c_0}\left(\sqrt{\frac{c_0}{c_2}} \frac{\cos\left(t_0\sqrt{c_0 c_2/m^2}\right) - e^{\frac{c_2}{m}x_0}}{\sin\left(t_0\sqrt{c_0 c_2/m^2}\right)} \right)^2} \right]. \quad (10)$$

Parameter estimates for c_0 and c_2 were generated by minimizing the squared difference between $x(t)$ from Equation 10 and the measured distance of 20 m.

3. OBJECTIVE

The ultimate goal of this thesis it to provide transportation professionals with ready-to-use physical characteristic distributions for real-world urban cyclists and illustrate associations with cycling behaviour. The goal is pursued by progressively investigating the followings:

(i) Available methods to gather bicycle resistances parameters: comparison to find the most suitable methods to be administered *in situ*, during an intercept cyclists' survey;

(ii) Selection and validation of test methodology based on results variability of indoor testing;

(iii) Coast-down testing expansion and validation to account for varying wind and grade conditions, typical of outdoor conditions;

(iv) Design and administration of coast-coast tests in an intercept survey in Vancouver, BC in summer 2016;

(v) Physical characteristics distribution illustration and correlation analysis among all measured parameters (physical, socio-demographic and behavioural).

In addition, to demonstrate how bicycle travel models could benefit from cyclists physical characterization, a context-sensitive speed model is developed and an application in traffic operations is illustrated.

4. BICYCLE COAST-DOWN TEST DESIGN

This section illustrates the process that led to the development of the final version of the coast-down test, eventually named the "12-switch" method. Trade-offs analysis was very important as the design had to consider the final usage in an intercept survey, so minimal imposition on cyclists and portability of instrumentation was paramount.

4.1. Suitable coast-down equipment

Measurement of bicycle motion when coasting (either, position, speed or acceleration) is required to model coast-down bicycle deceleration rate. Several technologies are available for such purpose. In general, motion-tracking devices can be installed on the vehicle (on-bicycle) or on the coast-down field (on-roadway). On-roadway devices are generally more laborious to install but they require less effort in gathering data when the coast down test is performed on intercepted cyclists. On the other hand, on-bicycle devices don't require any roadway installation, but they need to be of easy set-up and calibration on surveyed cyclists.

On-Bicycle motion sensors

Generally, on-bicycle devices provide a quasi-continuous tracking because they log bicycle motion with high frequency (<1Hz) to a memory slot.

(i) Accelerometers and Gyroscopes

Bicycle motion is described by accelerations collected with a certain selectable frequency. Smartphones often comprised of an Inertial Measurement Unit (IMU) including a three axial accelerometer and gyroscopes. Such technology could be easily and inexpensively provided to intercepted cyclists. However, such sensors

belong to the so-called MEMS (Micro Electro-Mechanical Systems) category. They are cheap and they are characterized by important errors. In particular, they have a systematic error component (bias, axis nonorthogonality, scale factor, thermal) and a random component (random noise), which can be potentially mitigated through calibration (Aggarwal, 2010).

(ii) Cycling computers

Bicycle motion is described by speed and distance collected with a relatively low frequency, usually of 1Hz for off-the-shelf devices, by measuring wheel revolutions. This method is inexpensive, but could perhaps generate reluctance in cyclists as it requires a non-trivial bicycle installation.

(iii) GNSS (Global Navigation Satellite System) receiver

Bicycle motion is described by geo-coordinates, collected with a certain frequency. A GNSS receiver can provide an absolute positioning in a reference frame (e.g. WGS84) with a precision in the order of 5 m, and with augmentation systems (e.g. WAAS - Wide Area Augmentation System) can be further improved (De Agostino, 2009). It requires at least four visible satellites, potentially limiting available testing locations, such as urban canyons or tree-lined streets.

(iv) Combined GNSS receiver + accelerometer and gyroscopes.

GNSS and inertial measurement can be integrated to measure more reliably bicycle motion. Due to the complementarity of GNSS measurements and accelerometers, coupling the two technologies is a technique that has been often proposed for vehicle positioning (especially during brief GNSS outages periods) (De Agostino, 2009). It implies the use of Kalman filters or neuronal networks to compute enhanced bicycle positioning (De Agostino, 2009).

On-roadway motion sensors

Generally, on-roadway devices provide a discrete tracking, because a finite number of sensors are installed on the coast down field. Sensors detect the movement of approaching bicycles.

(i) Ultrasonic rangefinders

Bicycle motion is described by proximity detection in time at finite locations along the coasting field. Ultrasonic sensors are used in many applications (presence, proximity or distance measurement). They work transmitting ultrasonic sound waves that, if reflected by an object, are returned and detected by the sensor itself. (Massa, 1999). For coast-down testing applications, there could be major concerns on detection of undesired objects, given the wide detection area of such sensors. Also, air temperature highly influence measurement accuracy.

(ii) Piezoresistive sensors (Pressure sensors)

Bicycle motion is described by detection in time at finite locations along the coasting field. Candau et al. (1999) used pressure sensors (in the form of pneumatic tubes) for coast-down testing. They are easy to install but they can interfere with the rolling resistance estimation as they introduce local energy losses.

(iii) Photoelectric sensors

Bicycle motion is again described by proximity detection in time at finite locations along the coasting field. Photoelectric sensors can detect distance and presence of an object through transmission/reception of light. Detection, in particular happens through interruption or reflection of a light beam by a moving objects. An important factor to consider for coast-down application is that the bicycle tire moving at typical bicycle speed must be thick enough to obstruct the light source for enough time for receiver's detection.

4.2. Coast-down equipment selection

It appears important to develop a coast-down method with minimal imposition on intercepted cyclists (i.e. nothing to be mount on bicycles). Therefore an "on-roadway" technology is preferred. Photoelectric (also called light-beam sensors) appears to be a good trade-off among "on-roadway" sensors because they do not affect the sought coefficients (as pressure sensors would) and because of small detection beam, it is unlikely that sensor will detect something that is not the targeted bicycle. In general there are three kinds of photoelectric sensors:

(i) Diffuse

Light receiver and emitter are located in the same sensor housing. Detection happens because the receiver is triggered by incoming object's reflected radiation;

(ii) Retro-reflective (reflex)

Light receiver and emitter are located in the same housing. A reflector, placed at a distance in front of the sensor itself, allows for the emitted light beam to be reflected into the receiver. Sensor is triggered when the light beam breaks (i.e. when the receiver does not see any light coming back);

(iii) Through-beam

Receiver and emitter are housed in two different boxes, installed one in front of the other, at a distance. As soon as the emitted radiation is not picked up by the receiver, the sensor registers detection (i.e. something obstructed the light beam).

Categories are listed from the least to the most accurate. Accuracy is mostly influenced by beam angle, different for each model: a diffuse sensor has the largest beam angle, whereas through-beam has the smallest (down to 1.5 degrees). A "beam-through" IR (infrared) photoelectric sensor pair (model SKU: SE-020101, Figure 1) is purchased because of its easiness in orientation an alignment and detection accuracy (small beam angle). The sensor pair was tested with respected to the following conditions:

- It must be compatible with a microcontroller (Arduino MEGA 2560), using a digital or analog pin (5V current);
- It must be easy to position and align in the field;
- It must be fairly insensitive to daylight (i.e. false triggering due to daylight contamination);
- It must be able to detect the very first part of the wheel of a bicycle, i.e. the sensor must have a small reaction time.

The first two requirements were fulfilled by wiring up sensors with the microcontroller and by verifying that sensors have a led indicating “alignment” or not (i.e. if the receiver reads infrared light beam generated by the emitter). The last two requirements are tested in the following two chapters.

Figure 1. Commercial-off-the-shelf, infrared photoelectric “beam-through” sensor pair (model SE-020101), utilized in the coast-down test.

Daylight sensitivity analysis

In order to verify daylight (that is comprised of an infrared component) sensitivity, IR receiver has been exposed to direct daylight, and the voltage output has been measured using analog pin with an Arduino microcontroller. The result of exposure to daylight over a few minutes, varying the exposure angle (i.e. inclination of sensor with respect to daylight source) led to the conclusions that IR sensors can be triggered by daylight. However, triggering happens only in case of perfect alignment with sunlight (i.e. only if receivers are

pointed towards the sun, or a surface that is reflecting sunlight towards the sensor). Since sensors in the field will be installed horizontally, risk of daylight-related false triggering is minimized. Also, as a precaution, receivers will be daylight-shielded using a washer, which will also serve as beam angle reduction for a better alignment.

Response time analysis

In order to perform a response time analysis an experiment was designed and developed. Such experiment aimed to see how fast could an object travel through the IR light-beam and being detected. A cylinder of hard paper, of diameter 4cm (comparable to bicycle tire + rim thickness) was repetitively dropped through the IR beam. This is to mimic a bicycle wheel travelling through the IR sensors in the field. The cylinder was dropped from a relative height Δh, with respect to the height of the IR beams. Energy conservation (in the simplified assumptions of no aerodynamic loss) is enforced according to $m\ g\ \Delta h = \frac{1}{2}\ m\ v_f^2$, where using as Δh 2.15 m, a speed v_f= 6.5 m/s (23.4 km/h) is expected for the cylinder at sensor's height. Such speed is deemed sufficient, as most cyclists do not ride at higher speeds. The test comprised ten cylinder drops and detection was checked using microcontroller's voltage readings. All ten executed drops were detected, deeming the IR light beam (Figure 1) as selected technology in the coast-down experiment.

Other pieces of equipment

(i) Microcontroller

The microcontroller chosen is illustrated in Figure 2. It is an Arduino MEGA 2560, capable of reading both analog and digital input, in the range 0-5V. To allow experimenters checking that equipment worked properly, an LCD-keypad

shield is wired on top. Finally, a microSD breakout was connected to the microcontroller to let the bicycle motion measurements be logged in a .csv format and easily post-processed.

(ii) Anemometer

Outdoor coast-down testing requires dynamic wind measurement. On the market there are three main typologies of anemometer available, being “mechanical”, “hot wire” and “ultrasonic”. The latter measures the time of flight of sonic pulses between emitter and receiver to estimate wind speed and direction. Ultrasonic anemometers can usually achieve very high accuracy, at low wind speed. Also, some models can be interfaced with Arduino microcontroller as it has two 0-5V signal output, one for wind speed and one for direction. For the cost-down test design, a 2D Ultrasonic anemometer (R.M. Young Company, 2004) is selected. The selected model is depicted in Figure 2.

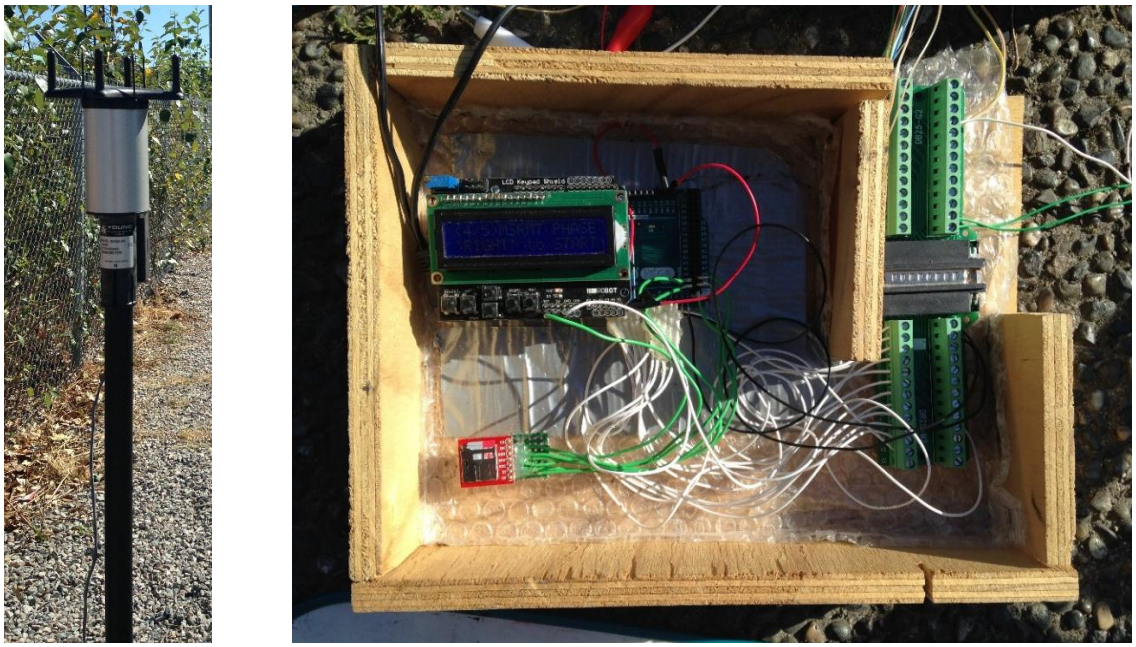

Figure 2. Left: 2D ultrasonic anemometer (Young ltd., model 85000). Right: Microcontroller (Arduino MEGA 2560) with LCD-keypad shield, and microSD breakout in an author's custom-made wooden housing.

4.3. Final equipment configuration: the "12-switch method"

Figure 3 provides an illustration of the test setup and instrumentation. The paired sensors at the start of the test were used to make a comparison with the method in Equation 10 (R. B. Candau et al., 1999). Infrared break-beam sensors were used as timing switches. The 15° default beam angle was reduced using washers on both the emitter and receiver. Response time and cross-interference of the sensors was tested during piloting and found to be sufficient to detect a 4cm diameter rod (approximatively the width of a bicycle tire) at 6.5m/s. Beam-break times were recorded by a microcontroller (Arduino Mega 2560) reading at ≤17µs intervals and logging on a microSD card. For details about microcontroller coding see Appendix D.

Wind speed and direction were measured using an ultrasonic anemometer (R.M. Young Company, 2004) connected to the microcontroller and logged at 1 Hz. Grade was measured every ten meters with an optical level (Leica Jogger 24) and a stadia rod. Break-beam sensors were aligned and positioned using a 100 m measuring tape and a five-point self-levelling laser. All beam heights were set at 0.31 m. For comparison to the 12-switch method, the bicycle was equipped with a cycle computer (Garmin Edge 500) recording distance and speed at 1 Hz (based on wheel revolutions).

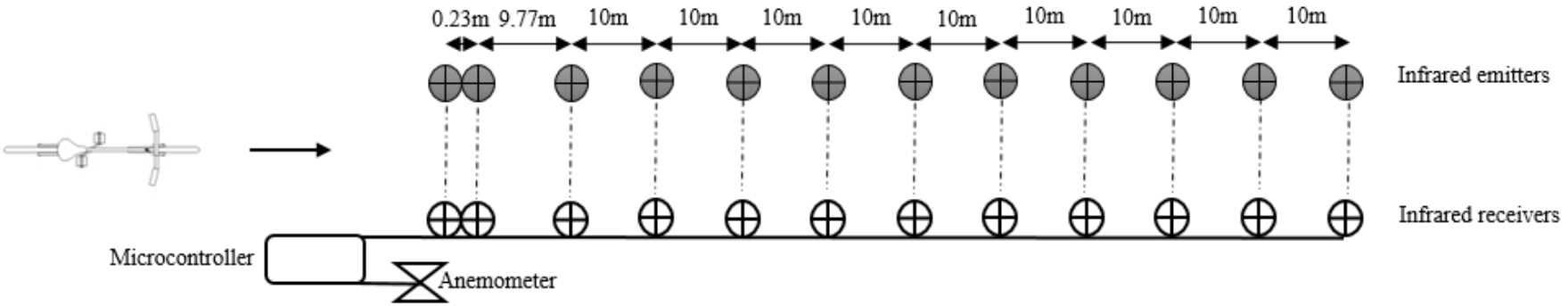

Figure 3. Illustration (top view) of coast-down test setup – not to scale.

4.4. Mathematical Formulation

Our field bicycle coast-down test builds on this past work by introducing dynamic wind and grade variables as well as multiple timing measurements over a longer coasting distance. The motivation for the additional measurements is to try to compensate for the noise expected to be introduced by varying on-road conditions (grade, wind, pavement) as well as to allow parameter estimation from a single test of an intercepted traveller (most previous coast-down testing involved dozens of runs for a single bicycle/rider, which would be a major burden for field intercept surveys). In addition, because the data are collected as $t(x)$, new expressions are derived that provide residuals in the measurement dimension (as opposed to $x(t)$).

Following previous coast-down studies, for an indoor test without wind or grade effects, rolling resistance force R_r is assumed to be independent of speed and drag resistance force R_d is assumed to be proportional to the square of speed (R. B. Candau et al., 1999; de Groot et al., 1995; Kyle & Burke, 1984; Waltham & Copeland, 1999; Wilson & Papadopoulos, 2004):

$$R_r = C_r m g \quad \text{and} \tag{11}$$

$$R_d = \frac{1}{2}\rho A_f C_d v^2 \,, \tag{12}$$

where C_r is a unit-less rolling coefficient, m is mass of bicycle and rider in kg, g is gravitational acceleration in m/s^2, ρ is air density in kg/m^3, A_f is frontal area in m^2, C_d is a unit-less drag coefficient, and v is speed in m/s. The product $A_f C_d$ is known as effective frontal area. Air density is a function of altitude (proxy for barometric pressure) and

temperature (di Prampero, 1986),

$$\rho = \rho_0 \cdot e^{-0.127h} \cdot \left(\frac{273}{T_K}\right) \quad (13)$$

where ρ_0=1.293 kg/m^3, h is the altitude above sea level (km) and T_K is the absolute temperature (°K).

Similar to Equation 7, coast-down resistance forces and deceleration can be formalized

$$m\frac{dv}{dt} = -R_r - R_d = -C_r mg - \frac{1}{2}\rho A_f C_d v^2 \ . \quad (14)$$

Using the simplifying parameters $A = gC_r$ and $B = \frac{1}{2\,m}\rho A_f C_d$, Equation 14 becomes the differential equation:

$$\frac{dv}{dt} = -A - Bv^2. \quad (15)$$

Integration is performed by separating variables and enforcing boundary conditions $v(t_0) = v_0$, leading to

$$v(t) = \frac{v_0 - \sqrt{\frac{A}{B}}\tan\left(t\sqrt{AB}\right)}{v_0\sqrt{\frac{B}{A}}\tan\left(t\sqrt{AB}\right)+1} \quad (16)$$

Then, using $v\frac{dv}{dx} = \frac{dv}{dt}$ and Equation 15, and integrating with the boundary condition $x(v_0) = 0$,

$$x(v) = \frac{1}{2B}ln\left(\frac{A+Bv_0{}^2}{A+Bv^2}\right) \quad (17)$$

Finally, substituting Equation 16 in Equation 17 and rearranging,

$$t(x) = \frac{1}{\sqrt{AB}} atan\left(\frac{\sqrt{AB}v_0 - \sqrt{A^2e^{2Bx} - A^2e^{4Bx} + ABv_0{}^2e^{2Bx}}}{Ae^{2Bx} - Bv_0{}^2}\right), \quad (18)$$

which is the indoor coast-down equation for multiple sensor locations (without wind and grade effects).

Velocity vectors for outdoor test conditions are illustrated in Figure 4, where absolute wind speed w_{abs} and direction α are measured by an anemometer. The apparent wind vector $\overrightarrow{w_{app}}$ is the vector difference between measured wind $\overrightarrow{w_{abs}}$ and bicycle ground speed $\vec{v}$; β is the yaw angle. For outdoor testing with varying wind and grade over x, Equation 12 is revised to

$$R_d = \frac{1}{2}\rho A_f C_d (w_{app} \cdot cos(\beta - \pi))\left|w_{app} \cdot cos(\beta - \pi)\right|. \quad (19)$$

Equation 19 can be rewritten $R_d = \frac{1}{2}\rho A_f C_d (v - w)|v - w|$, where w is wind speed (w_{abs}) in the direction of travel. The absolute value in Equation 19 ensures that the drag force acts in the correct direction when a tailwind exceeds the travel speed, i.e. $v - w < 0$ (Knight, 2008).

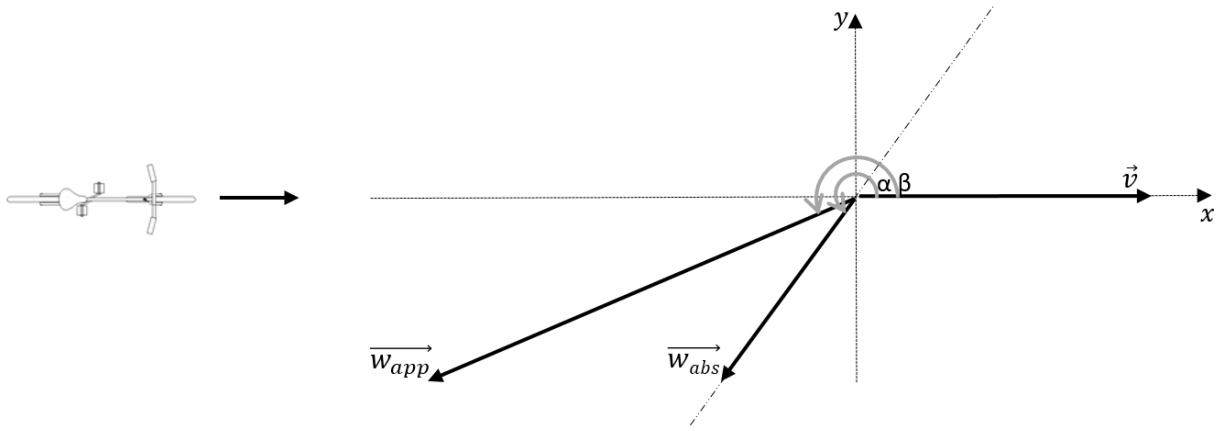

Figure 4. Illustration of speed vectors and angles

Grade resistance is $R_g = \frac{mgG}{\sqrt{1+G^2}}$, which for small grades can be simplified to

$$R_g = mgG \ . \qquad (20)$$

Equation 14 is then revised to

$$m\frac{dv}{dt} = -R_r - R_g - R_d = -mg(C_r + G) - \frac{1}{2}\rho A_f C_d (v-w)|v-w| \ . \qquad (21)$$

Equation 15 becomes the differential equation:

$$\frac{dv}{dt} = -A - gG - B(v-w)|v-w|, \qquad (22)$$

which can be inverted to:

$$\frac{d^2t}{dx^2} = \left(\frac{dt}{dx}\right)^3 \left[A + gG + B\left(\left(\left(\frac{dt}{dx}\right)^{-1} - w\right) \cdot \left|\left(\frac{dt}{dx}\right)^{-1} - w\right|\right)\right] . \qquad (23)$$

For outdoor conditions, G, v, and w all vary over t. Due to the time dependence of these variables and the presence of an absolute value function, no known indefinite integral exists

to generate an analytical solution to Equation 22. Therefore, a numerical, finite element method is used to generate $t(x)$ using Equation 23, starting from the boundary condition $t_0 = 0$, $x_0 = 0$, and $\left(\frac{dt}{dx}\right)_0 = \frac{1}{v_0}$, along with measured data for G and w. For further details about numerical integration of Equation 23 see Appendix D.

Equations 18 and 23 provide methods for generating $t(x)$ from the parameters A, B, and v_0. Parameter estimates $\hat{A}$, $\hat{B}$, and $\hat{v}_0$ are generated by minimizing the sum of square error between the predicted times $t(x)$ and observed times $\tau(x)$ at each measurement location x_i

$$\sum_i [\tau(x_i) - t(x_i)]^2 \, . \qquad (24)$$

Equations 18 and 23 are both highly non-linear, and the solution space contains many local minima. Parameter estimates are generated using a genetic algorithm for floating-point values with local nonlinear search optimization implemented in the statistical software R with the package 'GA' (Scrucca, 2013). Bounds for A and B were set using measured m, $g = 9.81$ m/s^2, ρ according to Equation 13, a C_r range of 0.001 to 0.02, and a $A_f C_d$ range of 0.2 to 1.2 m^2, based on the literature, especially (Wilson & Papadopoulos, 2004). Bounds for v_0 were set at 3 to 6 m/s, during validation testing based on protocol, whereas during intercepted survey based on field observations. The step size for the finite element method was set at 1 m to facilitate reasonable processing time; shorter step sizes were explored for individual tests and found to have no major impact on parameter estimates. The fitness function to maximize was the negative of Expression 24. Additional algorithm parameters were selected based on initial fitting trials: population size 50, maximum iterations 2,000, termination at 150 iterations without improved maximum

fitness, mutation probability 10%, and crossover probability 80%. As an alternative parameter fit for the simpler Equation 18 method, Expression 24 was minimized using a global nonlinear optimization search in MatLab (local solver ‘lsqcurvefit’ run from multiple starting points using ‘MultiStart’).

5. BICYCLE COAST-DOWN TEST VALIDATION

5.1. Indoor and outdoor validation testing

Validation testing was performed in three sessions. The first session was indoors to quantify test performance in a controlled environment (i.e. without wind and grade) and compare instrumentations (3 or 12-switch method, cycle computer). The second and third sessions were performed outdoors on relatively flat terrain in two different wind scenarios (crosswinds/tailwind and headwind) and on two different surfaces.

Indoors testing

Indoor tests were performed on May 29th, 2016 in a flat hallway with smooth concrete at the University of British Columbia. The hallway length limited the test setup to 90 m. Hallway altitude of 81 m and indoor temperature of approximately 20°C yielded air density of $\rho = 1.192$ kg/m^3. An early-model Centurion LeMans road bicycle (approximately 30 years old) was used for the test, equipped with 3 cm commuter tires and two rear panniers. The rider was a 22-year-old male (78.1 kg, 183 cm). The weight of the rider and bicycle was 94.5 kg. Six different tests were performed, with 10-30 runs (coast-downs) each. The tests for all sessions are summarized in Table 1: as an example, " Baseline" test comprised 30 coasting runs, with tires inflated at 80 psi, our volunteer riding in "tops" position (hands on the handlebar top part, as opposed to the hooks; see Figure 5), and aiming to a target initial speed v_0 of 4 m/s (the bicycle was equipped with a cycle computer, so the volunteer could target a speed before stop pedalling and entering the coasting field). The rider on the test bicycle in the test hallway is shown in Figure 5.

Table 1. Test protocols for indoor and outdoor sessions

Test	Number of runs	Tire pressure (psi)	Riding position	Target v_0 (m/s)	Other
Baseline	30	80	Tops	4	-
Mass	10	80	Tops	4	10 kg added to panniers
Tire Pressure	10	40	Tops	4	-
Riding Position	10	80	Drops	4	-
Low Speed	10	80	Tops	3	-
High Speed	10	80	Tops	5	-

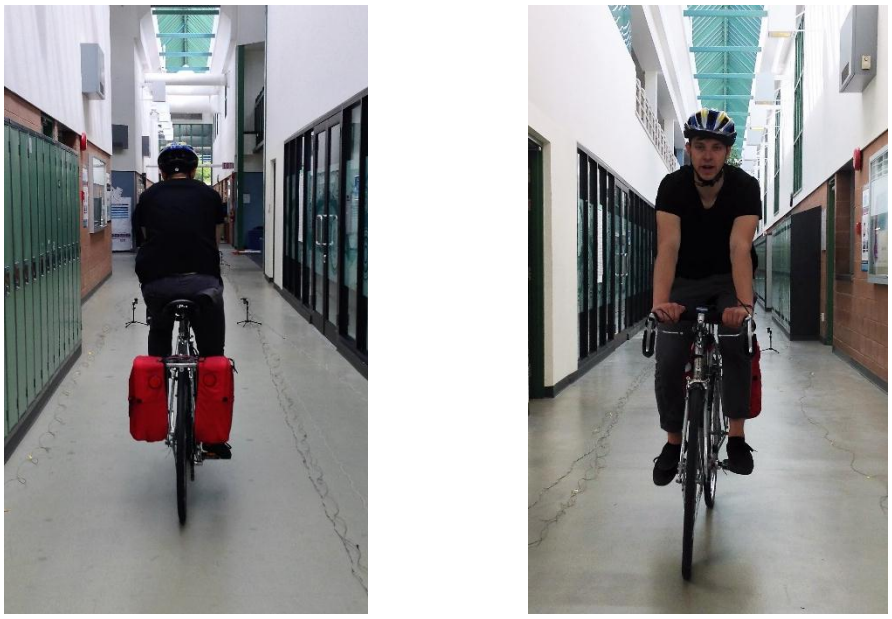

Figure 5. Indoor test rider and bicycle coasting in "tops" position

Outdoors testing

Outdoor tests were performed in two different sessions, the first (session "A") on a running track and the second (session "B") on an asphalt-paved bikeway. Session "B" was

designed to most closely represent typical riding conditions, on a real bikeway surface and with a dominant headwind. Session "A" represents less ideal test conditions, with a dominant tailwind and high-resistance riding surface.

Tests in session "A", were performed on June 24th, 2016 at Memorial South Park in Vancouver, British Columbia. The weather was cloudy, 18°C, with 75% relative humidity and track altitude of 98 m, leading to air density $\rho = 1.197$ kg/m^3. The track surface was a dry polyurethane, notably more rough and soft than the indoor test surface. The same rider, with same clothing and bicycle from the indoor test were used – see Figure 6. At the time of the test, the weight of the rider and bicycle was 95.1 kg. Grade was slightly negative in the first half of the test (minimum of –0.1%) and slightly positive in the second half of the test (maximum of 0.6%).

Figure 6. Rider coasting in "tops" position, outdoor session "A" (top) and "B" (bottom)

Tests in session "B", were performed on August 16th, 2016 on the "North Arm Trail" bikeway in Vancouver, British Columbia. The weather was sunny, 23°C, with 68% relative humidity and at an altitude of 41 m, leading to air density $\rho = 1.186$ kg/m^3. The same rider with similar clothing and a similar bicycle from indoor testing and outdoor testing session "A" were used – see Figure 6 (due to a crash, the LeMans was replaced with a Nishiki Rally road bicycle of similar age and condition, with 3 cm commuter tires and two rear panniers). At the time of the test, the weight of the rider and bicycle was 91.6 kg.

Grade was slightly negative in most of the test (minimum of –0.8%) and slightly positive at the end (maximum of 0.4%).

5.2. Indoor test results

Parameter estimation results for the indoor tests are given in Table 2. The results in the column “12-switch method” use the data from the infrared sensors illustrated in Figure 3, the next column “Cycle computer data” uses the Garmin data as a comparison. Both of these columns were generated using Equation 18. The last column, “3-switch method”, applies Equation 10 to the timing switch data as a comparison with Candau et al. (1999). Only the first 70 m of sensors were used for most of the indoor tests.

Table 2. Indoor test parameter estimates – mean (standard deviation)

	12-switch method			Cycle computer data			3-switch method		
TEST	C_r *[-]*	$A_f C_d$ *[m^2]*	v_0 *[m/s]*	C_r *[-]*	$A_f C_d$ *[m^2]*	v_0 *[m/s]*	C_r *[-]*	$A_f C_d$ *[m^2]*	v_0 *[m/s]*
Baseline	0.0051	0.449	3.99	0.0053	0.407	3.98	0.0062	0.502	4.17
	(0.0001)	(0.0285)	(0.10)	(0.0015)	(0.200)	(0.17)	(0.0003)	(0.0383)	(0.10)
Mass	0.0051	0.465	3.86	0.0047	0.436	3.73	0.0058	0.546	3.99
	(0.0002)	(0.0397)	(0.14)	(0.0015)	(0.216)	(0.14)	(0.0005)	(0.0675)	(0.12)
Tire Pressure	**0.0066**	**0.560**	3.79	0.0057	0.6217	3.68	0.0073	0.604	3.94
	(0.0001)	(0.0344)	(0.08)	(0.0015)	(0.146)	(0.06)	(0.0004)	(0.0716)	(0.09)
Riding Position	0.0052	**0.401**	3.94	0.0055	0.333	3.82	0.0057	0.475	4.06
	(0.0003)	(0.0497)	(0.08)	(0.0003)	(0.0413)	(0.08)	(0.0010)	(0.120)	(0.08)
Low Speed	**0.0046**	0.415	2.77	0.0036	0.712	2.75	0.0053	0.596	2.94
	(0.0002)	(0.0698)	(0.08)	(0.0005)	(0.1250)	(0.08)	(0.0004)	(0.118)	(0.08)
High Speed	**0.0054**	0.473	4.90	0.0062	0.375	4.70	0.0078	0.402	5.04
	(0.0003)	(0.0406)	(0.10)	(0.0013)	(0.131)	(0.13)	(0.0012)	(0.103)	(0.12)

Note: bold values significantly different from Baseline (two-tailed t-test with $p < 0.05$)

Parameter estimates are similar across the three methods in Table 2. Initial speed estimates are consistent with test protocols, and C_r and $A_f C_d$ values are in the range of literature values (Wilson & Papadopoulos, 2004). The 12-switch method provides the best results in terms of reproducibility, i.e. the lowest standard deviations. In addition, sensitivity analyses revealed that standard deviations decrease with test length and increase with sensor spacing.

Parameter estimates are compared across tests for the 12-switch method data using two-tailed t-tests with a significance threshold of $p < 0.05$. The test results reveal significantly higher rolling resistance due to tire deflation ($p < 0.001$ for Tire Pressure vs. Baseline tests) and significantly lower effective frontal area due to riding in a "drop" position ($p = 0.017$ for Riding Position vs. Baseline tests). Parameter estimates were not significantly affected by mass, which is expected ($p = 0.87$ and $p = 0.267$ for C_r and $A_f C_d$ respectively for Mass vs. Baseline tests). However, the C_r estimates were significantly affected by initial speed ($p < 0.001$ for Low Speed vs. Baseline tests and $p = 0.028$ for High Speed vs. Baseline tests), which could reflect a slight increase in C_r with speed, as suggested in some previous research (Wilson & Papadopoulos, 2004). Moreover, $A_f C_d$ estimates were unexpectedly affected by tire deflation ($p < 0.001$ for Tire Pressure vs. Baseline tests), which could be related to a nonlinear positive speed dependence of C_r.

Inspection of the residuals from the initial fit of the indoor validation test revealed spatial correlation across tests, which suggested small ~1 cm errors in the location data (i.e. sensor placement) – see Figure 7. Location correction was performed on the timing switch data according to: $\Delta x_i = \overline{v_{i,j}\ \varepsilon_{i,j}}$, where $v_{i,j}$ and $\varepsilon_{i,j}$ are the speed and time residual at location i in test j. Location corrections had a mean absolute value of 9 mm and a

maximum of 26 mm. The residuals from the parameter fits after location correction are shown in the right of Figure 7. The residual dispersion improved, but the parameter estimates were almost unchanged (<0.2% differences in C_r, $A_f C_d$, and v_0 estimates). The location correction was not applied to subsequent tests due to the negligible effect on parameter estimates and the doubling of the computational cost of fitting parameters (already ten min/test). Furthermore, inspection of residuals from the outdoor testing sessions did not reveal clear spatial correlation.

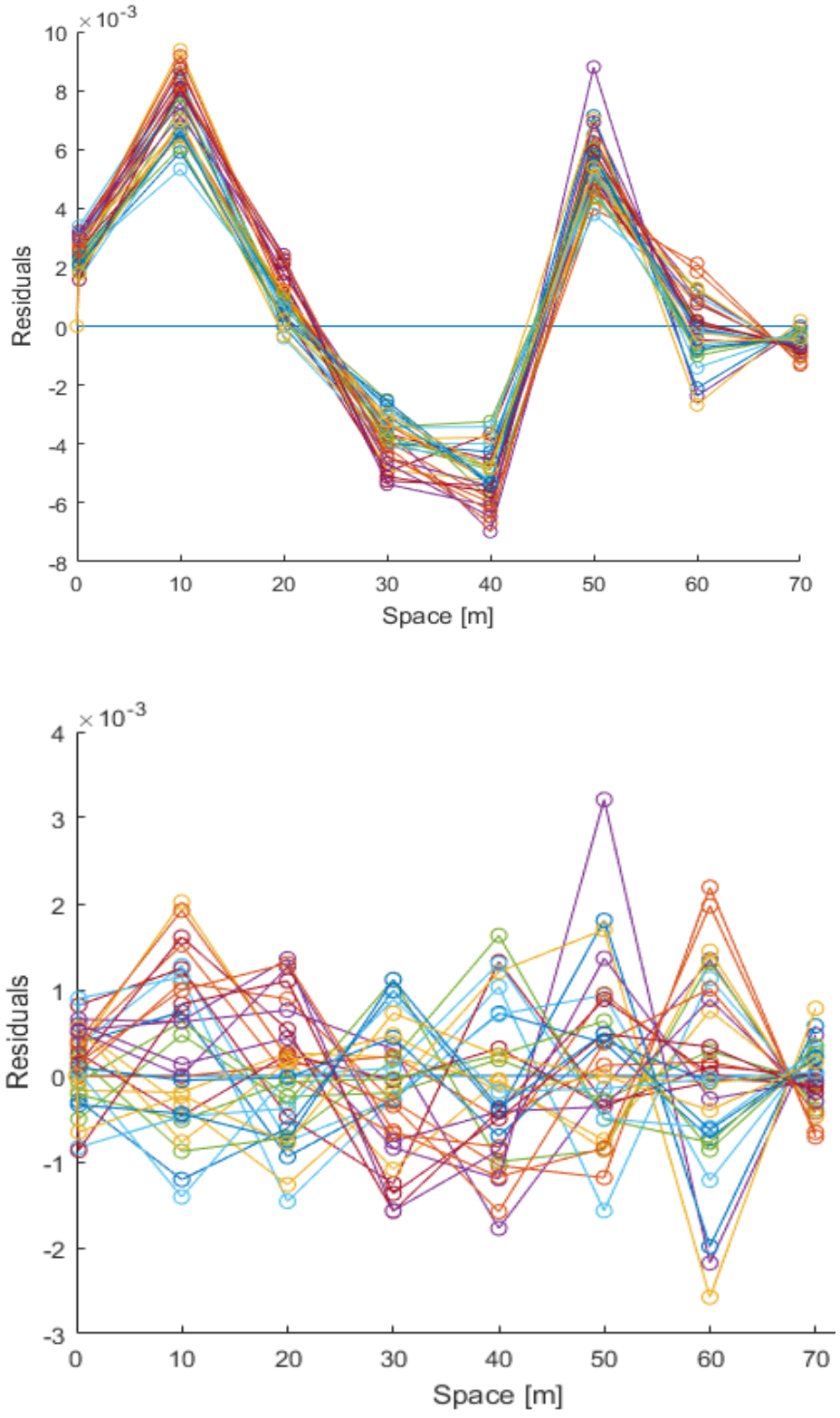

Figure 7. Time residuals before (top) and after (bottom) location correction

5.3. Outdoor test results

Based on the indoor test results, the 12-switch method was used for parameter estimates in the outdoor tests. Parameter estimation results for the outdoor tests are given in Table 3. The parameter estimates in Table 3 show increased variability for the outdoor tests as compared to the indoor tests. Higher variability is expected, due to the influence of varying wind and grade. The outdoor timing switch standard deviations are comparable to those of the cycle computer and 3-switch methods for the indoor tests. The initial speed estimates are again consistent with test protocols and cycle computer data, though the variation is higher than the indoor tests. Both the rolling resistance and effective frontal area parameters are higher than the indoor test results but still in the range of past reported values (Wilson & Papadopoulos, 2004). The higher C_r estimates can be expected from the rougher and softer surface on the running track in session "A" and the rougher asphalt-paved surface in session "B".

Table 3. Outdoor test parameter estimates – mean (standard deviation)

	Outdoor session "A"			Outdoor session "B"		
TEST	C_r *[-]*	$A_f C_d$ *[m^2]*	v_0 *[m/s]*	C_r *[-]*	$A_f C_d$ *[m^2]*	v_0 *[m/s]*
Baseline	0.0102 (0.0011)	0.692 (0.111)	4.25 (0.12)	0.0064 (0.0013)	0.630 (0.114)	3.91 (0.19)
Mass	**0.0116** (0.0008)	0.654 (0.0815)	4.28 (0.08)	0.0061 (0.0011)	0.567 (0.0984)	4.03 (0.14)
Tire Pressure	0.0098 (0.0011)	**0.793** (0.0839)	4.24 (0.11)	**0.0084** (0.0016)	0.594 (0.109)	3.87 (0.11)
Riding Position	0.0108 (0.0007)	0.670 (0.152)	4.29 (0.13)	0.0063 (0.0008)	**0.539** (0.0638)	3.96 (0.16)
Low Speed	0.0099 (0.0006)	0.736 (0.0638)	3.37 (0.13)	0.0057 (0.0012)	0.623 (0.163)	2.99 (0.16)
High Speed	0.0107 (0.0012)	0.676 (0.0726)	4.90 (0.14)	0.0062 (0.0014)	0.640 (0.105)	4.71 (0.19)

Note: bold values significantly different from Baseline (two-tailed t-test with $p < 0.05$)

The higher outdoor $A_f C_d$ estimates are likely due to the influence of real-world wind conditions as compared to the relatively still-air hallway. Previous wind tunnel tests and computational fluid dynamics simulations showed that crosswinds can increase effective frontal area due to increased frontal exposure (Fintelman, Hemida, Sterling, & Li, 2015; Fintelman, Sterling, Hemida, & Li, 2014). In addition, because the drag force is non-linear with respect to relative air speed $v - w$, wind speed and direction variability (within the 1 sec sampling frequency) would increase R_d and $A_f C_d$. Drag coefficient C_d generally varies with Reynolds number, particularly when apparent wind speed is below 10 m/s (Debraux et al., 2011; Defraeye, Blocken, Koninckx, Hespel, & Carmeliet, 2011), which could also lead to higher R_d and $A_f C_d$ in outdoor wind conditions. Crosswinds can also lead to small movements by the bicyclist to adjust for varying lateral drag force (Fintelman et al., 2014), which could increase deceleration and estimated $A_f C_d$.

To illustrate the wind direction differences between tests, Figure 8 shows the distribution of apparent wind speed and direction during the two outdoor sessions, separated into high (>3 m/s), medium (1.5-3 m/s), and low (<1.5) bicycle speed (v) ranges. Due to a dominant absolute crosswind/tailwind direction (α) during session "A", as bicycle coasting speed decreased the apparent wind direction (β) shifted away from a headwind. In contrast, session "B" had a dominant headwind direction (α), which led to a more stable yaw angle (β) around 180°. The influence of crosswind on effective frontal area is supported by higher $A_f C_d$ estimates with greater yaw angle (crosswind) in session "A" than "B". The still-air hallway had essentially no crosswind, and the lowest $A_f C_d$ estimates.

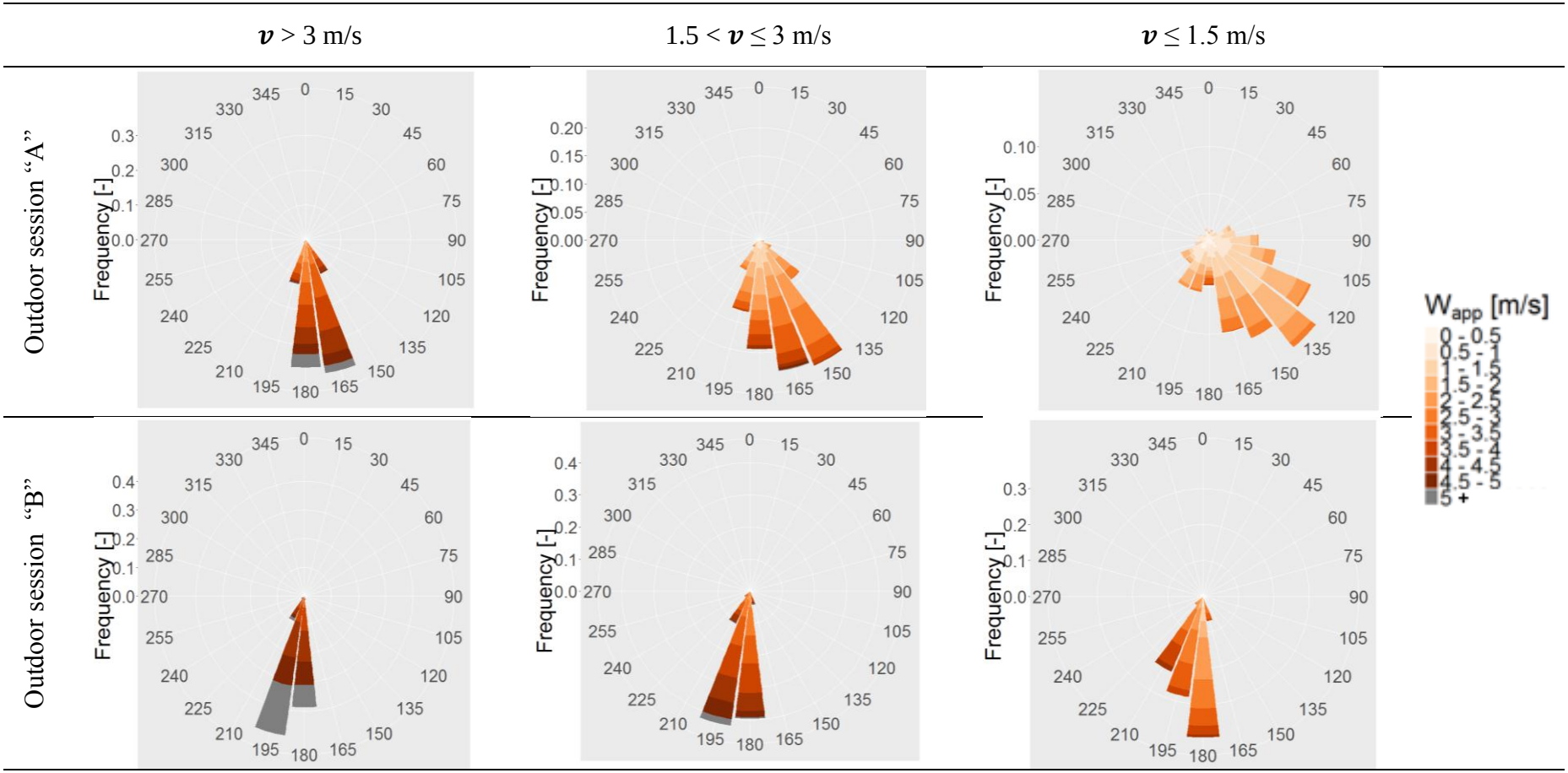

Figure 8. Apparent wind speed and direction (β) for three bicycle speed intervals (left: v>3 m/s; centre: 1.5<v≤3 m/s; right: v≤1.5 m/s) in outdoor sessions "A" (top row) and "B" (bottom row)

Outdoor parameter estimates are compared across tests using two-tailed t-tests with a significance threshold of $p < 0.05$. Parameter comparisons across tests for Session "B" are all in line with expectations. Rolling resistance was significantly higher after tire deflation ($p < 0.001$ for Tire Pressure vs. Baseline tests), effective frontal area was significantly lower riding in a "drop" position ($p = 0.031$ for Riding Position vs. Baseline tests), and parameter estimates were not significantly affected by mass ($p = 0.583, p = 0.136$ for C_r and $A_f C_d$ respectively in test Mass vs. Baseline) or initial speed ($p = 0.158$ and $p = 0.891$ for C_r and $A_f C_d$, respectively for Low Speed vs. Baseline tests, and $p = 0.720$ and $p = 0.808$ for C_r and $A_f C_d$, respectively in High Speed vs. Baseline tests). In contrast, session "A" generated the unexpected results that rolling resistance was significantly higher with added weight ($p = 0.025$ for Mass vs. Baseline tests) and effective frontal area was significantly higher after tire deflation ($p = 0.012$ for Tire Pressure vs. Baseline tests). These results are possibly due to the very soft riding surface, on which C_r could vary with mass and speed. Another consequence of the softer riding surface was shorter coasting distances for session "A" (typically between 60 and 70 m) than for session "B" (consistently the full 100 m), which generated fewer observations per test.

5.4. Validation summary

The novel outdoor *in situ* field coast-down test expands on past methods by accounting for varying wind and grade and allowing for more measurement locations per test. The 12-sensor outdoor test achieves comparable precision to a 3-sensor indoor test method, thus partially offsetting the effects of increased variability in outdoor conditions with increased observations per test.

Rolling resistance coefficient estimates were 0.0051 ±0.0001, 0.0064 ±0.0013, and 0.0102 ±0.0011 for tests on smooth concrete (indoors), asphalt pavement, and a polyurethane running track, respectively. Effective frontal area estimates were 0.45 ±0.03 m^2, 0.63 ±0.11 m^2, and 0.69 ±0.11 m^2 for tests in still air (indoors), in a headwind, and in varying crosswind/tailwind, respectively. The parameter estimates are in line with expectations, and demonstrate the importance of crosswind for aerodynamic drag resistance. The indoor test and the outdoor test on a hard surface with a dominant headwind were sufficiently sensitive to identify significant changes in resistance with tire pressure and riding position. The outdoor test in less ideal conditions (soft surface and varying apparent wind direction) was not sufficiently sensitive to these changes, revealing some limitations and constraints for outdoor testing.

Ultimately, if the parameters will be used to estimate on-road bicyclist energy expenditure and speed, the outdoor estimates in a dominant headwind (e.g. session "B") are expected to be the most representative. Indoor $A_f C_d$ estimates will likely be too low due to still air test conditions. Parameter estimates from outdoor tests with varying apparent wind direction (e.g. session "A") are less reliable and likely less representative of drag resistance at normal travel speeds.

The findings in this chapter will be useful in experimental design and estimation of measurement error for implementing field coast-down tests in traveller intercept surveys. Parameters standard deviations of 0.001 for C_r and 0.1 m^2 for $A_f C_d$ should be sufficient to characterize the broad range of urban bicyclists. Best estimates are expected if the tests are performed in headwind conditions that yield realistic yaw angles for normal travel speeds, and the riders start with enough speed to coast the full 100 m. Even if indoor testing is

possible, the resulting parameter estimates might not be representative of on-road cycling in varying wind conditions.

For further validation, future work should compare measured power output on an instrumented bicycle with modelled power based on indoor and outdoor test results. In addition, outdoor test results should be compared with wind tunnel testing. Application of the field coast-down test is expected to generate new information about the physical characteristics of real-world bicyclists, which will improve operations and microsimulation models and yield better understanding of on-road bicycle performance as seen in the following chapters.

6. CYCLISTS INTERCEPTED SURVEY

The objective of this chapter is to provide transportation researchers and practitioners with representative distributions of physical parameters for real-world urban cyclists that can readily be used in advanced bicycle travel modelling. Measured rolling and aerodynamic resistance parameter distributions for intercepted cyclists are presented, including fits to theoretical distributions. Additional measured physical parameters are also presented (tire pressure and width, bicycle and cargo weights, etc.), as well as an analysis of correlation among physical characteristics.

6.1. Design

The survey was designed so that socio-demographic and preferences of intercepted cyclists could be gathered to compare this study sample with other surveys in Vancouver, and to investigate relationships between resistance parameters and other physical characteristics as well as cyclist attributes, preferences and habits. To minimize the burden to intercepted cyclists and to make the study more appealing, the questionnaire (see Appendix B) was designed using user friendly Likert-scale and formulating questions as clearly as possible. Also, questions such as comfort on bicycle infrastructures were included to the benefit of cyclist classification according to a famous city of Portland, Oregon, classification (Dill & McNeil, 2013). As per UBC Ethics Board requirement, participants fulfilled a content form (see Appendix A) before taking part in the survey. Appendix C illustrates the sheet used by experimenters to note all the bicycles and cyclists related physical characteristics required by the study.

6.2. Field test administration

The coast down-test was administered to intercepted cyclists over 18 days in summer 2016 at 9 locations in Vancouver, Canada. Table 4 and Figure 10 provide testing session details. Locations were chosen based on flatness (grade approximatively null), uninterrupted length (at least 100 m long plus 20-30 m for acceleration), and accessing cyclists in a variety of contexts (university, downtown, waterfront paths, and residential areas). Data collection days were all weekdays (Monday-Friday), chosen based on experimenter availability and meteorological conditions (low probability of rain). Data collection times ranged from mid-day to early evening (approximately 12:00 to 19:00) to target peak and off-peak travellers. High-volume locations (over 3,000 bicycle trips per summer-weekday) were avoided during peak periods to minimise disruption on busy bicycle facilities and avoid participant queues (four experimenters together could process at most around 15 participants per hour). Figure 9 illustrates typical appearance of surveys stations.

Figure 9. Typical bicycle coast-down survey stations.

Table 4. Coast-down test location characteristics.

Date	Time	Location	Facility type	Sample size	Bicycle volume*	Mean (range) of grade in %
Tu 6/28	11:30-15:00	UBC	Path	10	not available	0.6 (0.4;1)
Th 6/30	11:30-15:00	UBC	Path	12	not available	0.6 (0.4;1)
We 7/06	13:00-16:00	York Ave	Cycle-track	22	2,475	-0.4 (-0.9;0.2)
We 7/13	12:00-16:30	Ontario North	Path	48	5,464	-0.1 (-0.9;0.4)
Fr 7/15	12:30-17:00	Science World	Path	20	3,985	0.2 (-0.6;0.9)
We 7/20	12:30-16:00	Ontario South	Cycle-track	10	442	0.3 (-0.4;0.9)
Th 7/21	12:00-16:30	Union St	Cycle-track	38	3,558	0.5 (-0.6;2.7)
Fr 7/22	12:00-16:00	Sunset Beach	Path	38	1,650	-0.1 (-2.6;0.7)
Mo 7/25	14:30-17:00	North Arm Trail	Path	11	229	0.3 (-0.9;0.8)
We 7/27	15:00-19:00	Ontario North	Path	59	5,464	-0.1 (-0.9;0.4)
Fr 7/29	15:00-17:00	York Ave	Cycle-track	29	2,475	-0.4 (-0.9:0.2)
Th 8/04	15:00-19:00	Union St	Cycle-track	50	3,558	0.5 (-0.6;2.7)
Fr 8/05	14:30-18:00	Expo Blvd	Cycle-track	34	1,379	0.6 (0.1;1.6)
We 8/10	16:00-19:00	Expo Blvd	Cycle-track	19	1,379	0.6 (0.1;1.6)
Th 8/11	15:00-19:00	Sunset Beach	Path	44	1,650	-0.1 (-2.6;0.7)
Fr 8/12	15:00-18::30	Science World	Path	45	3,985	0.2 (-0.6;0.9)
Tu 8/16	14:30-17:00	North Arm Trail	Path	10	229	0.3 (-0.9;0.8)
We 8/17	12:30-16:00	Ontario North	Cycle-track	58	5,464	-0.1 (-0.9;0.4)

* Bi-directional summer weekday average in 2012 (Acuere Consulting Inc., 2013).

Figure 10. Coast-Down test locations map.

Cyclists were first contacted with signage one block in advance of the testing area, followed by research team members with university branding, juice, and snack bars. After providing consent (see Appendix A), participants completed a 3-page questionnaire (see Appendix B) with socio-demographic and trip-related questions. Simultaneously, participant bicycle characteristics were measured (see Appendix C) by the research team (make, model, and year, number of gears, tire pressure, tire width, weight, and cargo). Bicycle type was categorised as "road" (drop handlebars, thin smooth tires), "mountain" (flat handlebars, large knobby tires, suspension), "hybrid" (flat handlebars, medium tires),

"cruiser" (cruiser handlebars, large smooth tires, upright seating position), and "other" (including e-bikes, tandems, and cargo bikes). Bicycles were weighed with any attached cargo due to participant reluctance to remove cargo in pilot testing. Participants were next instructed in performance of the coast-down test as follows:

(i) Accelerate up to a conformable, typical riding speed by the chalk-marked "stop pedalling line";

(ii) Coast, without pedalling or braking, along a dashed line chalk-marked every few meters throughout the coasting field;

(iii) Stop in case coasting speed becomes too low to proceed safely, or upon reaching the chalk-marked "end line".

(iv) Participants who braked, pedalled, swerved, or had some other observed violation of the test protocol were asked to re-perform the test.

6.3. Sample size and data filtering

Of 648 cyclists who gave consent to participate in the study, resistance parameters were successfully estimated for 557 (86%). Of the 91 (41%) discarded, 3 reported insufficient time to complete the test, 13 tests failed because of instrumentation issues (sensor power loss), 11 tests had an insufficient coasting length (<50m), and 64 tests yielded poor parameter fitting results (sum of square error over 1 second, or resistance parameters at bounds). Poor fit results could have been due to unobserved violations of testing protocols (braking, swerving, etc.). Wind was not an issue for any of the tests because of high initial speeds (average 6.4 m/s, standard deviation 1.1 m/s) and relatively

low-wind days so that apparent wind was within ±45° of the direction of motion for all tests (Tengattini & Bigazzi, 2017).

7. PHYSICAL CHARACTERIZATION RESULTS

7.1. Sample statistics and correlation analyses

Figure 11 summarises age and sex for the sample. Of the 557 participants, 348 were male, 188 were female, and 21 preferred not to state their sex. Excluding who did not provide their sex, the sample comprised 65% males, and 35% females. The average participant age was 40 (standard deviation 15, range 6-80). Table 5 shows age and gender for the sample and for cyclists in the Vancouver metropolitan area based on a 2011 household travel survey (TransLink, 2013). The sample is generally representative of the broader survey data, but with fewer youth under 18, and more females.

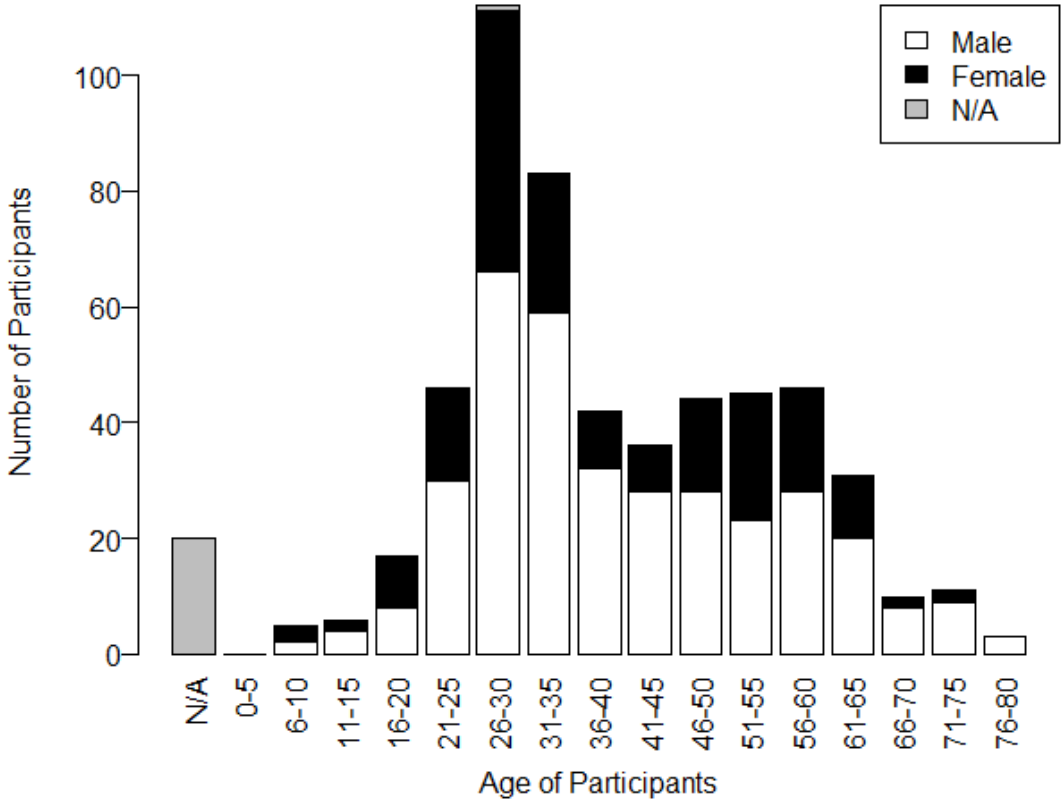

Figure 11. Participants by age and gender. N/A – Not Available.

Table 5. Age and sex in the study sample versus cyclists in a regional household travel survey.

	Range	Metro Vancouver, 2011*	This Study
	[-]	[%]	[%]
Age	5-12	8	1.5
	13-17	8	1.2
	18-24	5	8.8
	25-44	47	51.2
	45-64	28	30.2
	65-79	3	5
	80+	0	0.2
	Missing	-	2
Sex	Male	71	62
	Female	29	35.7
	Missing/Other	-	2.3

*(TransLink, 2013)

Figure 12 shows the distributions of participant and bicycle masses. Female cyclists rode heavier bicycles with more cargo, despite lower body weight. Bicycles with cargo were on average 4.6 kg heavier than bicycles without cargo. The average (standard deviation) of cyclist and cyclist + bike + cargo masses were 74.7 (15.4) and 92.2 (16.2) kg, respectively. Participant height was used to calculate Body Mass Index (BMI), defined as $mass/height^2$, with an average of 24.4 in the upper range of normal (standard deviation of 3.8).

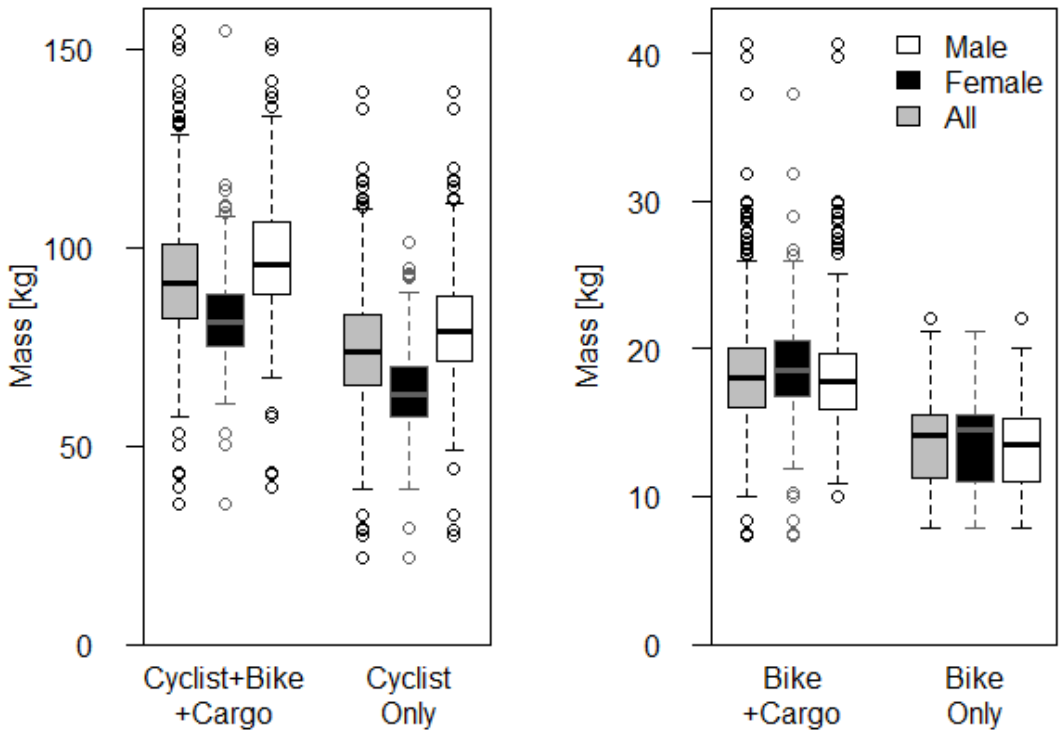

Figure 12. Boxplots illustrating participant, bicycle, and cargo mass by sex. Box height is the Inter Quartile Range (IQR), line in the box is median.

Rolling resistance parameter C_r averaged 0.0077 with a standard deviation of 0.0036 (95% Confidence Interval ±0.0003). Effective frontal area, $A_f C_d$, averaged 0.559 m^2 with a standard deviation of 0.170 m^2 (95% Confidence Interval ±0.014 m^2).

Figure 13 shows resistance parameter distributions by gender, revealing wide ranges of values, but without significant differences by gender (further examined below).

Summary statistics for measured physical characteristics are presented in Table 6. Sample sizes vary because not all participants consented to all questions or measurements.

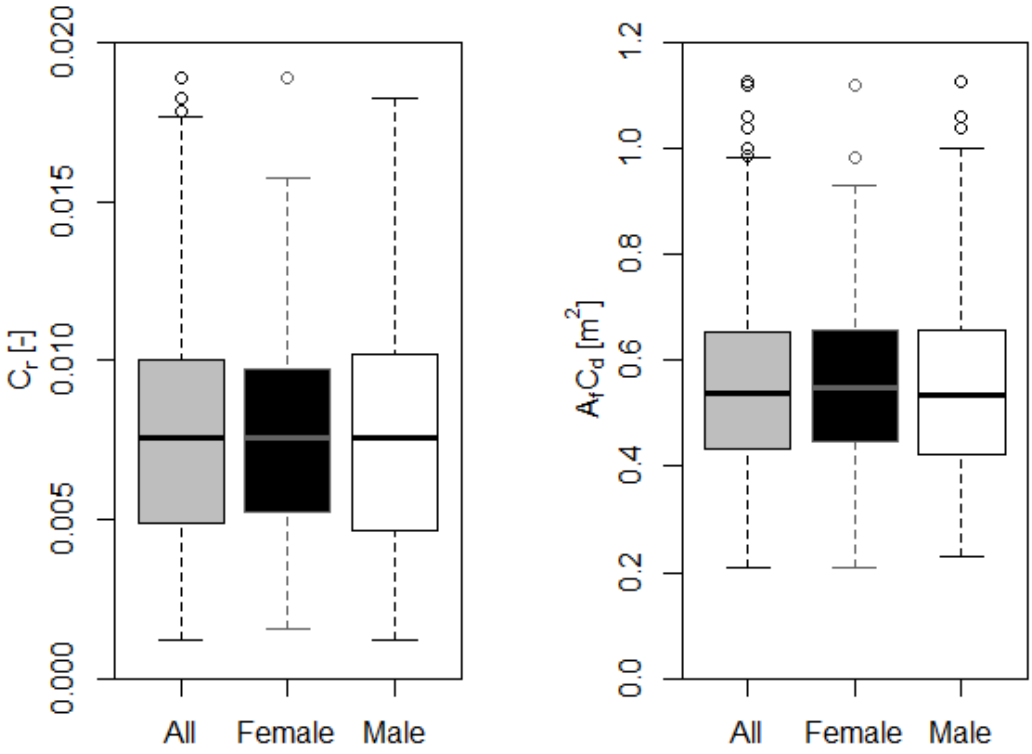

Figure 13. Boxplots illustrating Rolling and Drag resistance parameters by sex. Box height is the Inter Quartile Range (IQR), line in the box is median.

Table 6. Physical Characteristics sample statistics.

Parameter	Minimum	1st Quartile	Median	3rd Quartile	Maximum	Mean	Standard deviation	N
Cyclists+Bicycle+Cargo Mass [kg]	35.4	82.0	90.9	100.9	154.7	92.2	16.2	552
Bicycle+Cargo Mass[kg]	7.3	16.0	18.0	20.0	40.7	18.3	4.1	423
Bicycle Mass [kg]	7.8	11.4	14.2	15.5	22.0	13.7	3.3	118
Cyclist Mass [kg]	21.9	65.0	73.5	83.0	139.0	74.7	15.4	552
BMI [kg/m^2]	15.8	22.0	23.8	26.3	45.0	24.4	3.8	513
Cr [-]	0.0012	0.0049	0.0076	0.0100	0.0189	0.0077	0.0036	557
$A_f C_d$ [m^2]	0.209	0.434	0.539	0.655	1.128	0.559	0.170	557
Front Tire Pressure [kPa]	55	234	317	431	872	347	154	553
Back Tire Pressure [kPa]	48	234	317	445	876	352	157	553
Front Tire Width [cm]	2.0	2.8	3.3	4.2	9.6	3.5	0.9	553
Back Tire Width [cm]	2.0	2.8	3.3	4.2	9.6	3.5	0.9	553
Bicycle Year [-]	1945	2005	2009	2014	2016	2006	10	505
Bicycle Gears [-]	1	14	21	24	30	19	8	502

Resistance parameters are positive by definition, finitely bounded, and positively skewed (moment coefficient of skewness of 0.47 for C_r and 0.58 for $A_f C_d$), so Weibull and Gamma distributions were fit to observed data, using Maximum Likelihood estimation with the "fitdistrplus" software package in R (Delignette-Muller & Dutang, 2015). Visual inspection (Figure 14) and five test statistics (Kolmogorov-Smirnov, Cramer-von Mises, Anderson-Darling statistics; Aikake's Information Criterion and Bayesian Information Criterion) were used to select the most appropriate distributions. Measured rolling resistance coefficient, C_r, values were better approximated by a Weibull distribution (shape and scale parameters $k_w = 2.28$, $\lambda_w = 0.00874$), while effective frontal area parameter, $A_f C_d$, values were better approximated by a Gamma distribution (shape and rate parameters $\alpha_\Gamma = 10.99$ and $\beta_\Gamma = 19.68$).

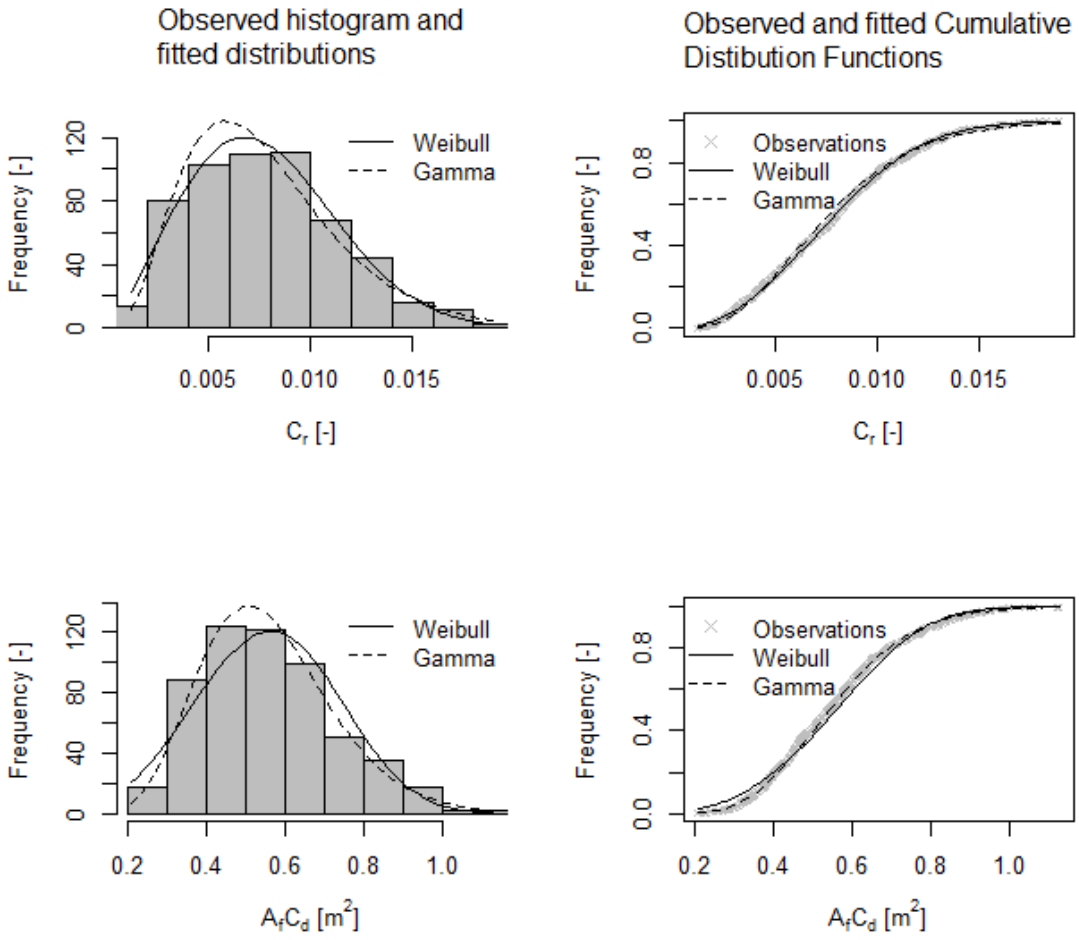

Figure 14. Resistance parameter observed and fitted distributions.

Measured resistance parameters and masses are segmented by categorical variables in Table 7. Most cyclists rode in "tops" position (typical for flat handlebars); "drops" is the typical aerodynamic position, and "hoods" is a position in between the two. Fewer cyclists wore sport clothing (i.e. tight cycling shorts and jersey) than those who wore casual clothing. About half the participants had "commuter" tires, with a medium texture compared to smooth "slick" tires and "knobby" treaded tires.

Table 7. Measured resistance parameters and masses, segmented by categorical variables, with mean (standard deviation) and [Sample Size]*.

Parameters	Category					
	I	II	III	IV	V	
Gender	**Male [348]**	**Female [188]**				**NA [21]**
C_r [-]	0.0077 (0.0038)	0.0077 (0.0033)				
$A_f C_d$ [m^2]	0.559 (0.175)	0.56 (0.161)				
Cyclist+Bike+ Cargo Mass [kg]	97.7 (15.4)	82.1^{I} (13.2)				
Cyclist Mass [kg]	80.5 (14.3)	63.9^{I} (11.5)				
Riding Position	**Drops [22]**	**Hoods [90]**	**Tops [438]**			**NA [7]**
C_r [-]	0.0056 (0.0032)	0.0061 (0.0029)	0.0081^{I,II} (0.0036)			
$A_f C_d$ [m^2]	0.463 (0.13)	0.477 (0.122)	0.579^{I,II} (0.173)			
Cyclist+Bike+ Cargo Mass [kg]	92.9 (13.8)	89.8 (14.6)	92.5 (16.6)			
Cyclist Mass [kg]	76.8 (12.8)	75.3 (13.3)	74.5 (16.3)			
Cyclist Apparel	**Sport [78]**	**Casual [477]**				**NA [2]**
C_r [-]	0.0063 (0.0032)	0.0079^{I} (0.0036)				
$A_f C_d$ [m^2]	0.486 (0.145)	0.570^{I} (0.170)				
Cyclist+Bike+ Cargo Mass [kg]	87.5 (13.9)	92.9^{I} (16.4)				
Cyclist Mass [kg]	72.6 (13)	75.1 (16.1)				
Tire type	**Slick [137]**	**Commuter [273]**	**Knobby [138]**			**NA [9]**
C_r [-]	0.0070 (0.0035)	0.0074 (0.0033)	0.0092^{I,II} (0.0039)			
$A_f C_d$ [m^2]	0.498 (0.148)	0.579^{I} (0.172)	0.576^{I} (0.174)			
Cyclist+Bike+ Cargo Mass [kg]	89.9 (14.7)	93.3 (15.6)	92.3 (18.5)			
Cyclist Mass [kg]	75.1 (13.9)	75.3 (15.4)	73.9 (18.0)			
Bicycle type	**Road [225]**	**Hybrid [181]**	**Mountain [90]**	**Cruiser [37]**	**e-bike [7]**	**NA [17]**
C_r [-]	0.0070 (0.0034)	0.0079^{I} (0.0035)	0.0089^{I,II} (0.0041)	0.0078 (0.0039)	0.0103 (0.0042)	
$A_f C_d$ [m^2]	0.505 (0.135)	0.579^{I} (0.176)	0.603^{I} (0.187)	0.64^{I} (0.179)	0.614^{I} (0.210)	
Cyclist+Bike+ Cargo Mass [kg]	91.5 (14.5)	91.1 (15.9)	93.3 (18.3)	93.7 (16.0)	106.3^{I,II,III} (11.0)	
Cyclist Mass [kg]	75.8 (13.9)	73.5 (16.4)	75.1 (17.8)	74.0 (16.1)	74.2 (9.5)	

* Two-sample, two-sided, Kolmogorov-Smirnov tests for differences by category; Roman numeral superscripts indicate the comparison categories for which significant difference were found ($p < 0.05$).

Non-parametric Kolmogorov-Smirnov tests were used to examine differences in C_r, $A_f C_d$ and m by category; results are included in Table 7 with Roman numerals indicating comparison categories for which significant difference were found ($p < 0.05$). Participants riding in tops position had significantly higher resistance parameters, likely due to the drag effect and correlation with other bicycle characteristics (such as larger, knobbier tires). Cyclists wearing casual clothing had significantly higher resistances and overall mass. As expected, knobby tires were associated with significantly higher in C_r. Cyclists with slick tires had significantly lower drag parameters, likely due to association with riding position. Bicycle type differences also reflect associations with other characteristics (riding position, tire type, etc.). E-bikes had significantly higher overall mass and $A_f C_d$. Resistance parameters were not significantly different by gender. Presence of a helmet (for 79% of participants, not included in the Table 7) was not associated with any significant differences in C_r, $A_f C_d$, or m.

Figure 15 shows correlations significantly different from zero (at $p < 0.05$) among continuous variable characteristics. The highest correlations are for front/back tire pressures and widths, which is expected because they are likely of the same type and inflated simultaneously. Tire pressures and widths are negatively correlated, also expected because thin tires (usually for sport cyclists) are inflated to higher pressures. Age is positively correlated with number of gears, mass, and BMI. Number of gears is also correlated with bicycle year, meaning that newer bicycles have more gears.

As for resistance parameters, the correlations in Figure 15 indicate that rolling resistance coefficient decreases with tire pressure, as expected (Wilson & Papadopoulos, 2004). An increase in tire width increases C_r as well, probably due to negative correlation

between tire width and pressure. Aerodynamic drag depends on the frontal area and shape of the cyclist and bicycle. Effective frontal area was significantly positively correlated with overall mass (including cargo), age, and BMI, a measure of body "slenderness" of participants (Debraux et al., 2011). In addition, $A_f C_d$ was negatively (positively) correlated with tire pressures (widths), likely due to the indirect effect of bicycle type, as seen in Table 7. A positive correlation between C_r and $A_f C_d$ (0.04) was not significant ($p = 0.36$).

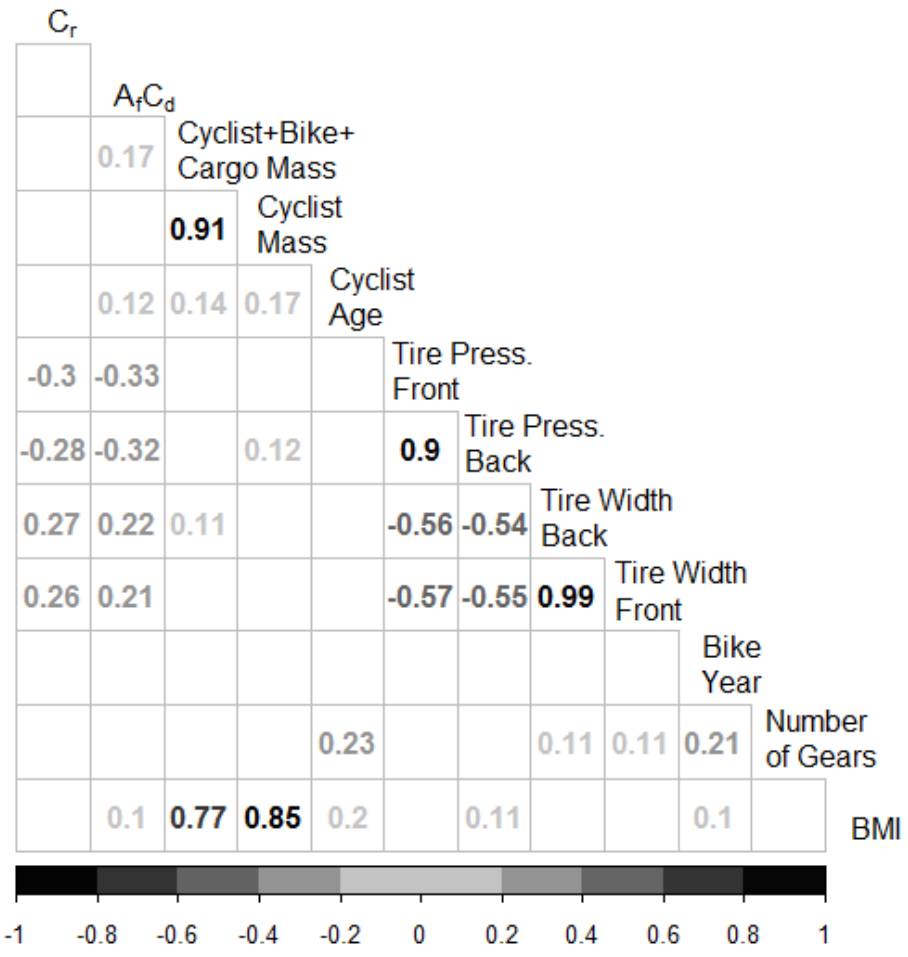

Figure 15. Correlation matrix (Pearson's linear correlation) of measured physical characteristics. Values shown are significantly different from zero at $p < 0.05$.

7.2. Discussion of results

The measured resistance values in this study show that real-world urban cyclists have a very wide range of physical characteristics. Two published sources report typical values for a range of vehicles, measured with different techniques, but no known study reports systematic measurements from a sample of real-world in-use bicycles. Gross et al. (1983, pp. 150–151) report ranges for C_r of 0.003-0.014 and for $A_f C_d$ of 0.31-0.56 m^2 for "standard bicycles", and $C_r = 0.006$ and $A_f C_d = 0.56$ m^2 for an "upright commuter" bicycle. Wilson & Papadopoulos (2004, pp. 188, 215) reports ranges for C_r on smooth surfaces of 0.002-0.010 and for $A_f C_d$ of bicycles ranging from recumbents to upright commuters of 0.04-0.63 m2. They also report $C_r = 0.006$ and $A_f C_d = 0.63$ m^2 for a typical upright cyclist. The measured values in this study generally agree with the limited information available in the literature, but observed distributions are wider than previously suggested ranges, especially on the upper end of values. A summary is available in Table 8.

Table 8. Resistance estimates comparison with available literature.

Studies	Ranges		"Upright Commuter"*	
	C_r	$A_f C_d$	C_r	$A_f C_d$
	[-]	[m^2]	[-]	[m^2]
Gross et al. (1983, pp. 150–151)	0.003-0.014	0.31-0.56	0.006	0.56
Wilson (2004, pp. 188, 215)	0.002-0.010	0.04-0.63	0.006	0.63
This study	0.002-0.02	0.2-1.2	0.008	0.56

* "Upright commuter" is an estimate for a typical urban rider (Gross et al., 1983; Wilson & Papadopoulos, 2004). Mean values from this thesis survey are given for "This study".

Correlations among measured physical characteristics show consistency with expectations and literature. Tire pressure is negatively correlated with C_r, while tire width and knobby tire type are positively associated with C_r. More upright riding position, casual clothing, and BMI are positively associated with $A_f C_d$. More generally, resistance

parameters are significantly higher for cyclists on non-road bikes (more than half the sample) than on road bikes.

The results in this chapter can improve understanding of on-road bicycle performance for a realistic range of urban travellers. The main physical characteristics in this study, C_r, $A_f C_d$, and m, can be used in advanced bicycle travel models to estimate speed, power, and energy expenditure of cyclists, applicable to geometric design, speed choice and route choice modelling, health and safety impact assessments, and more. Using the reported parameter distributions, these estimates can be applied in probabilistic designs and stochastic models. Simulations could sample from these distributions to generate synthetic travellers with realistic ranges of physical characteristics. The statistical comparisons above provide insights that could be used to select context-sensitive values for assumed cyclist parameters.

Existing literature suggests narrower and lower ranges of cyclist parameter distributions. Applying lower ranges could lead to under-estimates of cyclist power and energy, and over-estimates of cyclist speeds, which would be non-conservative in many applications. Major studies including cyclist physical characteristics are encouraged to perform similar testing to determine the attributes of the sample or population of interest.

This study characterised cyclists in Vancouver, Canada during summer and results may not be applicable in other contexts. Cities with significantly different bicycle mode shares would likely have different populations of cyclists. Other countries might have substantially different bicycle fleets, such as more cruiser-style bikes in Northern Europe or more mountain bikes in South America. Another limitation is that rolling resistance was only measured on dry pavement; effects of wet weather were not assessed.

The next chapter will investigate relationships between physical characteristics and other travel and traveller attributes, such as socio-demographics, trip type, and route preferences. Relationships between resistances and travel preferences (mode, route, speed) could reveal systematic differences relevant to policy, network, and infrastructure design. Other future work should conduct similar intercept studies in other locations for cross-city comparisons of cyclist physical characteristics.

8. THREE PHYSICAL URBAN CYCLIST TYPOLOGIES: ASSOCIATIONS WITH PREFERENCES AND HABITS

This chapter aims to categorize the cohort of cyclists intercepted in the survey presented previously, by using cluster analysis to discern three physical-based typologies, to explore relationships with cycling preferences and habits. Typologies are based on observed physical attributes of the bicycle and cyclist (see Appendix C). The analysis indicates that cycling efficiency, perceptions, preferences, and habits are related, to physical typology in a complex but consistent manner. Usage of more efficient bicycles might result in higher cycling rates as a result of an internal feedback effect. Physical typologies might help unveiling active travel behaviour and encouraging urban cycling by a wider range of people.

8.1. Motivation

Cycling in urban environments has been fostered by many cities around the world because it benefits to individuals and the environment (de Hartog, Boogaard, Nijland, & Hoek, 2010; Fox, 1999; David Rojas-Rueda, Nazelle, Tainio, & Nieuwenhuijsen, 2011). As the number of cyclists grows, there is the need to develop more sophisticated bicycle travel models, comprising behavioural, safety, health, and microsimulation models. Cyclist energy expenditure and power output modelling is important for realistic bicycle travel modelling, because cycling is a physical activity (Bigazzi & Figliozzi, 2015b).

In chapter 6 an extensive data collection in Vancouver, Canada, has been carried out, where distributions of cyclist physical characteristics were measured. Cyclist characterisation is manifold. Firstly, it comprises measurement of bicycle resistances, namely rolling resistance coefficient C_r (unit-less), and aerodynamic resistance parameter

$A_f C_d$ (m^2), often referred as effective frontal area. Secondly, it includes measurement of cyclist, bicycle and cargo masses, together with other parameters such as tire pressure and width, riding position, and cyclist apparel, all parameters that were observed to affect resistances. Lastly, other non-physical cyclist parameters, such as socio-demographics (e.g. sex, age, income, education), preferences (e.g. comfort on bicycle infrastructures), and habits (e.g. transport modes use, weekly physical activity) were collected as well.

C_r, $A_f C_d$, and m have an explicit role in modelling cyclists power output, whereas other cyclists physical characteristics (e.g. riding position, tire pressure, cargo, etc.) contribute implicitly as they affect either C_r, $A_f C_d$, m, or a combination of them (Burke, 2003b; Wilson & Papadopoulos, 2004). Socio-demographics, preferences and habits might be also correlated with physical characteristics. Investigating such correlations might be important to understand underlying systematic patterns among cyclists and be able to model power output from indirect sources (i.e. without actual measurement of mass and resistances). Also, it could be the ground for policy development aiming to foster cycling (Damant-Sirois & El-Geneidy, 2015; Dill & McNeil, 2013; Gatersleben & Haddad, 2010).

This chapter explores weather within the cohort of urban cyclists, systematic typologies can be discerned based on simple cyclist and machine physical attributes (e.g. tire type or riding position). If so, also, significant relationships among cyclists typologies and (i) C_r, $A_f C_d$, m (and therefor power output); (ii) cycling preferences and (iii) habits will be explored.

To pursue the objective, survey data collected in the previous chapter are used. Cluster analysis is employed to find cyclists physical typologies. Cluster-to-cluster

comparisons determine significant differences in resistances parameters, habits and preferences.

8.2. Method

Measurable physical cyclist attributes are used as input parameters in a cluster analysis to determine whether such characteristics can be used to group the cohort of cyclists and to unveil latent systematic differences among groups of cyclists. The study follows this steps:

(i) Determination of a physical typology of cyclists based on cluster analysis of observed physical attributes;

(ii) Examination of relationships between cyclist types and:

  (a) Resistance parameters C_r, $A_f C_d$, and equipment mass m (bicycle + cargo), which relate to power output and energy expenditure;

  (b) Cyclist attitudes and preference, such as comfort on different types of facility;

  (c) Travel habits, such as cycling frequency and seasonality.

Survey and sample description

In 2016, in Vancouver, Canada during 18 summer days, at 9 locations the physical characteristics of cyclists were measured in a survey presented in the previous chapter. The survey comprised four main parts. Firstly, an interested cyclist (usually enticed to participate in exchange of refreshments) was instructed about survey's protocol and invited to sign a consent form. Upon signing, a cyclist became a survey's participant. Overall, 648 cyclists signed the consent form. Secondly, a participant was asked to fulfill a

questionnaire. The purpose was to gather socio-demographics, trip information, transport preferences and travel behaviour of participants. The second part usually happened simultaneously with the third one, which involved measurement of physical cyclists and bicycle characteristics, but for resistance parameters. For example, mass, cargo, tire pressure, tire width, riding position were measured/observed and recorded. Lastly, the participant was invited to take the coast-down test. The test involved coasting from a cursing speed to a stop over 100 m of a flat stretch of paved bikeway, while time sensors were recording bicycle motion. From the data collected by the sensors, resistances parameters could be extrapolated by fitting the coast-down equation (Tengattini & Bigazzi, 2017). The questionnaire was administered in hard-copy. It comprised three main parts. The first one regarded trip information (i.e. origin, destination, purpose, trip length/distance). The second included both travel habits and preferences questions. The last part included socio-demographics like sex, age, income and gender. The majority of the answers were formulated in a "checkbox" form (Likert-type scale). For example, a level of comfort question would be answered using four checkboxes, with a gradually increasing meaning, such as "very uncomfortable", "uncomfortable", "comfortable", "and very uncomfortable". Other answers were left free, especially ones related to socio-demographics questions. Figure 16 illustrates that the collected sample compares well with a Vancouver metropolitan area 2011 household travel survey (TransLink, 2013), in terms of age, sex and income, but with fewer youth, more females, and fewer high income (75k-100k CAD) people. K-S tests for income and age, and χ^2 for sex proved insignficant difference in the two samples ($p > 0.9$).

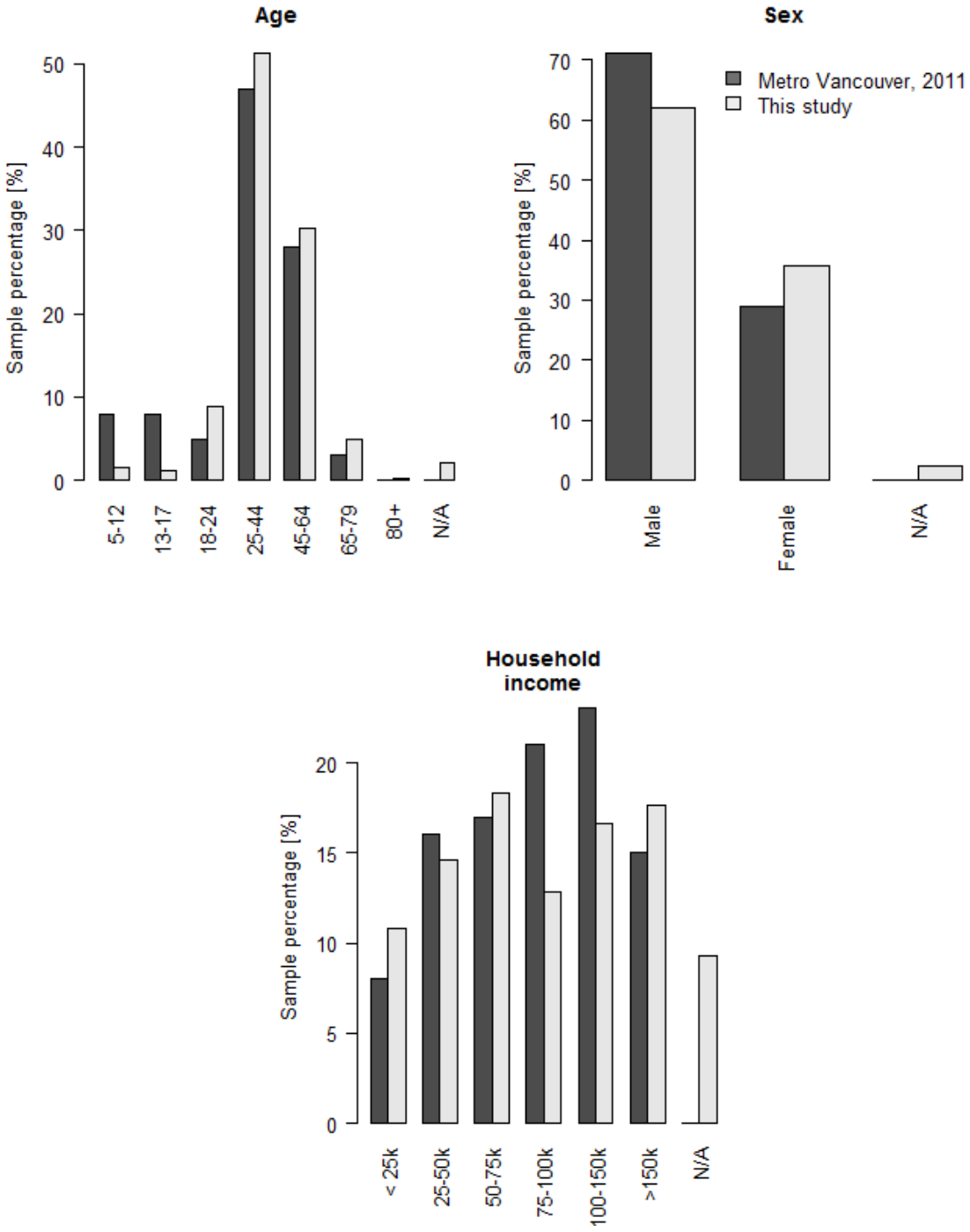

Figure 16. Sample size comparison with a Metro Vancouver survey in 2011 (TransLink, 2013)

Cluster and statistical analyses

Cluster-based grouping of riders is performed using only observed physical attributes assessed by experimenters during the survey, as opposed to other information that was stated by the participant, leading to more objectivity. Variables used are both categorical and continuous in nature. Categorical variables comprises Bicycle Type (Road, Hybrid, Mountain, Cruiser, and Other); Tire Type (Slick, Commuter, and Knobby); Cyclist Apparel (Sport, and Casual); and Riding Position (Drops, Hoods, and Tops). Continuous variables comprised Tire Pressure, Tire Width, Number of Cargo Pieces.

Cluster analysis was performed in the environment R using "cluster" and "fcp" packages (Hennig, 2015; Maechler, Rousseeuw, Struyf, Hubert, & Hornik, 2016). Because of the heterogeneity of variables' nature, a meaningful dissimilarity matrix cannot be computed using classic Euclidean metric. Instead, Gower metric (Gower, 1971) was used and k-medoid clustering was performed, where k is the number of clusters. Maximization of the mean of average silhouette width for growing k (Reynolds, Richards, Iglesia, & Rayward-Smith, 2006) is used to reveal the optimum cluster number, which is found to be three. Each variable used to generate cluster will be examined as to characterize composition and attach physical meaning to the three clusters.

Resistances parameters (C_r, $A_f C_d$, and m), cycling preferences, and habits, which are not used to generate clusters, will be analysed, so to see if there are systematic relationships between clusters (i.e. physical cyclists typologies) and all the aforementioned variables. Non-parametric Kolgoromov-Smirnov (K-S) and chi-squared (χ^2) tests are used to test significant differences of continuous and categorical variables, respectively, among the three clusters.

8.3. Clustering results and associations

Physical typologies

As seen in Chapter 7, Of 648 participants, 91 coast-down tests were discarded (mainly due to poor fit), so resistance parameters for 557 participants were successfully computed. However, because not all participants consented to all measurements used in the cluster analysis, 531 data points were used. Figure 17 shows clusters data point membership along the first two principal components.

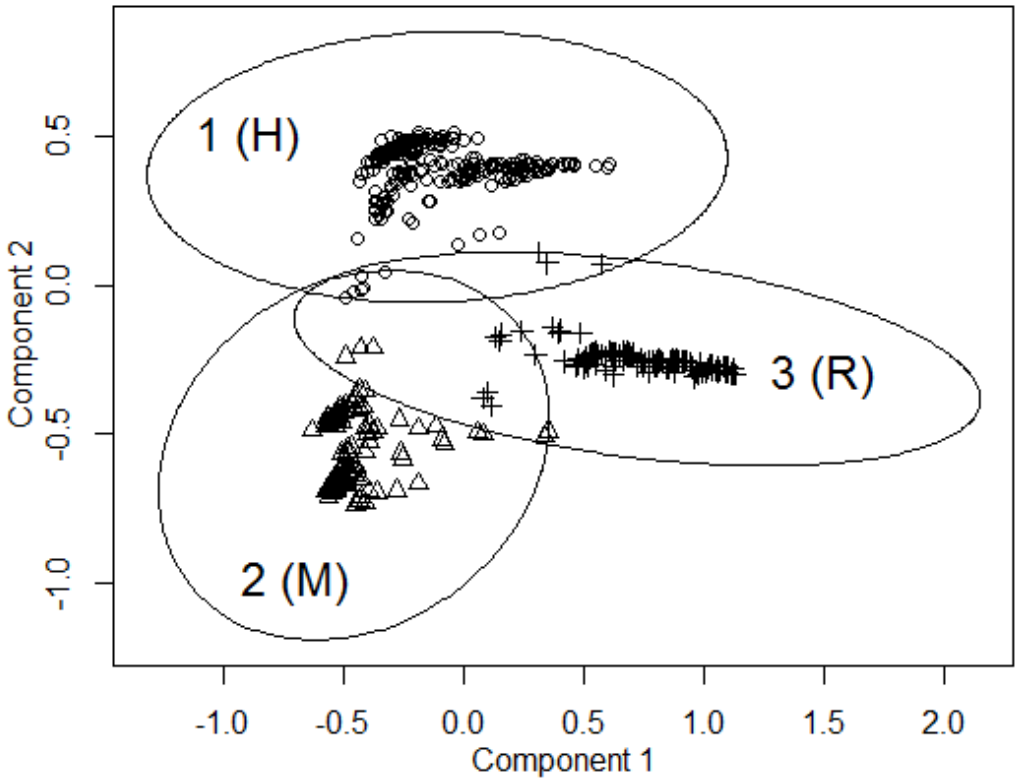

Figure 17. *k*-medoids clustering output with respect to two principal components. Visible is cluster number and (name).

To attach physical meaning to each cluster,

Figure 18, Figure 19 show a cyclist's physical characteristic share in each cluster. Statistical tests are used to check significant difference in parameters distribution among clusters. Tyre types, pressure and width (

Figure 18) are all significantly different among all clusters ($p<0.001$). In Figure 18, bicycle type is shown and it is significantly different among all clusters ($p<0.001$). Also, riding position is significantly different ($p<0.05$) among clusters. Cyclist apparel and number of gears are both significantly different ($p<0.001$) only among cluster 1-3, and 2-3. Number of cargo pieces is not significantly ($p>0.6$) different among clusters.

In the interests of convenience and clarity, cluster number one, two, and three (as per Figure 17) are re-named Hybrid-styled cyclist (H), Mountain-styled cyclist (M), and Road-styled cyclist (R). Cluster size is 270, 133, and 128 for cluster H, M, and R, respectively. Cluster's names are derived from the major (>50%) bike type per cluster, as seen in Figure 18. Generally speaking, bicycles are designed for different riding conditions and purposes, so it is expected to see systematic correlations among physical characteristics, hence the suitability for cluster analysis. For example, cluster M is comprised by more than half Mountain bikes, it is largely characterized by knobby, wide and low-pressure tires, and mainly ridden in tops positions. On the other hand, cluster R includes almost exclusively highly pressurized, slick, thin tires. Also, almost half of such cyclists rode in drops or hoods positions.

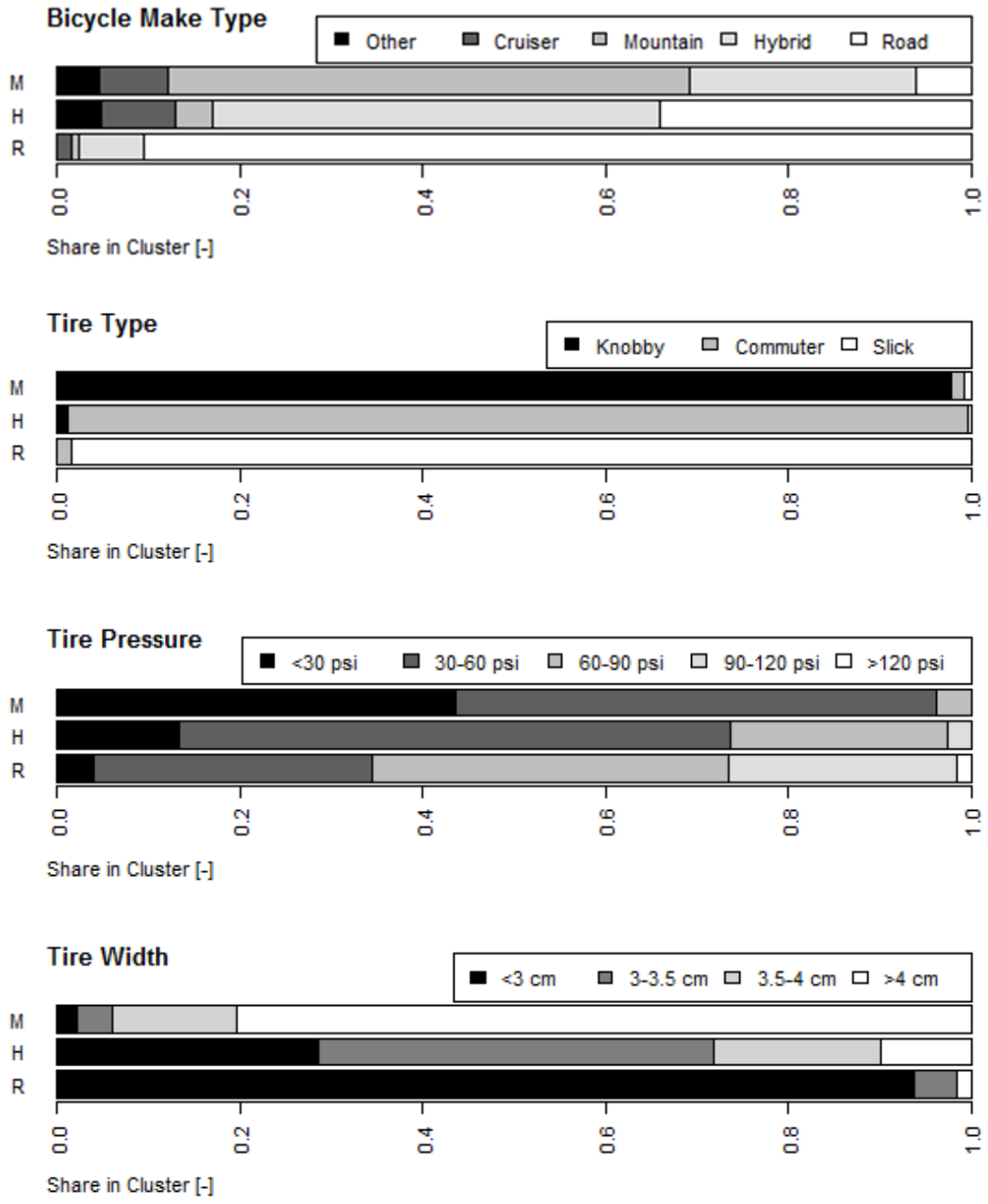

Figure 18. Bicycle characteristics by cluster.

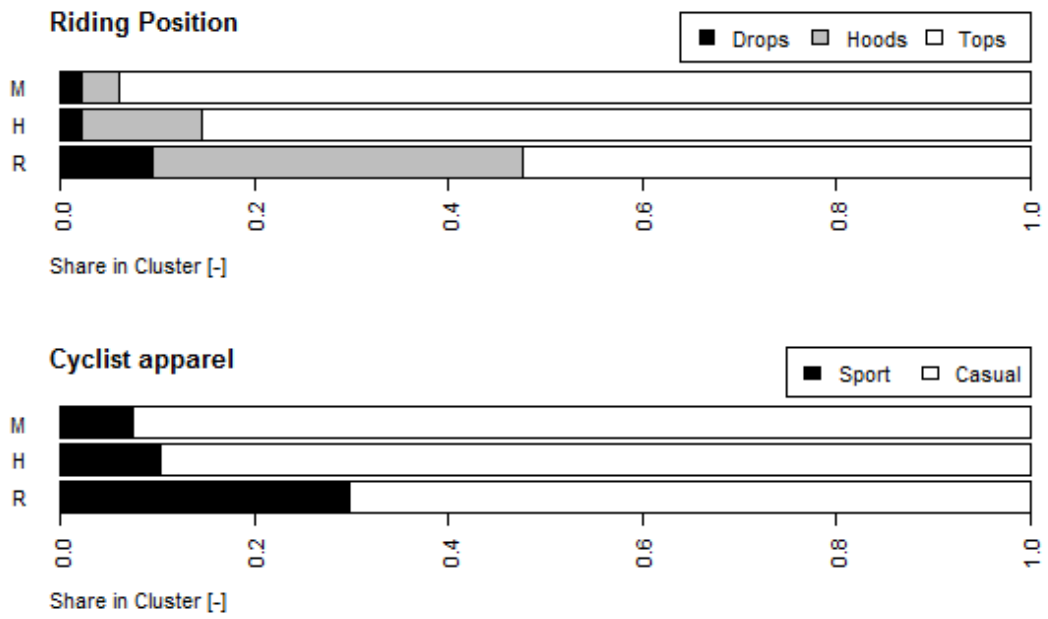

Figure 19. Cyclist characteristics by cluster.

Physical typology relationships with day or location of sample data collections were investigated, resulting in insignificant differences (p≥0.1). Sex difference among physical typologies was also insignificant (p>0.4), as well as cyclist body mass (p>0.45). Other socio-demographic participant characteristics revealed significant differences among clusters, as illustrated in Table 9. In particular, in our sample, lower income are more likely to be M members. Not reported in Table 9 is a less significant ($p \leq 0.10$) difference, for "level of education", where M-type is significantly lower than R and H.

Table 9. Socio-demographics mean and (standard deviation) per cluster. Subscripts indicate the comparison categories for which significant difference were found with K-S tests ($p \leq 0.05$)

	R	H	M
Age	37.25 (12.63)	41.00^{R} (14.95)	38.65 (15.63)
Household income [CAD]	92,415 (51,039)	93,879 (54,182)	$78{,}491^{R,H}$ (57,063)
Household size	2.34 (1.08)	2.49 (1.31)	2.57 (1.31)
Number of motorized vehicle in household	2.03 (0.77)	2.12 (0.87)	2.07 (0.91)
Level of education*	3.78 (0.91)	3.84 (1.1)	3.48 (1.27)

*1-"high school or less", 5-"master's or doctorate degree"

Relationships with resistances parameters

Typologies outlined in the previous chapter suggests there might be some difference in resistances parameters. As found in previous chapters and (Wilson & Papadopoulos, 2004) rolling, drag and mass parameters were significantly correlated with physical characteristics such as tire pressure, width, and riding position. Figure 20 shows differences in resistances per physical typology (i.e. cluster). Table 10 illustrates that for C_r, $A_f C_d$, and equipment mass significant ($p \leq 0.001$) differences between R and M clusters are always found.

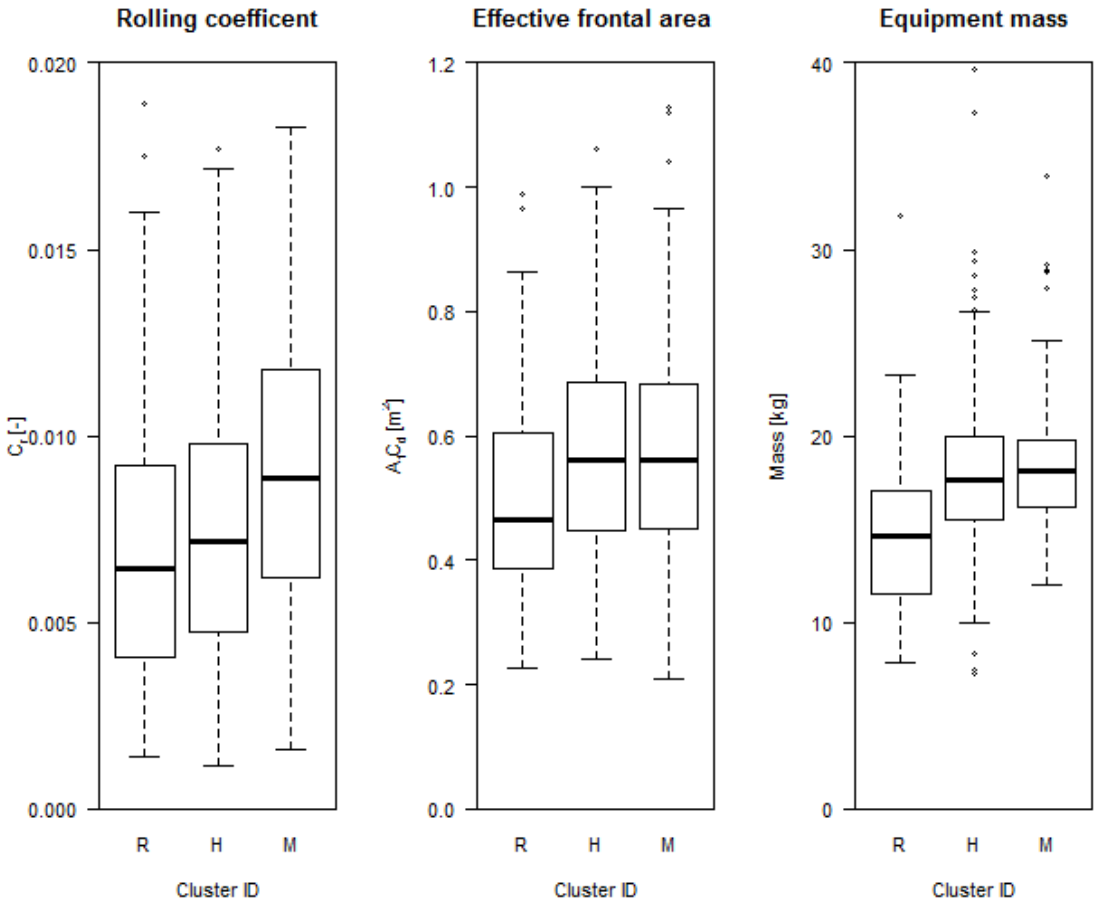

Figure 20. . Boxplots illustrating rolling, aerodynamic coefficients and equipment mass by cluster. Box height is the Inter Quartile Range (IQR), line in the box is median.

Table 10. Resistances mean and standard deviation per cluster. Superscripts indicate the comparison categories for which significant difference were found with K-S tests ($p \leq 0.001$).

	R	H	M
C_r [-]	0.0069 (0.0035)	0.0074 (0.0034)	$0.0092^{R,H}$ (0.0039)
$A_f C_d$ [m^2]	0.495 (0.148)	0.577^{R} (0.171)	0.579^{R} (0.178)
Cargo+Bike mass [kg]	14.6 (4.1)	18.5^{R} (6.2)	18.4^{R} (3.5)

Relationships with cycling preferences and attributes

Cycling preferences and attributes comprises variables presented in Table 11 and were obtained using a questionnaire filled by each participant. Interestingly, a clear trend, although not always significant, can be seen across physical typologies where R type cyclists seem less concerned about mixed-traffic cycling condition than M type. M-type of cyclists stated to be significant less comfortable than R-type when no physical separation is present on major streets. Also, the gain in comfort can be related to the perception of physical activity enjoyment that makes cycling a less stressful activity. "Would bike more" is short for the question "I would like to travel by bicycle more than I do now" and interestingly R type cyclists would bike more than others probably because they enjoy physical activity more and consider cycling as a physical activity. Not reported in Table 11 is a less significant ($p \leq 0.10$) difference for "stated bicycle maintenance conditions", where M-type have a self-reportedly less maintained bicycles, if compared to R and H.

Table 11. Mean (standard deviation) preferences and perceptions responses per typology. Superscripts indicate the comparison categories for which significant difference were found with K-S tests ($p \leq 0.05$).

		R	H	M
	Stated bicycle maintenance conditions*	3.02 (0.89)	3.02 (0.75)	2.8 (0.81)
	Would cycle more**	3.87 (1.11)	3.78 (1.12)	3.67 (1.23)
	Cycling is a form of exercise**	4.63 (0.75)	4.56 (0.8)	4.33 (1.07)
	Physical Activity Enjoyment**	4.75 (0.6)	4.68 (0.71)	4.54 (0.99)
Comfort*** on	Path - away from motor vehicles	3.9 (0.31)	3.89 (0.39)	3.8 (0.51)
	Local st. - low traffic and speeds	3.8 (0.4)	3.65 (0.58)	3.7 (0.48)
	Major st. w/ physical separation	3.57 (0.68)	3.46 (0.68)	3.39^{R} (0.71)
	Major st. w/ painted separation	3.29 (0.69)	3.03 (0.79)	2.94^{R} (0.81)
	Major st. w/o any separation	2.43 (0.95)	2.11^{R} (1.02)	2.06^{R} (0.91)

* 1-"poor", 4-"excellent".
** 1-"strongly disagree", 5-"strongly agree".
*** 1-"very uncomfortable", 4-"very comfortable".

Relationships with cycling habits

Table 12 illustrates habits participant responses per physical typology. None of the travel mode or bicycle by purpose habits revealed significant difference among typologies. Interestingly a significant difference is found in the type of cyclist, therefore we are able to link physical typology to cyclist behaviour. Findings show that R-type of cyclists (i.e. "efficient" riders) are significantly more likely to belong to "confident & enthused" or "strong and fearless" than if they were part of the M-type (i.e. "inefficient"). This relationship is probably a consequence of significantly higher comfort in mixed traffic of

R-type cyclists and them being significantly more “year-round” cyclists. This information it’s of primary importance as having a more efficient bicycle (like R type) can be related to more cycling and with more confidence.

Self-reported intercepted-trip distance and time did not reveal any significant difference among physical typologies. Also, self-reported intercepted trip purpose did not show significant difference, however, R type had the highest share of commuters, whereas M were mostly recreational.

Table 12. Mean (standard deviation) habits responses per typology. Superscripts indicate the comparison categories for which significant difference were found with K-S tests ($p \leq 0.05$).

		R	H	M
Mode usage*	Private vehicle (driver or passenger)	2.88 (1.21)	2.73 (1.36)	2.71 (1.45)
	Car share (driver or passenger)	1.68 (0.87)	1.56 (0.9)	1.39^{R} (0.75)
	Taxi	1.42 (0.62)	1.41 (0.68)	1.37 (0.64)
	Public transit	2.56 (1.03)	2.68 (1.11)	2.93 (1.23)
	Bicycle and e-bikes	4.56 (0.73)	4.34 (1.06)	4.23 (1.01)
	Walk	4.16 (1.1)	4.26 (1.13)	4.07 (1.26)
Cycling by purpose [day/mo]	Commuting	14.5 (10.35)	13.79 (10.84)	12.48 (10.67)
	Shopping	11.12 (8.55)	10.51 (8.86)	10.17 (9.72)
	Recreational	10.18 (8.66)	8.83 (8.5)	11.15 (9.47)
Other habits	Year-round cyclist**	3.94 (1.32)	3.72 (1.42)	3.42^{R} (1.45)
	Typical self-reported speed***	2.56 (0.57)	2.18^{R} (0.61)	2.1^{R} (0.68)
	Moderate Physical Activity [hrs/wk]	4.86 (1.87)	4.63 (1.91)	4.7 (1.9)
	Vigorous Physical Activity [hrs/wk]	4.27 (2)	3.24^{R} (2.15)	3.27^{R} (2.22)
	Equivalent Physical Activity [hrs/wk]****	12.46 (2.69)	11.15^{R} (3.15)	11.16^{R} (3.29)
	Type of cyclist*****	1.79 (0.71)	1.64 (0.72)	1.49^{R} (0.69)

* 1-"almost never", 5-"almost daily".

** 1-"strongly disagree", 4-"strongly agree".

*** 1-"slower than most cyclists", 3-"faster than most cyclists".

**** Computed as (moderate physical activity) + 2(vigorous physical activity).

***** 0-"no way, no how", 1-"interested but concerned", 2-"confident & enthused", 3-"strong and fearless". Deduced from other responses according to Dill & McNeil (2013)

8.4. Discussion of findings

This study explicates associations among purely physical grouping of cyclists and cyclists socio-demographics, resistance parameters, preferences and habits. Overall, considering R, H, and M typology, in order, a consistent shift in participants' characteristics and responses can be seen, but not always significant as per Table 10, Table 11, Table 12.

Firstly, resistance parameters are significantly lower for R members, if compared to H and M. Implications are mainly related to power output modelling which has uses in ventilation, speed, and route choice models (Bigazzi, 2017; Bigazzi & Figliozzi, 2015b; Mercat, 1999b; Mueller et al., 2015b). In fact, more fine-detailed analysis can be carried out because based on easily measurable physical characteristic cyclists typology can be deduced, and resistance parameters selected accordingly.

Secondly, looking at cycling preferences and attributes R, H and M type participants, in order, consistently had a better bicycle maintenance perception (perhaps related to actual lower resistances), enjoyed more and were willing to do more physical activity and were less sensitive to a comfort loss on progressively less separated bicycle facilities. In particular, significantly difference were found in comfort levels in mixed traffic condition (no separation). Implications might be regarding facility usage and route choice. Because in most cities cycling network is still a very limited subset of the overall road network, mixed traffic routes can be distance/time/topographically-wise more convenient, and they would probably be chosen only by cyclists who feel comfortable on them, leading to systematic route choice depending on physical typology.

Thirdly, cycling habits revealed that R, H and M members, in that order, cycled more often for commute and shopping purpose (but not significantly). However,

recreational/leisure cycling is mostly done by M-type of cyclists, perhaps indicating that because they commute less often by bicycle they are more willing to leisurely cycle. Mode share among typology interestingly revealed that R-cyclists do significantly more car sharing. This could potentially reflect a more sharing-economy mind-set of R typology of people. However, public transit was used more (but insignificantly) by M-type, perhaps correlated to their lower income. Time spent doing physical activity, cycling year-round, self-reported bicycle speed shows how R-types of cyclist are significantly more "dedicated" to cycling, to work out and possibly as a consequence they tend to ride faster.

Finally, using behavioural-related questions (comfort on facilities, willingness to cycle more and frequency of cycling in the past 30 days), each cyclist was labelled as one of the four types of cyclists (Dill & McNeil, 2013). Our physical typology showed significant difference in the "four type of cyclists" distribution among our "three physical types". In particular, R type cyclists, if compared to M, were significantly more on the "enthused and confident" side than the "interested but concerned" one. Educating cyclist on bicycle maintenance (e.g. keep well-inflated pneumatics), and incentivising road or hybrid type of bicycle, might contribute to a cyclist transition from M type to R type meaning that they would be more likely to be "enthused and confident", i.e. they would bike more and more confidently. Also, such relationship might help to physically identify "interested but concerned" cyclist, which, at least in Portland, OR, are the majority (Dill & McNeil, 2013) and should be the first targeted people to foster modal shift towards cycling.

Overall, interesting and reasonable correlations among physical typologies and all the other parameters were found perhaps opening more questions than finding answers. The definition of R for Road, H for Hybrid, and M, for Mountain, purely physical could be mapped into an Efficient, Moderate and Inefficient type of cyclists because the three

typologies, in that order, systematically have lower resistances (energetic efficiency), they go faster (time efficiency), and their route set is wider because they are more comfortable in mixed traffic (route choice efficiency).

It is true that correlation does not imply causation. However, a positive feedback effect seems to be present in the cohort of cyclist. In fact, previous research investigated how leisure cycling (a form of physical activity) could positively affect commuting cycling and vice versa (Kroesen & Handy, 2014; Park, Lee, Shin, & Sohn, 2011). In this study we also see that more cycling could be fostered by a more efficient vehicle and equipment, and by more physical activity which will result in cyclists to cycle even more, making them more comfortable to mixed-traffic facilities as vulnerable user, also possibly going faster so to reduce speed differential with motorized vehicles and feel safer.

All this is fascinating and may have important policies implication to increase cycling rates in cities. Because of the consistency in answers among the three physical typologies, and correlations with cycling behaviour and habits, it is believed that effective policies should aim to educate cyclist about bicycle types and efficiency (e.g. maintenance and equipment selection). For example, community bicycle shops should be built, and community centre should offer practical classes about bicycle maintenance, and proper usage for a more enjoyable ride. Also, policies aiming to reduce bicycle thefts should be simultaneously implemented (e.g. attended bicycle parking lots), as theft could be major factor restraining cyclists from purchasing a more efficient, road-style bicycle. Such efforts might accelerate the internal feedback effect that make cyclist progressively shifting to R type, meaning they will cycle more and come comfortably. Other incentives, such as distance-based bicycle commute reimbursement, could be used as to entice cyclist to cycle more while upgrading their bicycle. Also, as a possible consequence of more cycling there

is some evidence that more cycling could improve safety because of driver's adaptation to cyclists presence in the road environment (Jacobsen, 2003; Phillips, Bjørnskau, Hagman, & Sagberg, 2011; Wegman, Zhang, & Dijkstra, 2012), showing again an internal feedback effect that could contribute a cyclist to feel more comfortable and therefore ride more.

The study has several limitations. Although the clustering is performed with objective measures carried out by experimenters, all the questionnaire answers are self-reported and might be biased. For example, people tend not to answer in an extreme manner when using a Likert-type scale, or inflate their amount of exercise (Van de Mortel & others, 2008). Also, some question may have been unclear to some participants, leading to unintentional answers. However, the experimenters were always available for clarifications. This study was conducted in the summer and people may have been biased by the steady favourable weather of Vancouver during summer months. In particular in Table 12, three questions ("cycling by purpose") explicitly referred to habit in the previous 30 days (i.e. warm, summer days).

Overall, further investigation need to be pursued. As an example, a longitudinal survey would help exploring if there is a natural cyclist's growth and learning process that manifests as a physical typology shift over time. Also, further research needs to address the causality sequence in the physical typology shift, i.e. whether upgrading the equipment, bicycle, and better maintenance precede or follow behavioural and habits changes, and perhaps if there is any "novelty" or "guilt" effect, i.e. an owner invested money on a new bicycle, feeling the need to use it. Finally, further investigation should focus on mode substitution, because, as a cyclists type shift towards R type, it uses more private cars and less transit (although insignificantly).

9. CONTEXT-SENSITIVE, FIRST PRINCIPLE CRUISING SPEED MODEL, USING CYCLISTS CHARACTERIZATION

This chapter addresses the non-trivial and practical problem of estimating bicycle free-flow cruising speed given a bicyclist's physical characteristics, power output, and road conditions. The method described in this paper can be implemented to compute design speed on varying road grades or target/desired speed in microsimulation models. A "bottom-up" or mechanical perspective is used for speed estimation from first principles. A closed formula for speed is derived from equilibrium of traction and resistance forces, and applied using parameters from the literature and analysis of an observational data set. Results are compared to speed distributions in the literature. The method is extended to the problem of speed estimation for bicycles with a limited range of gearing and applied to the problem of clearance interval calculation.

9.1. Bicycle speed modelling

Currently, bicycle speeds are considered constant in many transportation analysis contexts, likely due to a lack of bicycle speed modelling tools. Travel time is a key factor in travel mode and route choices (Broach, Dill, & Gliebe, 2012; Sener, Eluru, & Bhat, 2009), and yet most travel models use constant-speed assumptions for bicyclists. Health impact assessment models assessing crash risk, pollution inhalation and physical activity also make assumptions about bicycle speeds based on limited information (Mueller et al., 2015a; D Rojas-Rueda, de Nazelle, Teixidó, & Nieuwenhuijsen, 2013).

Several empirical studies have shown that observed bicycle speeds can vary systematically with factors such as facility type and topography (Bernardi & Rupi, 2015; El-Geneidy, Krizek, & Iacono, 2007; Parkin & Rotheram, 2010). Still, studies of bicycle

speeds and travel times are relatively rare, and the literature lacks tools for estimating bicycle speeds based on roadway and traveller conditions. Speed analysis for a transportation system can be performed from a "top-down" or "flow-constrained" perspective where speed is determined by facility conditions. For motorized vehicle speeds, this approach has led to development of classical traffic flow theory (May, 1989). The flow-constrained approach is less applicable to modelling bicycle speeds because many bicycle facilities carry volumes well below levels at which bicyclist interactions impede travel. Bicycle facility capacity is of growing interest, however, and as bicycle mode share grows, flow-constrained speed may become a more important issue (Jiang, Hu, Wu, & Song, 2016; Jin et al., 2015).

9.2. Mechanical Speed Determination

Bicycle speed results from a set of forces, F_i, applied to the bicycle,

$$\sum_i F_i = T - R = m\frac{dv(t)}{dt} \quad (25)$$

where $v(t)$ is the linear speed of the bicycle (in m/s) as a function of time t (in s), T and R are traction and resistance forces respectively (in N), and m is the mass of the bicycle and bicyclist (in kg). Resistance R is the resultant of several forces acting against the forward motion while traction T is the propelling force tangential at the wheel as a result of the power that the bicyclist is providing. Full traction force is successfully exploited if and only if it is less than the available adherence (otherwise slippage occurs). If $T > R$ then the bicycle accelerates, and if $T < R$ the bicycle decelerates. This paper examines bicycle steady-state cruising speed, where $T = R$.

Resistance R can be modelled according to Equation 5, rewritten for convenience here

$$R = mg(C_r + G) + \frac{1}{2}\rho A_f C_d v_{rel}|v_{rel}|, \quad (26)$$

which for $v_{rel} > 0$ is of the general parabolic form

$$R = A + Bv_{rel}^2 \quad (27)$$

with parameters $A = mg(C_r + G)$ and $B = \frac{1}{2}\rho A_f C_d$ fixed over a road section of homogenous grade and surface.

Traction force is complex because it depends on energy expenditure and power output of the bicyclist, and the literature provides little guidance on modelling these factors for utilitarian bicyclists. Traction force T is a function of the power applied at the traction wheel P_w (in W) and bicycle speed v as

$$T = \frac{P_w}{v} \quad (28)$$

Positive P_w depends on the power input by the bicyclist at the crank P_c (in W) and the drivetrain efficiency η: $P_w = \eta P_c$, leading to $T = \frac{\eta P_c}{v}$. Braking leads to negative values of P_w and T.

Bicyclist power output is expected to vary with road conditions and across individuals. In particular, it has been observed that power increases with road grade. Previous research (Parkin & Rotheram, 2010) suggests the linear relationship:

$$P_c = 127 + 2590 \cdot G. \quad (29)$$

As a comparison to Equation 29, we estimate a similar relationship using an observational data set from (Bigazzi & Figliozzi, 2015a). Assuming the same $\eta = 0.95$ from (Parkin & Rotheram, 2010),

$$P_c = 112 + 2441 \cdot G \quad (30)$$

for observations with G of -3% to 7% and power of 20 to 300 W (R^2 = 0.46). The power-grade models compare well despite substantially different data sources. For the rest of this section, it is assumed that P_c can be considered an exogenous choice of the bicyclist unconstrained by speed; limitations of power output at certain speeds due to gearing limitations are explored below. Investigation of power choices in more varying bicycling conditions is left for future work.

Traction and resistance force equilibrium is illustrated in Figure 21, where cruising speeds are at the intersections of the traction (dashed) and resistance (solid) lines. Illustrative resistance parameters are shown in Table 13. Four equilibria speeds can be seen in Figure 21: 21.5 km/h for R at $G = 0\%$ and T at 127 W, 26.8 km/h for R at $G = 0\%$ and T at 205 W, 17.5 km/h for R at $G = 3\%$ and T at 205W, and 12.1 km/h for R at $G = 3\%$ and T at 127 W. With no power adjustment, a rider at $P_w = 127$ W on level ground would slow from 21.5 to 12.1 km/h at 3% grade, but only to 17.5 km/h if P_w were increased to 205 W as a consequence of Equation 29. According to Equations 29 and 30 and $\eta = 0.95$, P_w is expected to increase by almost 80 W with a 3% increase in grade, which would lead to an equilibrium speed reduction from about 22 to 18 km/h at the higher grade.

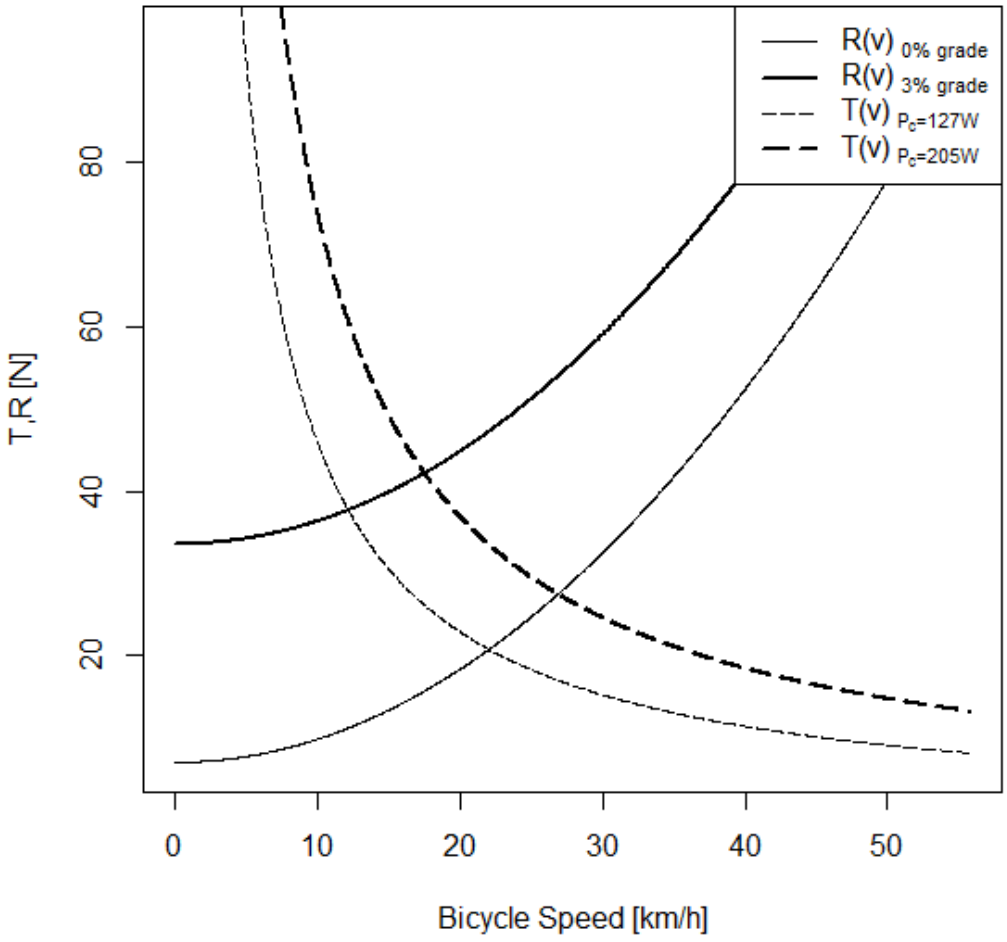

Figure 21. Traction and resistance forces at varying grades and power. Power computed as a function of grade according to Equation 29.

Table 13. Sensitivity analysis for bicycle speed calculation*

Parameter	units	Mean	Standard deviation	Speed range from +/- 1 standard deviation of parameter [km/h]
m	kg	90	20	± 0.72
C_r	-	0.008	0.004	± 1.61
G	-	0	0.03	± 4.66
$A_f C_d$	m^2	0.6	0.2	± 1.70
P_w **	W	127	78	± 4.78
A ***	N	7.06	38.23	± 7.70
B ***	kg/m	0.368	0.122	± 1.70

* Sources: (Bigazzi & Figliozzi, 2015a; Chowdhury & Alam, 2012; Faria et al., 2005; Gross et al., 1983; Launer & Harris, 1996; Martin, Milliken, Cobb, McFadden, & Coggan, 1998; Olds et al., 1995; Wilson & Papadopoulos, 2004); in addition, $g = 9.81$ m/s^2, $\rho = 1.225$ kg/m^3, and m includes bicycle mass.
** calculated from G and Equation 29, with $\eta = 0.95$.
*** calculated from other parameters.

Setting Equation 25 equal to zero, $T = R$ and from Equations 27 and 28, neglecting wind so that $v_{rel}|v_{rel}| = v^2$,

$$\frac{P_w}{v} = A + Bv^2 \quad (31)$$

which rearranges to

$$v^3 + \frac{A}{B}v - \frac{P_w}{B} = 0\ . \quad (32)$$

B is positive by definition and the sign of A depends on G. Thus, from Descarte's rule of signs, if $P_w > 0$, exactly one positive solution to Equation 32 exists. If the discriminant

$$\frac{P_w^2}{4B^2} + \frac{A^3}{27B^3} \quad (33)$$

is non-negative, the solution to Equation 32 can be computed

$$v = \sqrt[3]{\frac{P_w}{2B} + \sqrt{\frac{P_w^2}{4B^2} + \frac{A^3}{27B^3}}} + \sqrt[3]{\frac{P_w}{2B} - \sqrt{\frac{P_w^2}{4B^2} + \frac{A^3}{27B^3}}}\,. \qquad (34)$$

The discriminant will be negative if $A^3 < -\frac{27}{4}P_w^2 B$, which will only occur on negative grades ($< -4\%$) with low P_w where braking probably occurs.

9.3. Sensitivity and Second Moment Analyses

Second moment analysis is performed for Equation 34 to investigate the effects of variability of input parameters on cruising speed. Input parameter values are summarized in Table 13, along with data sources. Second moment analysis was performed using the reliability analysis software "Rt" (Mahsuli & Haukaas, 2013). Propagating the variability of all parameters of Table 13 together, the resulting mean (standard deviation) of speed is 21.5 (8.1) km/h. In case of fixed, null grade, the mean (standard deviation) of speed is 21.5 (3.9) km/h which compares well with observed speed distributions reported in the literature (Bernardi & Rupi, 2015; El-Geneidy et al., 2007). The last column in Table 13 shows the range of speeds that results from ± 1 standard deviation of individual parameter values. Speed increases with P_w and decreases with all other parameters. Grade can be a major factor for speed, as expected, as can bicyclist power, which is related to grade. Drag and rolling resistance parameters are somewhat less important factors, followed by mass.

9.4. Constrained Power and Cadence

The power at the crank P_c (W) is the product of the torque applied at the crank τ_c (Nm) and pedalling cadence c (s^{-1}). Cadence, in turn, is related to speed through the gearing

or "development" D as $c = v/D$, where $D = 2\pi r_w m_i$, r_w is the rear wheel radius, and m_i is the gear conversion ratio at gearing i, defined as $\frac{front\ chainring\ teeth}{rear\ cog\ teeth}$. Thus,

$$P_c = \tau_c c = \tau_c \frac{v}{D}. \quad (35)$$

With an infinite range of D, a bicyclist can use a desired cadence at any speed (and similarly apply a preferred P_c and τ_c). Real bicycles have a limited range of D, which in turn limits the available c at a given speed. At low cadences, P_c could be constrained by maximum leg strength to apply force at the pedals or by the maximum available static friction between wheel and pavement; at high cadences, P_c could be constrained by leg strength available at high leg speed. Previous work (Wilson & Papadopoulos, 2004) suggests a linear torque-cadence relationship,

$$\tau_c = \gamma - \delta c \quad (36)$$

which leads to a second-order power-cadence relationship

$$P_c = \gamma c + \delta c^2 \quad (37)$$

with maximum $P_c^* = \frac{-\gamma^2}{4\delta}$ at $c^* = -\frac{\gamma}{2\delta}$.

Rearranging, $\gamma = 2\frac{P_c^*}{c^*}$ and $\delta = \frac{-P_c^*}{c^{*2}}$, which leads to a constrained power model for a bicyclist that must depart from $c \neq c^*$ due to limited gearing:

$$P_c = 2\frac{P_c^*}{c^*} c - \frac{P_c^*}{c^{*2}} c^2, \quad (38)$$

or equivalently,

$$P_c = \frac{2P_c^*}{c^*D} v - \frac{P_c^*}{(c^*D)^2} v^2 \ . \quad (39)$$

For a single-geared bicycle, $P_c < P_c^*$ at speeds higher and lower than c^*D. Traction force for a single-geared bicycle can be modeled from $T = \frac{\eta P_c}{v}$ and Equation 39

$$T = \frac{\eta P_c^*}{(Dc^*)^2}(2Dc^* - v) \quad (40)$$

which is a linear function of speed, as opposed to the inverse relationship in Equation 28.

A more flexible definition for a bicycle with a limited and continuous range of gears from D_{min} to D_{max} is:

$$P_c = \begin{cases} \frac{2P_c^*}{c^*D_{min}} v - \frac{P_c^*}{(c^*D_{min})^2} v^2 & v < c^*D_{min} \\ P_c^* & o/w \\ \frac{2P_c^*}{c^*D_{max}} v - \frac{P_c^*}{(c^*D_{max})^2} v^2 & v > c^*D_{max} \end{cases} \quad (41)$$

In this model, $P_c = P_c^*$ where v is between c^*D_{min} and c^*D_{max}, and drops off at higher and lower speeds. Again in terms of traction power, we have a continuous and differentiable function of v:

$$T(v) = \begin{cases} \frac{\eta P_c^*}{(D_{min}c^*)^2}(2D_{min}c^* - v) & v < c^*D_{min} \\ \frac{\eta P_c^*}{v} & o/w \\ \frac{\eta P_c^*}{(D_{max}c^*)^2}(2D_{max}c^* - v) & v > c^*D_{max} \end{cases} \quad (42)$$

which yields the following equilibrium equations from $T = R = A + Bv^2$:

$$\begin{aligned} 0 &= A - \frac{2\eta P_c^*}{c^* D_{min}} + \frac{\eta P_c^*}{(c^* D_{min})^2} v + Bv^2 \quad && v < c^* D_{min} \\ 0 &= -\eta P_c^* + Av + Bv^3 && o/w \\ 0 &= A - \frac{2\eta P_c^*}{c^* D_{max}} + \frac{\eta P_c^*}{(c^* D_{max})^2} v + Bv^2 && v > c^* D_{max} \end{aligned} \quad (43)$$

These equilibrium equations can be solved as for Equation 32 and by using the quadratic formula as:

$$v = \frac{-\frac{\eta P_c^*}{(c^* D_{min})^2} + \sqrt{\frac{(\eta P_c^*)^2}{(c^* D_{min})^4} + \frac{\eta 8 B P_c^*}{c^* D_{min}} - 4AB}}{2B} \quad (44)$$

for $\eta P_c^* < Ac^* D_{min} + B(c^* D_{min})^3$;

$$v = \frac{-\frac{\eta P_c^*}{(c^* D_{max})^2} + \sqrt{\frac{(\eta P_c^*)^2}{(c^* D_{max})^4} + \frac{\eta 8 B P_c^*}{c^* D_{max}} - 4AB}}{2B} \quad (45)$$

for $\eta P_c^* > Ac^* D_{max} + B(c^* D_{max})^3$; and as per Equation 34 otherwise.

The data from (Bigazzi & Figliozzi, 2015a) (with $P_c > 0$, $c > 0$ and $-1 < G < 1$ %) are again used to examine the relationship between P_c and c on level terrain, by fitting a second-order polynomial for $P_c(c)$ with robust standard errors. The fitted equation is $P_c = 80 + 108c - 58c^2$; all three parameters are significant at $p < 0.01$, supporting the hypothesis that power falls at high and low cadences. Peak power (here $P_c^* = 132$ W) is at $c^* = 0.93$ rps (56 rpm) and compares well with power at $G = 0$ in Equation 29.

A visualization of the model is provided in Figure 22, which illustrates P_c (Equation 41) and T (Equation 40) for a bicycle equipped with unlimited gears (equivalent to case in Figure 21), limited range of gears (from $D_{min} = 2.78$ m to $D_{max} = 8.56$ m, corresponding to gear ratios m_i of 34/23 and 50/11, respectively and wheel radius assumed r_w = 0.3m) and

single speed ($D = 5.67$ m, the midpoint between D_{min} and D_{max}). Even on level ground, both traction and power are reduced at high and low speeds due to the gearing constraint. For any given value of T, unlimited-gear bicycles allow the highest speeds. All else equal, a wider range of gearings increases the speed that a bicyclist will attain for a preferred power output.

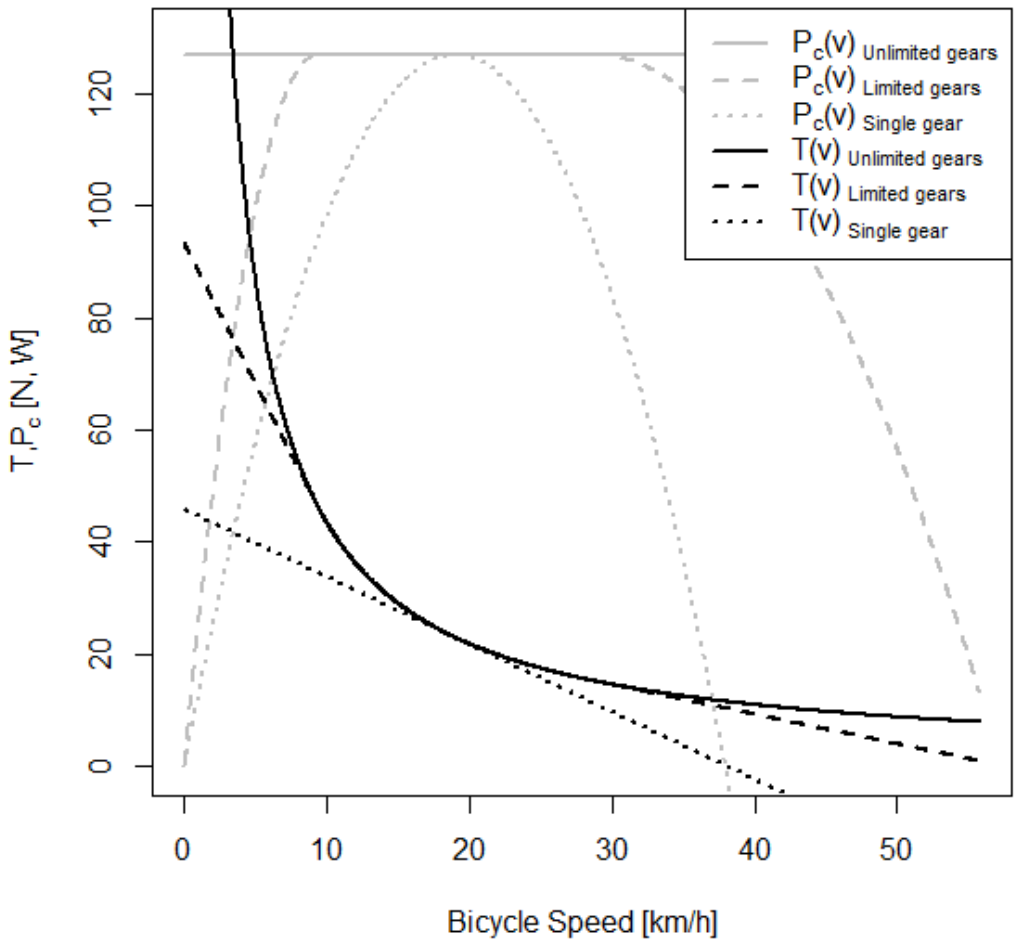

Figure 22. Crank power (P_c) and traction (T) as a function of bicycle speed, for single gear, limited gear and unlimited gear bicycle at preferred power output P_c^* of 127 W and $c^* = 0.93$.

Figure 23 and Figure 24 illustrate the potential importance of accounting for gear limitations in speed modelling, particularly at high power and on hills. Figure 23 shows equilibrium speed at different grades and gearings. At higher positive grades, lower gearing allows for higher speeds, and vice-versa. Equilibrium speeds for limited and unlimited gear

bicycles are equivalent at these grades due to the wide gearing range in the example. Gearing becomes more important for bicycles with narrower gear ranges, such as found in many bike-share systems. Figure 24 shows equilibrium speed at different preferred powers and gearings, and illustrates that a single gearing can limit the attainment of high speeds, whereas limited but wide gearing has little impact on speed (similar to Figure 23).

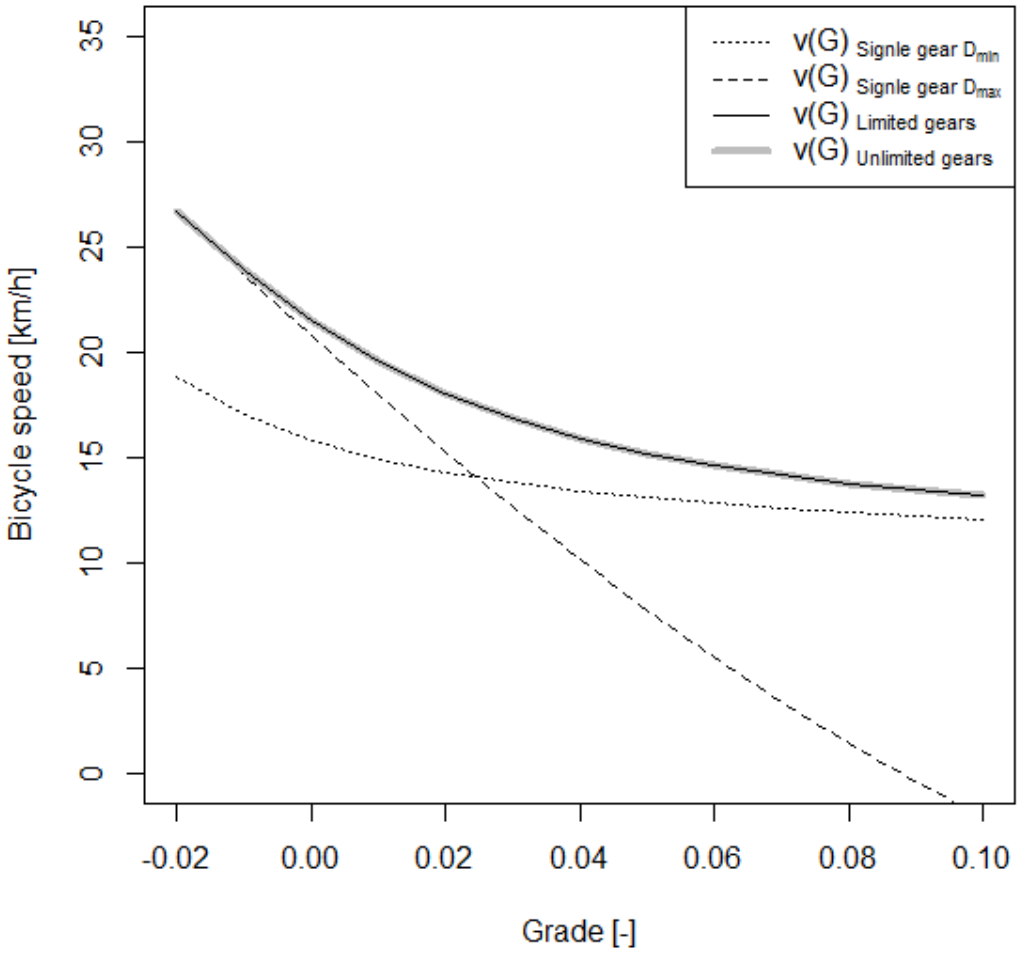

Figure 23. Bicycle speed as a function of grade for four different gearing cases, with P_c^*, according to Equation 29, $c^* = 0.93$ rps and other parameters as per mean values in Table 13.

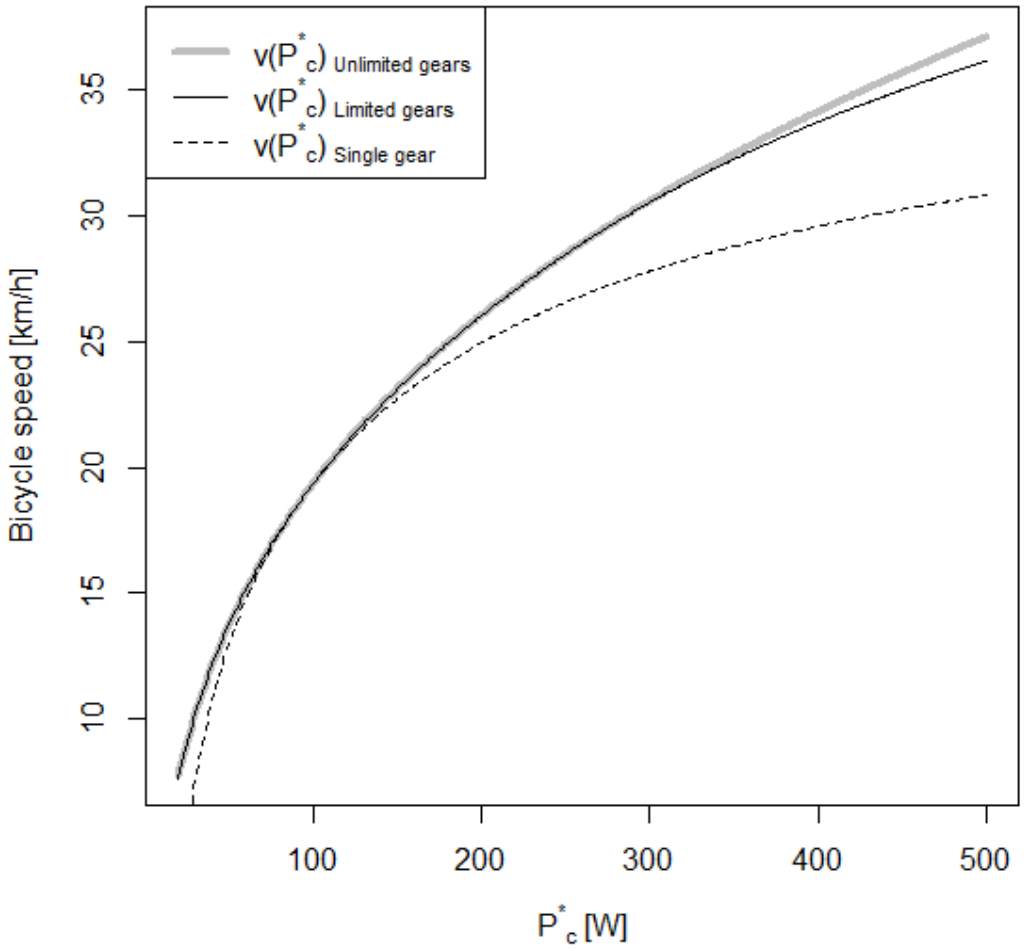

Figure 24. Bicycle speed as a function of P_c^* for single ($D = 5.67$ m), limited ($D_{min} = 2.78$ m to $D_{max} = 8.56$ m), and unlimited gears with $c^* = 0.93$ rps and other parameters as per mean values in Table 13

9.5. Application of the Method

This bicycle speed calculation framework is suitable for many applications in intelligent transportation systems design, operations, and management. In particular, it can

be easily implemented in microsimulation models to determine target cruising speeds for bicyclists based on their personal characteristics and road grade. Furthermore, it can be used to generate context-specific bicycle design speeds for advanced traffic management systems. For example, signal timing design according to the NACTO *Urban Bikeway Design Guide* (National Association of City Transportation Officials, 2014) requires calculation of the clearance interval C_i (sec) according to

$$C_i = 3 + 3.6\frac{w_i}{v} \quad (46)$$

where w_i is the width of the intersection in meters and v is in km/h. The guide suggests assuming $v = 15$ km/h on level ground, if no local bicycle speed data are available (which is commonly the case).

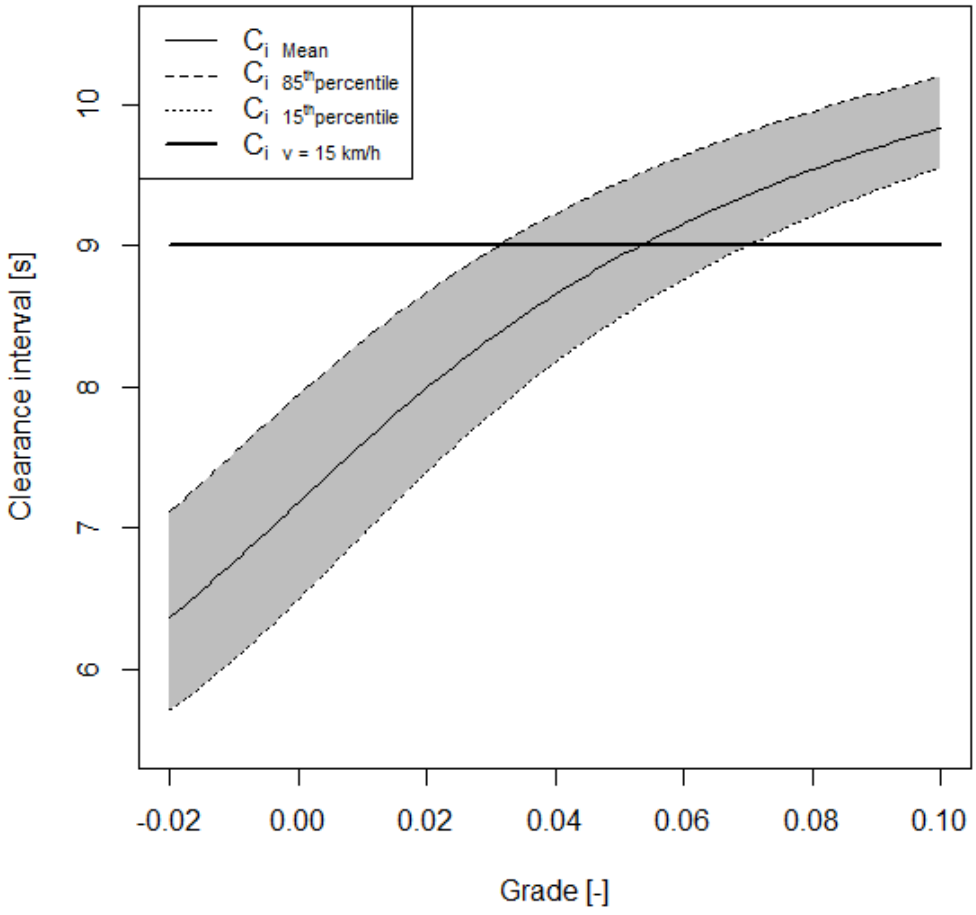

Figure 25. Clearance interval C_i for crossing a 25 m wide intersection (w_i) at different grades; grey area gives the 15th to 85th percentile C_i values, propagating m, C_r, and $A_f C_d$ uncertainty as per Table 13.

Figure 25 illustrates how the method can be used to estimate context-sensitive and probabilistic design speeds by propagation of parameter uncertainty in the equilibrium speed model (m, C_r, and $A_f C_d$ as in Table 13 and P_w from Equation 29). The 85th percentile clearance interval exceeds the mean by up to 0.8 sec, and the mean varies from the default value by up to 2.6 sec. At $G = 3\%$ C_i 85th percentile exceeds the default value, possibly

leading to unsafe clearance interval for higher grades and inefficient for level ones. More specific information about local bicyclist characteristics (e.g. high bike-share usage with heavier bicycles and a more limited gear range) can be applied for optimized and safer designs, especially in hilly terrain.

9.6. Discussion and limitations

This chapter presented a novel, first principles approach to estimating bicycle cruising speed from cyclist power output, bicycle resistance parameters, and road grade, including a sophistication for limited-gearing bicycles. Closed-form solution equations are presented which can be easily integrated into various analysis tools, including spreadsheet software. This framework allows for implementation of more refined microsimulation and travel models that are sensitive to resistance characteristics (road grade, rolling and drag parameters), gearing characteristics and power output of bicyclists. The framework with second moment analysis can be used for probabilistic geometric design, reliability and safety analysis, as bicycle speed variability is the results of the propagation of all the others context-related parameters variability. Finally, the framework can be applied to stochastic route choice modelling. The methodology can also be expanded to include other factors potentially affecting bicycle speed such as power assistance and wind.

The framework presented is steady-state, and does not address start and stop phases or interactions with other road users. Moreover, power is an exogenous input only affected by road grade and without consideration of crash risk or stress due to motor vehicle traffic. Another limitation of the method is that application requires knowledge of bicycle parameters and power output, for which there is limited information in the literature. The linear relationship between power and grade presented in this paper is a start, and future

work will further investigate the determinants of on-road power output by utilitarian bicyclists. The recent proliferation of moderate-cost bicycle power meters enables large-scale collection of power data from urban bicyclists. Additional next steps include modelling of speed dynamics and electric-assist bicycles.

10. CONCLUSION AND THE FUTURE

10.1. Contributions to the body of knowledge

Nowadays cycling is not only a sport or recreational activity, as it represents the principal mode of transportation for growing shares of travellers. Transportation professionals recognise the trend, but lack of proper and reliable bicycle travel models and data.

This thesis contributes to fill the knowledge gap represented by elementary urban cyclists' physical characteristics quantification, such as bicycle resistance parameters. These parameters can be used in health, and ventilation models, but can also be used for sophisticated bicycle speed modelling, which is in turn important for infrastructure and geometric design, mode and route choice modelling. Also, results found in this thesis can be used by policy makers to foster cycling in urbanized environments, as systematic cycling behavioural associations were found with physical characteristics.

Firstly, the lack of real-world bicycle rolling and drag resistance is addressed by development and validation of a novel outdoor coast-down test. The method expands on previous methods found in the literature by accounting for wind and grade variation. Results revealed that the test significantly detects changes in resistances for a tire pressure or riding position change. It was noted that only those test sessions performed in head-wind conditions (most representative of cycling conditions) could revel significant differences. Also the novelty of this outdoor coast down-test technique lies in the fact that indoor testing (wind tunnels) might not be representative of on-road condition especially because of the dependence of effective frontal area from relative wind speed (Reynolds number) and direction. For further details, please refer to Chapter 4 and 5.

Secondly, the validated outdoor method has been implemented in an intercept bicycle survey in Vancouver, BC in summer 2016. Testing sessions were conducted during 18 different days at 9 different location so to obtain a representative sample of the cyclists' population. Detail of testing sessions are outlined in Chapter 6. For the first time, a significant sample of real-world urban cyclists contributed to the estimation of in-use bicycle resistances parameters distribution (rolling, aerodynamic resistance and mass, comprising cyclist, bicycle and cargo). The estimated distribution seems to agree with resistances estimates available in the literature (mostly for sport cycling) but the measured range found in this study is wider, possibly because of the wide range of bicycle types and conditions involved in the survey.

By clustering cyclists using physical characteristics, particularly bicycle type, tire conditions, and riding position, systematic behavioural pattern were found in the cohort of cyclists. In particular, more frequent cyclists used more efficient bicycles, and also enjoyed and practised more physical activity. This suggests that policy makers might effectively develop cycling-friendly strategy by education on bicycle efficiency and the importance of physical activity. Physical-behavioural relationships might also be important for a better modelling of cyclist power output, having implications for health studies and speed modelling.

Lastly, a context-sensitive speed model shows the applicability of cyclist physical characterization process undertaken in this thesis. Making use of power-grade trade-off relationships, bicycle resistances parameters and road topography, speed distributions are obtained so that enhanced bicycle transportation designed can be pursued.

10.2. Limitations to look forward

This study has a few limitations, consequences of the methodology used. Firstly, the bicycle coast-down test validation phase could involve comparison with other resistances methodologies such as wind tunnels, towing method and comparison with power-meters measurements. Also, physical characterization was obtained for a sample in Vancouver, Canada, in summer 2016. As such, only a picture of cyclists' physical conditions is provided and it is not known how it would change if the survey was carried out in other times of the year or in other cities. Therefore, repeating the study in different cities with different bicycle fleets and mode shares could significantly affect this study's results. Also, we did not do testing in wet, cold weather conditions, a factor that could significantly affect results as well. Longitudinal studies, involving panels of cyclists, and cross-sectional studies (in different cities and different seasons), should be therefore carried out in the future. The questionnaire used is a stated preference survey methodology and, as such, response biases could be present (e.g. misinterpreting questions, tendency to answer in a non-extreme manner). Finally, the speed model should use more refined power-cadence and power-grade relationships, especially with the rising of e-bicycles. For micro-modelling, non steady-state cycling condition should be explored by investigating and accounting for acceleration and decelerations rates. Interaction with other road users and comfort/safety perceptions, likely to affect bicycle speed were not modelled as well.

REFERENCES

Acuere Consulting Inc. (2013). Acuere Consulting's annual average daily bicycle (AADB) traffic volume database. [Database].

Aggarwal, P. (2010). *MEMS-based Integrated Navigation*. Artech House.

Andersen, L. G., Larsen, J. K., Fraser, E. S., Schmidt, B., & Dyre, J. C. (2014). Rolling resistance measurement and model development. *Journal of Transportation Engineering*, *141*(2), 04014075.

Bernardi, S., & Rupi, F. (2015). An Analysis of Bicycle Travel Speed and Disturbances on Off-street and On-street Facilities. *Transportation Research Procedia*, *5*, 82–94. https://doi.org/10.1016/j.trpro.2015.01.004

Bigazzi, A. Y. (2016). Determination of active travel speed for minimum air pollution inhalation. *International Journal of Sustainable Transportation*, *in press*. https://doi.org/10.1080/15568318.2016.1238984

Bigazzi, A. Y. (2017). Determination of active travel speed for minimum air pollution inhalation. *International Journal of Sustainable Transportation*, *11*(3), 221–229. https://doi.org/10.1080/15568318.2016.1238984

Bigazzi, A. Y., & Figliozzi, M. A. (2014). Review of urban bicyclists' intake and uptake of traffic-related air pollution. *Transport Reviews*, *34*(2), 221–245. https://doi.org/10.1080/01441647.2014.897772

Bigazzi, A. Y., & Figliozzi, M. A. (2015). Dynamic ventilation and power output of urban bicyclists. *Transportation Research Record: Journal of the Transportation Research Board*, *2520*, 52–60. https://doi.org/10.3141/2520-07

Broach, J., Dill, J., & Gliebe, J. (2012). Where do cyclists ride? A route choice model developed with revealed preference GPS data. *Transportation Research Part A: Policy and Practice*, *46*(10), 1730–1740. https://doi.org/10.1016/j.tra.2012.07.005

Burke, E. (2003). *High-tech Cycling*. Human Kinetics.

Candau, R. B., Grappe, F., Ménard, M., Barbier, B., Millet, G. Y., Hoffman, M. D., … Rouillon, J. D. (1999). Simplified deceleration method for assessment of resistive forces in cycling. *Medicine and Science in Sports and Exercise*, *31*(10), 1441–1447.

Candau, Robin B., Grappe, F., Menard, M., Barbier, B., Millet, G. Y., Hoffman, M. D., … Rouillon, J. D. (1999). Simplified deceleration method for assessment of resistive forces in cycling. *Medicine & Science in Sports & Exercise*, *31*(10), 1441. https://doi.org/10.1097/00005768-199910000-00013

Chowdhury, H., & Alam, F. (2012). Bicycle aerodynamics: an experimental evaluation methodology. *Sports Engineering*, *15*(2), 73–80. https://doi.org/10.1007/s12283-012-0090-y

CROW. (2007). *Design manual for bicycle traffic*. The Netherlands: Centre for Research and Contract Standardisation in Civil Engineering.

Damant-Sirois, G., & El-Geneidy, A. M. (2015). Who cycles more? Determining cycling frequency through a segmentation approach in Montreal, Canada. *Transportation Research Part A: Policy and Practice*, *77*, 113–125. https://doi.org/10.1016/j.tra.2015.03.028

De Agostino, M. (2009). *I sensori inerziali di basso costo per la navigazione geodetica*. Politecnico di Torino. Retrieved from https://www.researchgate.net/profile/Mattia_De_Agostino/publication/268009971_I

_SENSORI_INERZIALI_DI_BASSO_COSTO_PER_LA_NAVIGAZIONE_GEODETICA/links/54ec4eb00cf27fbfd76f3db7.pdf

de Groot, G., Sargeant, A. J., & Geysel, J. (1995). Air friction and rolling resistance during cycling. *Medicine and Science in Sports and Exercise*, *27*(7), 1090–1095.

de Hartog, J. J., Boogaard, H., Nijland, H., & Hoek, G. (2010). Do the Health Benefits of Cycling Outweigh the Risks? *Environmental Health Perspectives*, *118*(8), 1109–1116.

Debraux, P., Grappe, F., Manolova, A. V., & Bertucci, W. (2011). Aerodynamic drag in cycling: methods of assessment. *Sports Biomechanics*, *10*(3), 197–218. https://doi.org/10.1080/14763141.2011.592209

Defraeye, T., Blocken, B., Koninckx, E., Hespel, P., & Carmeliet, J. (2011). Computational fluid dynamics analysis of drag and convective heat transfer of individual body segments for different cyclist positions. *Journal of Biomechanics*, *44*(9), 1695–1701. https://doi.org/10.1016/j.jbiomech.2011.03.035

Delignette-Muller, M. L., & Dutang, C. (2015). fitdistrplus: An R Package for Fitting Distributions. *Journal of Statistical Software*, *64*(4). https://doi.org/10.18637/jss.v064.i04

di Prampero, P. E. (1986). The energy cost of human locomotion on land and in water. *International Journal of Sports Medicine*, *7*(2), 55–72.

di Prampero, P. E., Cortili, G., Mognoni, P., & Saibene, F. (1979). Equation of motion of a cyclist. *Journal of Applied Physiology*, *47*(1), 201–206.

Dill, J., & McNeil, N. (2013). Four Types of Cyclists? *Transportation Research Record: Journal of the Transportation Research Board*, *2387*, 129–138. https://doi.org/10.3141/2387-15

El-Geneidy, A. M., Krizek, K. J., & Iacono, M. J. (2007). Predicting bicycle travel speeds along different facilities using GPS data: A proof-of-concept model. Presented at the Transportation Research Board 86th Annual Meeting. Retrieved from http://trid.trb.org/view.aspx?id=802502

Faria, E. W., Parker, D. L., & Faria, I. E. (2005). The science of cycling: factors affecting performance-part 2. *Sports Medicine*, *35*(4), 313–337.

Fintelman, D. M., Hemida, H., Sterling, M., & Li, F.-X. (2015). CFD simulations of the flow around a cyclist subjected to crosswinds. *Journal of Wind Engineering and Industrial Aerodynamics*, *144*, 31–41. https://doi.org/10.1016/j.jweia.2015.05.009

Fintelman, D. M., Sterling, M., Hemida, H., & Li, F.-X. (2014). The effect of crosswinds on cyclists: An experimental study. *Procedia Engineering*, *72*, 720–725. https://doi.org/10.1016/j.proeng.2014.06.122

Fox, K. R. (1999). The influence of physical activity on mental well-being. *Public Health Nutrition*, *2*(3a). https://doi.org/10.1017/S1368980099000567

Gatersleben, B., & Haddad, H. (2010). Who is the typical bicyclist? *Transportation Research Part F: Traffic Psychology and Behaviour*, *13*(1), 41–48. https://doi.org/10.1016/j.trf.2009.10.003

Gower, J. C. (1971). A General Coefficient of Similarity and Some of Its Properties. *Biometrics*, *27*(4), 857–871. https://doi.org/10.2307/2528823

Gross, A. C., Kyle, C. R., & Malewicki, D. J. (1983). The Aerodynamics of Human-Powered Land Vehicles. *Scientific American*, *249*, 142–152. https://doi.org/10.1038/scientificamerican1283-142

Hay, W. W. (1982). *Railroad Engineering*. John Wiley & Sons.

Heinen, E., van Wee, B., & Maat, K. (2010). Commuting by bicycle: An overview of the literature. *Transport Reviews*, *30*(1), 59–96. https://doi.org/10.1080/01441640903187001

Hennig, C. (2015). fpc: Flexible Procedures for Clustering (Version R package version 2.1-10). Retrieved from https://CRAN.R-project.org/package=fpc

Iseki, H., & Tingstrom, M. (2013). A New Approach in the GIS Bikeshed Analysis with Consideration of Topography, Street Connectivity, and Energy Consumption. Presented at the Transportation Research Board 92nd Annual Meeting. Retrieved from http://trid.trb.org/view.aspx?id=1241168

Ismail, K., & Sayed, T. (2009). Risk-based framework for accommodating uncertainty in highway geometric design. *Canadian Journal of Civil Engineering*, *36*(5), 743–753.

Jacobsen, P. (2003). Safety in numbers: more walkers and bicyclists, safer walking and bicycling. *Injury Prevention*, *9*(3), 205–209. https://doi.org/10.1136/ip.9.3.205

Jiang, R., Hu, M.-B., Wu, Q.-S., & Song, W.-G. (2016). Traffic dynamics of bicycle flow: Experiment and modeling. *Transportation Science*. Retrieved from http://pubsonline.informs.org/doi/abs/10.1287/trsc.2016.0690

Jin, S., Qu, X., Zhou, D., Xu, C., Ma, D., & Wang, D. (2015). Estimating cycleway capacity and bicycle equivalent unit for electric bicycles. *Transportation Research Part A: Policy and Practice*, *77*, 225–248. https://doi.org/10.1016/j.tra.2015.04.013

Knight, R. (2008). The Bicyclist's Paradox. *The Physics Teacher*, *46*(5), 275–279. https://doi.org/10.1119/1.2909744

Kroesen, M., & Handy, S. (2014). The relation between bicycle commuting and non-work cycling: results from a mobility panel. *Transportation*, *41*(3), 507–527. https://doi.org/10.1007/s11116-013-9491-4

Kyle, C. R., & Burke, E. (1984). Improving the racing bicycle. *Mechanical Engineering*, *106*(9), 34–45.

Launer, L. J., & Harris, T. (1996). Weight, height and body mass index distributions in geographically and ethnically diverse samples of older persons. Ad Hoc Committee on the Statistics of Anthropometry and Aging. *Age and Ageing*, *25*(4), 300–306.

Lupi, M. (2004). Elementi di Meccanica della Locomozione (Appunti dalle lezioni di Tecnica ed Economia dei Trasporti). Universita' degli Studi di Bologna.

Maechler, M., Rousseeuw, P., Struyf, A., Hubert, M., & Hornik, K. (2016). cluster: Cluster Analysis Basics and Extensions (Version R package version 2.0.4 --- For new features, see the "Changelog" file (in the package source)).

Mahsuli, M., & Haukaas, T. (2013). Computer Program for Multimodel Reliability and Optimization Analysis. *Journal of Computing in Civil Engineering*, *27*(1), 87–98. https://doi.org/10.1061/(ASCE)CP.1943-5487.0000204

Martin, J. C., Milliken, D. L., Cobb, J. E., McFadden, K. L., & Coggan, A. R. (1998). Validation of a mathematical model for road cycling power. *Journal of Applied Biomechanics*, *14*, 276–291.

Massa, D. P. (1999). Choosing an ultrasonic sensor for proximity or distance measurement. *Sensors*, *16*(2).

May, A. (1989). *Traffic Flow Fundamentals*. Prentice Hall.

Mercat, N. (1999a). Modelling of bicycle journeys: using energy expended rather than journey time or distance. In *Proceedings of the 11th international bicycle planning conference, Graz, Austria.*

Mueller, N., Rojas-Rueda, D., Cole-Hunter, T., de Nazelle, A., Dons, E., Gerike, R., … Nieuwenhuijsen, M. (2015a). Health impact assessment of active transportation: A

systematic review. *Preventive Medicine*, *76*, 103–114. https://doi.org/10.1016/j.ypmed.2015.04.010

Mueller, N., Rojas-Rueda, D., Cole-Hunter, T., de Nazelle, A., Dons, E., Gerike, R., … Nieuwenhuijsen, M. (2015b). Health impact assessment of active transportation: A systematic review. *Preventive Medicine*, *76*, 103–114. https://doi.org/10.1016/j.ypmed.2015.04.010

National Association of City Transportation Officials. (2014). *Urban bikeway design guide* (2nd ed.). Island Press.

Navin, F. P. D. (1994). Bicycle traffic flow characteristics: Experimental results and comparisons. *ITE Journal*, *64*(3), 31–37.

Olds, T. S. (2001). Modelling human locomotion: Aapplications to cycling. *Sports Medicine*, *31*(7), 497–509.

Olds, T. S., Norton, K. I., Lowe, E. L., Olive, S., Reay, F., & Ly, S. (1995). Modeling road-cycling performance. *Journal of Applied Physiology*, *78*(4), 1596–1611.

Park, H., Lee, Y. J., Shin, H. C., & Sohn, K. (2011). Analyzing the time frame for the transition from leisure-cyclist to commuter-cyclist. *Transportation*, *38*(2), 305–319. https://doi.org/10.1007/s11116-010-9299-4

Parkin, J., & Rotheram, J. (2010). Design speeds and acceleration characteristics of bicycle traffic for use in planning, design and appraisal. *Transport Policy*, *17*(5), 335–341. https://doi.org/10.1016/j.tranpol.2010.03.001

Phillips, R. O., Bjørnskau, T., Hagman, R., & Sagberg, F. (2011). Reduction in car–bicycle conflict at a road–cycle path intersection: Evidence of road user adaptation? *Transportation Research Part F: Traffic Psychology and Behaviour*, *14*(2), 87–95. https://doi.org/10.1016/j.trf.2010.11.003

Preda, I. C., & Ciolan, D. (2010). Coast-Down Test–Theoretical and Experimental Approach. In *The Automobile and the Environment* (pp. 277–288).

Reynolds, A. P., Richards, G., Iglesia, B. de la, & Rayward-Smith, V. J. (2006). Clustering Rules: A Comparison of Partitioning and Hierarchical Clustering Algorithms. *Journal of Mathematical Modelling and Algorithms*, *5*(4), 475–504. https://doi.org/10.1007/s10852-005-9022-1

R.M. Young Company. (2004). ULTRASONIC ANEMOMETER MODEL 85000. Retrieved from http://www.youngusa.com/Manuals/85000-90(J).pdf

Rojas-Rueda, D, de Nazelle, A., Teixidó, O., & Nieuwenhuijsen, M. (2013). Health impact assessment of increasing public transport and cycling use in Barcelona: A morbidity and burden of disease approach. *Preventive Medicine*. https://doi.org/10.1016/j.ypmed.2013.07.021

Rojas-Rueda, David, Nazelle, A. de, Tainio, M., & Nieuwenhuijsen, M. J. (2011). The health risks and benefits of cycling in urban environments compared with car use: health impact assessment study. *BMJ*, *343*, d4521. https://doi.org/10.1136/bmj.d4521

Scrucca, L. (2013). GA: A Package for Genetic Algorithms in R. *Journal of Statistical Software*, *53*(4). https://doi.org/10.18637/jss.v053.i04

Sener, I. N., Eluru, N., & Bhat, C. R. (2009). An analysis of bicycle route choice preferences in Texas, US. *Transportation*, *36*(5), 511–539. https://doi.org/10.1007/s11116-009-9201-4

Taylor, D., & Mahmassani, H. (2000). Coordinating Traffic Signals for Bicycle Progression. *Transportation Research Record: Journal of the Transportation Research Board*, *1705*, 85–92. https://doi.org/10.3141/1705-13

Tengattini, S., & Bigazzi, A. Y. (2017). A Field Bicycle Coast-Down Test to Measure Resistance Parameters. Presented at the 96th Annual Meeting of the Transportation Research Board, Washington D.C.

TransLink. (2013). *2011 Metro Vancouver Regional Trip Diary - Analysis Report.* Retrieved from http://www.translink.ca/-/media/Documents/customer_info/translink_listens/customer_surveys/trip_diaries/2011%20Metro%20Vancouver%20Regional%20Trip%20Diary%20%20Analysis%20Report.pdf

Twaddle, H., Schendzielorz, T., & Fakler, O. (2014). Bicycles in Urban Areas. *Transportation Research Record: Journal of the Transportation Research Board*, *2434*, 140–146. https://doi.org/10.3141/2434-17

Van de Mortel, T. F., & others. (2008). Faking it: social desirability response bias in self-report research. *Australian Journal of Advanced Nursing, The*, *25*(4), 40.

Waltham, C., & Copeland, B. (1999). Power requirements for rollerblading and bicycling. *The Physics Teacher*, *37*(6), 379–382. https://doi.org/10.1119/1.880355

Wegman, F., Zhang, F., & Dijkstra, A. (2012). How to make more cycling good for road safety? *Accident Analysis & Prevention*, *44*(1), 19–29. https://doi.org/10.1016/j.aap.2010.11.010

White, R. A., & Korst, H. H. (1972). The Determination of Vehicle Drag Contributions from Coast-Down Tests, *SAE Transactions*. https://doi.org/10.4271/720099

Wilson, D. G., & Papadopoulos, J. (2004). *Bicycling Science*. MIT Press.

Wong, J. Y. (2008). *Theory of Ground Vehicles*. John Wiley & Sons.

APPENDIX A: SURVEY CONSENT FORM

a place of mind
THE UNIVERSITY OF BRITISH COLUMBIA
Civil Engineering
Faculty of Applied Science

Department of Civil Engineering
Faculty of Applied Science

Consent Form
Bicycle coast-down test

I. Who is conducting the study?

Principal Investigator:

Dr. Alex Bigazzi, Assistant Professor
The University of British Columbia
Department of Civil Engineering

Co-Investigator:

Simone Tengattini, Masters Student
The University of British Columbia
Department of Civil Engineering

II. Who is collaborating on this study?

This study is carried out solely by Simone Tengattini & Dr. Alex Bigazzi, employees of the University of British Columbia (UBC).

III. Why are we doing this study? Why should you take part in this study?

The goal of the project is to estimate real-world bicyclists' resistance forces, in particular rolling resistance (between the wheel and pavement) and aerodynamic resistance (due to drag) through measurement of deceleration rate when coasting to a stop. This information on bicycle resistance forces will be used in travel models and health models that will help transportation planners and engineers make more informed decisions when developing bicycle infrastructure.

IV. What happens if you say "Yes, I want to be in the study"? How is the study done?

If you agree to participate in this study, you will be asked to perform the following tasks, that overall will require from 5 to 10 minutes.

Before the test

- You shall understand and sign this consent form;
- Complete the questionnaire by providing general information about you (such as age, gender, education, income) and your trip (such as origin, destination, purpose). Please note that you may to decline to answer any questions on the questionnaire that you choose; and
- Allow us to weigh you and your bike, and measure the pressure of your tires.

During the test

- You shall wear your helmet and adhere to all traffic laws;
- Allow us to capture a video of you completing the test;
- From a starting location well beyond the test corridor, you shall accelerate up to full riding speed (no faster than you feel comfortable and safe riding);
- Stop pedaling just before reaching the test corridor (marked with a "stop pedaling" line in chalk);
- Coast without braking or pedaling, until you reach the end of the test corridor (marked with another chalk line), or you are going too slow to ride safely.

V. Study Results

The results of this study will be reported in a Master of Applied Science thesis at UBC and may also be published in academic journals.

If you are interested in viewing the results, provide your email address below, and we will send you the published results along with personal data from your test (around spring 2017). Your email address will be stored along with your test/questionnaire data, but will not be used for any other purpose.

Email:_____

VI. Is there any way this study could harm you?

The risks to you in the study include:

- Risks typical of riding a bicycle on an off-street path; you are reminded to adhere to safe riding procedures and obey all traffic laws. In addition, caution must be taken in relation to the sensors placed along the sides of the path, which will be highlighted by cones.
- Providing personal information through the questionnaire; all questionnaire responses are non-compulsory, and after each data collection day, personal information will be transferred to and stored only on a secure server at UBC.

Please let one of us know if you have any concerns, and remember that you can quit the test at any time without providing any reason.

VII. What are the benefits of participating in this study?

Although taking part in this study will not provide immediate benefit to you directly, it will provide future indirect benefits because data collected will be used in development of better urban bicycle networks and bicycle infrastructure.

VIII. How will your identity and privacy be protected?

All collected information (including video and questionnaire data) will remain confidential: stored securely at UBC and only accessible to the researchers. Only

a place of mind
THE UNIVERSITY OF BRITISH COLUMBIA
Civil Engineering
Faculty of Applied Science

aggregate and non-personally-identifiable results will be published. We will not record your name; participants will be identified in the data only by serial number. Study data will be kept in electronic format at UBC for a period of 5 years after the study ends.

IX. Will you be paid for the time spent taking part in this research study?

You will not be paid for the time to take part in this study. However, light refreshments (water, juice) will be available for you.

X. Who can you contact if you have questions about the study?

If you have any questions or concerns about the study, please contact a member of the Study Team. Their names, telephone numbers, and email addresses are listed in part I of the first page of this form.

XI. Who can you contact if you have complaints or concerns about the study?

If you have any concerns or complaints about your rights as a research participant and/or your experiences while participating in this study, contact the Research Participant Complaint Line in the UBC Office of Research Ethics a f long distance e-mai or call toll free

XII. Your consent and signature

Taking part in this study is entirely up to you. You have the right to refuse to participate in this study. If you decide to take part, you may choose to withdraw from the study at any time without giving a reason and without any negative impact on you.

- Your signature below indicates that you consent to participate in this study.
- Your signature also indicates that you have received a copy of this consent form.
- **If you are under age 14**, your parent or guardian must also provide consent for you to participate by signing below.

_____	_____	_____
Printed Name of Participant	Signature	Date
_____	_____	_____
Printed Name of Participant	Signature	Date
_____	_____	_____
Printed Name of Parent or Guardian (Required if a Participant is under age 14)	Signature	Date

APPENDIX B: SURVEY QUESTIONNAIRE

a place of mind
THE UNIVERSITY OF BRITISH COLUMBIA
Civil Engineering
Faculty of Applied Science

Bicycle coast-down test: Questionnaire [Test #:_____]

Part I: Trip Information

Where did you start your trip?	Address, intersection, or landmark: City:
Where are you going?	Address, intersection, or landmark: City:
How long is this trip?	Distance: _____km AND Time: _____minutes
What is the purpose of this trip? (check one)	____ Commuting to/from work or school ____ Shopping, errands, restaurant/dining, etc. ____ Recreation or exercise: no destination, just riding ____ Other - please, specify:_____

Part II: Travel Characteristics

How often do you use the following modes for personal travel around Metro Vancouver?
Include commuting to/from work, but exclude work-related travel.

Check one box per row:	Almost never	Monthly or less often	Several times a month	Several times a week	Almost every day
Private vehicle, driver or passenger					
Carshare, driver or passenger (Car2Go, Evo, Modo, etc.)					
Taxi, rideshare companies					
Public transit (bus, Skytrain, HandyDART, etc)					
Bicycle					
Walk					

In the past 30 days, how many days did you ride a bicycle for each of the following purposes?

Check one box per row:	0 days	1-4 days	5-9 days	10-19 days	20+ days
Commuting to/from work or school					
Shopping, errands, restaurant/dining, etc.					
Recreation or exercise: no destination, just riding					

How much do you agree or disagree with the following statements?

Check one box per row:	Strongly disagree	Somewhat disagree	Neither agree nor disagree	Somewhat agree	Strongly agree
I bicycle year-round, regardless of the weather (rain or cold)					
I would like to travel by bicycle more than I do now.					
Bicycling is a form of exercise for me.					
I enjoy physical activity.					
I consider energy expenditure (physical effort) when choosing a bicycle route					
I consider air pollution (air quality) when choosing a bicycle route					

How comfortable would you feel cycling on your own in each of the following situations?

Check one box per row:	Very Uncomfortable	Uncomfortable	Comfortable	Very Comfortable
On bicycle paths far away from motor vehicles				
On local neighbourhood streets with little traffic and low speeds				
On major streets, provided they have bicycle lanes separated from traffic with a physical barrier				
On major streets, provided they have painted bicycle lanes				
On major streets without bicycle lanes				

How would you describe the maintenance condition of the bicycle you are riding today?	____ Excellent condition ____ Good condition ____ Fair condition ____ Poor condition
Do you consider the bicycle you are riding today to be heavy or light?	____ My bicycle seems heavy ____ My bicycle seems about average ____ My bicycle seems light
How would you compare your typical riding speed, compared to other cyclists?	____ Slower than most cyclists ____ About average speed ____ Faster than most cyclists

Part III: Personal Information

What is your home postal code? (for example V5M 1P1, or neighborhood if unknown)	
How many people live in your household, including yourself?	_____ person(s) total, including _____ licensed driver(s)
How many motor vehicles does your household own or lease? (include cars, vans and light trucks, but exclude motorcycles, scooters, bicycles and car-share vehicles)	____ None ____ One ____ Two ____ Three or more
What is the highest level of education you have completed? (check one)	____ Some high school or less ____ Completed high school/equivalency ____ College/University certificate or diploma ____ Bachelor's degree ____ Graduate degree (master's degree or doctorate)
What is your sex?	
What is your age?	
What is your height?	
How much time in a typical week do you spend in moderate and vigorous-intensity physical activities? (include bicycling and work activities)	*moderate* activity, such as brisk walking, with *small* increases in breathing and heart rate **(circle one)** Less than ½ hour | ½ - 1 ¼ hours | 1 ¼ - 2 ½ hours | 2 ½ - 5 hours | over 5 hours *vigorous* activity, such as running, with *large* increases in breathing and heart rate **(circle one)** Less than ½ hour | ½ - 1 ¼ hours | 1 ¼ - 2 ½ hours | 2 ½ - 5 hours | over 5 hours
What is your gross annual *household* income? (in CAD, check one)	____ under $24,999 ____ $25,000 to $49,999 ____ $50,000 to $74,999 ____ $75,000 to $99,999 ____ $100,000 to $149,999 ____ $150,000 or more

APPENDIX C: BICYCLE MEASUREMENTS FORM

a place of mind
THE UNIVERSITY OF BRITISH COLUMBIA
Civil Engineering
Faculty of Applied Science

BMP (Bicyclists' Measured Parameters) - Test #_____

General Info

Bicycle type	_____road _____hybrid _____mountain _____cruiser _____other, specify:_____
Bicycle gearing	_____# of gears OR _____fixed-gear
Bicycle make & model	Make:_____ Model:_____
Bicycle made year	Year:_____
Cargo description	#Back panniers:_____ #Backpacks:_____ #Front panniers:_____ Other:_____
Test riding position	___ aero (drops) ____ halfway (hoods) ____ upright/top bar
Helmet	___Yes ___No
Outfit	___Cycling specific clothing ___General/casual

Weight

bicycle+holder	_____ kg
cargo+holder	_____kg or ___Cargo is absent
Bicyclist	_____kg
Holder (if not bicyclist)	_____kg (blank if bicyclist is holder)

Tires details

Tire pressure front	_____ psi or _____bar
Tire pressure back	_____ psi or _____bar
Tire width front	_____cm
Tire width back	_____cm
Tire type front	___slick ___commuter ___knobby
Tire type back	___slick ___commuter ___knobby

APPENDIX D: CODES

For convenience and accessibility, coding implemented by the author are freely available on the GitHub author's account. In particular, repository /BCDT comprises the Arduino IDE sketch (.ino) loaded in the microcontroller, used during the data collection. Also, an R Script (.R) illustrates main functions and algorithms used in the data post-processing phase.